AD-A191 629 MIXED-MODE FRACTURE OF UNIAXIAL FIBER REINFORCED COMPOSITES(U) DREXEL UNIV PHILADELPHIA PA DEPT OF MECHANICAL ENGINEERING AN.. A S WANG ET AL. APR 87 1/2

UNCLASSIFIED NADC-87133-60 N62269-85-C-0246 F/G 11/4 NL

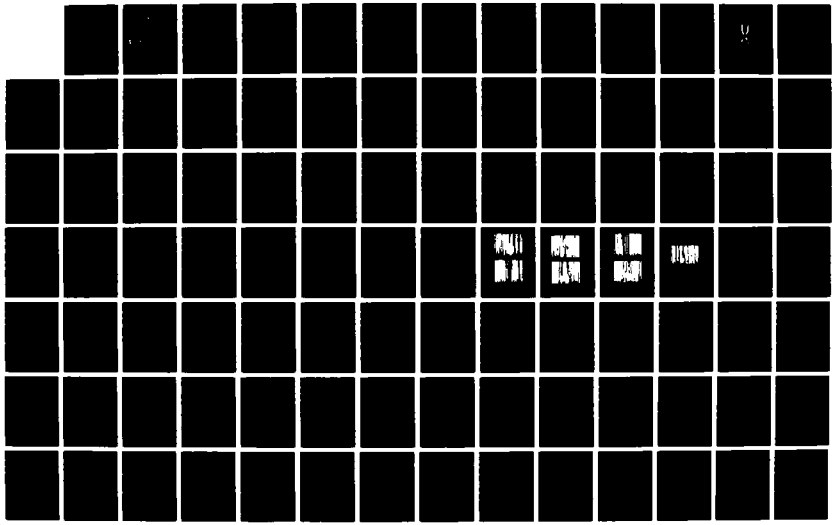

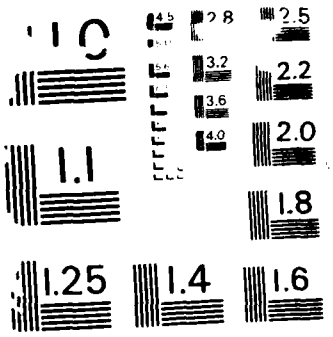

TEST CHART
NATIONAL BUREAU OF STANDARDS - 1963

DTIC FILE COPY

(2)

REPORT NO. NADC-87133-60

AD-A191 629

MIXED-MODE FRACTURE OF UNIAXIAL FIBER REINFORCED COMPOSITES

A. S. D. Wang, W. Binienda, E. S. Reddy, and Y. Zhong
Department of Mechanical Engineering and Mechanics
Drexel University
Philadelphia, PA 19104

DTIC
ELECTE
FEB 1 9 1988
S D
D

APRIL 1987

FINAL REPORT
Contract No. N-62269-85-C-0246

Approved for Public Release: Distribution is Unlimited

Prepared for
Air Vehicle and Crew Systems Technology Department
(Code 6043)

NAVAL AIR DEVELOPMENT CENTER
Warminster, PA 18974

88 2 19 06 6

SECURITY CLASSIFICATION OF THIS PAGE

REPORT DOCUMENTATION PAGE

1a REPORT SECURITY CLASSIFICATION UNCLASSIFIED	1b RESTRICTIVE MARKINGS
2a SECURITY CLASSIFICATION AUTHORITY	3 DISTRIBUTION/AVAILABILITY OF REPORT Approved for Public Release: Distribution is Unlimited
2b DECLASSIFICATION/DOWNGRADING SCHEDULE	
4 PERFORMING ORGANIZATION REPORT NUMBER(S)	5 MONITORING ORGANIZATION REPORT NUMBER(S) NADC-87133-60
6a NAME OF PERFORMING ORGANIZATION Drexel University 6b OFFICE SYMBOL (If applicable)	7a NAME OF MONITORING ORGANIZATION Air Vehicle and Crews Systems Technology Dept. Naval Air Development Center
6c ADDRESS (City, State, and ZIP Code) 32nd and Chestnut Streets Philadelphia, PA 19104	7b ADDRESS (City, State, and ZIP Code) Warminster, PA 18974
8a NAME OF FUNDING/SPONSORING ORGANIZATION NADC 8b OFFICE SYMBOL (If applicable) 6043	9 PROCUREMENT INSTRUMENT IDENTIFICATION NUMBER N-62269-85-C-0246
8c ADDRESS (City, State, and ZIP Code) Warminster, PA 18974	10 SOURCE OF FUNDING NUMBERS PROGRAM ELEMENT NO. 61153N PROJECT NO. TASK NO. R02303001 WORK UNIT ACCESSION NO. 106364

11 TITLE (Include Security Classification)
MIXED-MODE FRACTURE OF UNIAXIAL FIBER REINFORCED COMPOSITES

12 PERSONAL AUTHOR(S) A. S. D. Wang, W. Binieda, E. S. Reddy and Y. Zhong

13a TYPE OF REPORT	13b TIME COVERED	14 DATE OF REPORT (Year, Month, Day)	15 PAGE COUNT
Final Report	FROM 1 Jul 85 TO 31 Dec 86	15 April 1987	57 + 79 Appendix

16 SUPPLEMENTARY NOTATION

17 COSATI CODES			18 SUBJECT TERMS (Continue on reverse if necessary and identify by block number)
FIELD	GROUP	SUB-GROUP	Composite material, Graphite-epoxy, Mixed-mode fracture matrix cracking, Singular integral equation, Finite element simulation, Experiment-analysis correlation
11	04		
20	11		

19 ABSTRACT (Continue on reverse if necessary and identify by block number)

Mixed-mode matrix fracture in notched off-axis unidirectional composite is investigated. First the problem is treated by an exact formulation based on elastic fracture mechanics. It is then simulated by a finite element model. Correlation with experiment suggests a fracture criterion based on total strain energy release rate as the fracture parameter.

20 DISTRIBUTION/AVAILABILITY OF ABSTRACT ☒ UNCLASSIFIED/UNLIMITED ☐ SAME AS RPT ☐ DTIC USERS	21 ABSTRACT SECURITY CLASSIFICATION Unclassified
22a NAME OF RESPONSIBLE INDIVIDUAL Lee W. Gause	22b TELEPHONE (Include Area Code) (215) 441-1330 22c OFFICE SYMBOL 6043

DD FORM 1473, 84 MAR 83 APR edition may be used until exhausted. All other editions are obsolete

SECURITY CLASSIFICATION OF THIS PAGE

U.S. Government Printing Office 1986—607-044

TABLE OF CONTENTS

	Page
Foreword	
I. MIXED-MODE MATRIX CRACKING	1
Introduction	1
Objective of Research	4
Research Plan	4
Figures 1.1 to 1.2	7-8
II. MIXED-MODE FRACTURE ANALYSIS MODELS	9
Elasticity Solution for a Kinked Crack	9
Finite Element Simulations	12
Table 2.1	14
Figures 2.1 to 2.20	15-34
III. EXPERIMENT AND RESULTS	35
Material and Specimens	35
Test Method and Test Data	36
Finite Element Simulation	37
Critical Strain Energy Release Rate at Onset of Kink	38
Table 3.1	40
Figures 3.1 to 3.11	41-54
IV. CONCLUDING REMARKS	55
REFERENCES	56
APPENDIX A	
- Exact Solution of a Kinked Crack in an Orthotropic Plate -	58

FOREWORD

Results contained in this report were obtained during the course of research conducted under the contract N-62269-85-C-0246, from the Naval Air Development Center to Drexel University. The NADC program manager is Mr. Lee W. Gause. The program principal investigator at Drexel University is Professor A. S. D. Wang. Contributors to this program are Dr. E. S. Reddy, Mr. W. Binienda and Mr. Y. Zhong of Drexel University, and Professor F. Delale of the City College of New York. The authors wish to thank Mr. Gause for his many helpful suggestions during the course of this work.

QUALITY INSPECTED 2

Accesion For
NTIS CRA&I ☑
DTIC TAB ☐
Unannounced ☐
Justification
By
Distribution /
Availability Codes
Dist Avail and / or Special
A-1

I. MIXED MODE MATRIX CRACKING

Introduction.

Structural composite laminates, notably those made of unidirectional tape systems, are known to suffer extensive matrix cracks before the failure of the load-carrying fibers. These matrix cracks occur because of the interfacial stresses that arise from local load-transfer. For instance, load transfer from a weakened fiber bundle to an adjacent stronger fiber bundle may induce debonding between these two fiber bundles. Similarly, load transfer from a weakened lamina to an adjacent stronger lamina may induce delamination between these two laminae. Thus, the initiation and propagation of matrix cracks in laminates of multi-directional plies usually follow either the fiber/matrix interface or the ply/ply interface, or both.

Fig. 1.1 shows the extensive matrix cracking that occurred in a notched graphite-epoxy $[0_2/90_2]_s$ laminate subjected to uniaxial tension. Two major types of matrix cracking occurred when viewed at the phenomenlogical scale. Namely, in-ply cracking between two adjacent fiber bundles and delamination between two adjacent plies. The four vertical cracks were initiated first near the hole and propagated inside the 0^0-plies. The driving force here was clearly due to the load-transfer from the fiber bundle cut by the hole to the fiber bundle which is uncut. As the vertical cracks propagated away from the hole, load transfer then took place locally between the cracked 0^0-plies and the uncracked 90^0-plies. This in turn induced interply stresses along the root of the vertical cracks; and delamination in the 0/90 interface initiated and propagated with the applied load.

A closer analysis of the cracked specimen stress field at each major stage of crack development would reveal a complex three-dimensional stress state. Stress concentration is high near the crack-root regions; and the resulting crack propagation is mixed-mode (with both opening and shearing

actions [1]).

The basic mechanisms of in-ply trans-fiber cracking and interply delamination have recently been treated at the phenomenlogical scale by a unifed energy method [2]. The energy release rate concept of elastic fracture mechanics was employed as a criterion for crack propagation. This method, when coupled with a three-dimensional stress analysis and limitted to mode-I propagation conditions, has proven useful for predicting brittle matrix cracks in graphite-epoxy systems. For mode-I cracking, it is necessary to determine the strain energy release rate G_I as the crack-driving force and validate the corresponding critical strain energy release rate G_{IC} as a material property [2].

As for matrix cracks that involve mixed modes, such as those illustrated in Fig. 1.1, the applicabilty of the energy method has not been as firmly established. One major difficulty is that the specimen geometry effects on mixed-mode crack propagation are intrinsically coupled with the material effects. Separation of these effects requires a rigorous analysis of the cracked specimen at each major stage of crack development.

There have been several studies aimed at establishing criteria for mixed-mode matrix cracking in unidirectional laminates. Most of the studies used graphite-epoxy systems. Wilkins, et. al. [3] and Ramkumar, et.al [4] used the cracked-lap shear specimen loaded in uniaxial tension to induce mixed mode-II/mode-I delamination between the cracked lap-layer and the substrate layer. By varying the thickness of the lap-layer relative to the substrate layer, the mixed-mode ratio G_{II}/G_I in the measured total critical strain energy release rate could be varied from 0.35 to 0.45. They observed that the total strain energy release rate $(G_I+G_{II})_C$ is somewhat greater than G_{IC} obtained under pure mode-I conditions. Bradley and Cohen [5] used a cantiliver

split-beam specimen loaded by a pair of upward and downward loads applied at the tip of the cantilliver. Variation of the mixed-mode ratio G_{II}/G_I was achieved by changing the ratio of the upward and downward loads. In this way, they obtained a range for the G_{II}/G_I ratio from 0 to about 0.6. They observed that the measured total strain energy release rate $(G_I+G_{II})_C$ increased uniformly with G_{II}/G_I in those systems made of brittle matrix material, but decreased slightly with G_{II}/G_I in systems made of ductile matrix material. Wang, et. al. [6] used a doubled side-notched off-axis unidirectioal laminate coupon loaded in axial tension. By varying the off-axis angle from 0^0 to 90^0, the mixed-mode strain energy release rate for G_{II}/G_I ratio ranging from 0 to about 3 could be determined. They found that the total strain energy release rate $(G_I+G_{II})_C$ first increased with G_{II}/G_I monotonically up to about G_{II}/G_I = 1.5, and then reached an asymptotic value which is about three times G_{IC}. Russell and Street [7] used four different test specimen configurations and obtained mixed-mode strain energy release rates for a wide range of mixed-mode cracking conditions. Their results showed that the measured strain energy release rate values were test specimen dependent.

Clearly, no firm agreement could be reached toward establishing a general criterion for mixed-mode matrix cracking, despite these and many other efforts. It is believed that one principal reason for the disagreement in results is that the effects of specimen geometry on mixed-mode matrix cracking were not rigorously separated from material effects. Specifically, the mathematical analysis for the cracked specimen was based on either one-dimensional beam theory or a finite element laminated plate model. These approximate methods lack the required precision to treat highly three-

dimensional stress fields that often contain stress singularities. This is especially true when applied to mixed-mode cracking conditions, where significant errors could result in the computed G_I and G_{II} energy release rates.

Objectives of Research.

The purpose of this study is to overcome the above stated difficulty by developing an analysis for mixed-mode fracture employing an ideal specimen configuration and loading condition. This problem can be treated rigorously on the basis of the theory of elasticity and fracture mechanics. Concurrently, a finite element procedure is developed to simulate the same problem and yield accruate numerical solutions. Mathematical rigor and numerical accuracy are needed at the same time in order to ensure correct separation of the specimen geometry effects from the material effects. Finally, experiments are conducted using specimems of similar configurations to generate mixed-mode fracture data on a wide range of G_{II}/G_I ratios. The corresponding fracture analysis is performed using the finite element simulation model. This will provide a final correlation between experiment and analysis.

It should be mentioned that an exact elasticity solution for the test specimen configurations cannot presently be obtained, requiring use of a numerical model with established accuracy.

Research Plan.

To this end, the following research plan involving four analysis steps as illustrated in Fig. 1.2 was implemented.

Step A. We begin with a unidirectional laminate of infinite domain. Let the laminate contain a through-thickness kinked crack and subject to a uniform far-field tensile stress σ_0. Let the base of the crack be orientated normal to the far-field tension, while the kink be in the direction of the fibers. The angle between the fiber and the applied tension is denoted by θ. Assuming linear

elastic response under the applied stress σ_0, a pair of dissimilar stress singularities develop at the two crack tips. At some critical σ_0, the kink will propagate in mixed-mode along the fiber direction. Our plan is to determine the crack tip stress intensity factors K_I and K_{II} as well as the strain energy release rates G_I and G_{II}. By treating the laminate as an elastic, homogeneous and orthotropic body that contains the prescribed kinked crack we solve the elastostatic problem exactly based on the theory of elasticity. Note that the determined mixed-mode G_{II}/G_I ratio at the tip of the kink will vary with the angle θ as well as the length of the kink, a'. We are especially interested in the cases where a' is arbitrarily small.

Step B. Next, we simulate the problem by a finite element model. Here, we represent the infinite plate by a rectangular plate which contains the same kinked crack. The length and width of the plate are so large that the effects of the plate boundaries will not affect the stress state near the kinked crack. The finite element shape and mesh size selections must be tuned to yield a result as close as possible with that obtained by the exact elasticity solutions. This step establishes the degree of accuracy of the finite element model.

Step C. Having established confidence in the accuracy of the finite element model, we then use the model and simulate a finite width, off-axis unidirectional tensile coupon with double side-notches. We assume that the far-field stress, σ_0, will initiate a kinked crack and propagate unstably along the direction of the off-axis fibers at some critical value. The finite element model simulates this mixed-mode cracking and yields both the kink-tip stress intensity factors K_I and K_{II} and the strain energy release rates G_I and G_{II}. The computed mixed-mode G_{II}/G_I ratio at the tip of the kink will vary not only with the off-axis angle θ but also with the depth of the side-notch, a.

Note that this problem differs from the previous one in that the kink-tip behavior in this problem is affected significantly by the free edge boundary and the notch depth relative to the width of the tensile coupon.

Step D. The final step involves experiments in which off-axis tensile coupons with double side-notches are tested the same way as those simulated in Step-C. Here, the critical far-field stress, σ_{cr}, at the propagation of the kink is recorded. This provides the necessary data for correlation with the analysis performed in step-C.

In order to effect a realistic and reliable correlation, the off-axis angle θ of the test specimens is varied from 0^0 to 90^0 in seven different increments and the initial depth of the side-notches is varied from 0.1 to 0.175 inch in four increments (the width of the coupon is 1.0 inch).

The analytical treatment for the problem as described Step-A and the finite element simulation for the same problem as described in Step-B are outlined in Section 2. The detailed mathematical derivations and solution procedures for the analytical problem are included in Appendix A, while the details of the finite element calculation routine are referred to an earlier publication. Section 3 discusses the experiment, the experimental results, the finite element simulations and the final experiment/analysis correlations as described in steps C and D above. Finally, a set of concluding remarks is presented in Section 4.

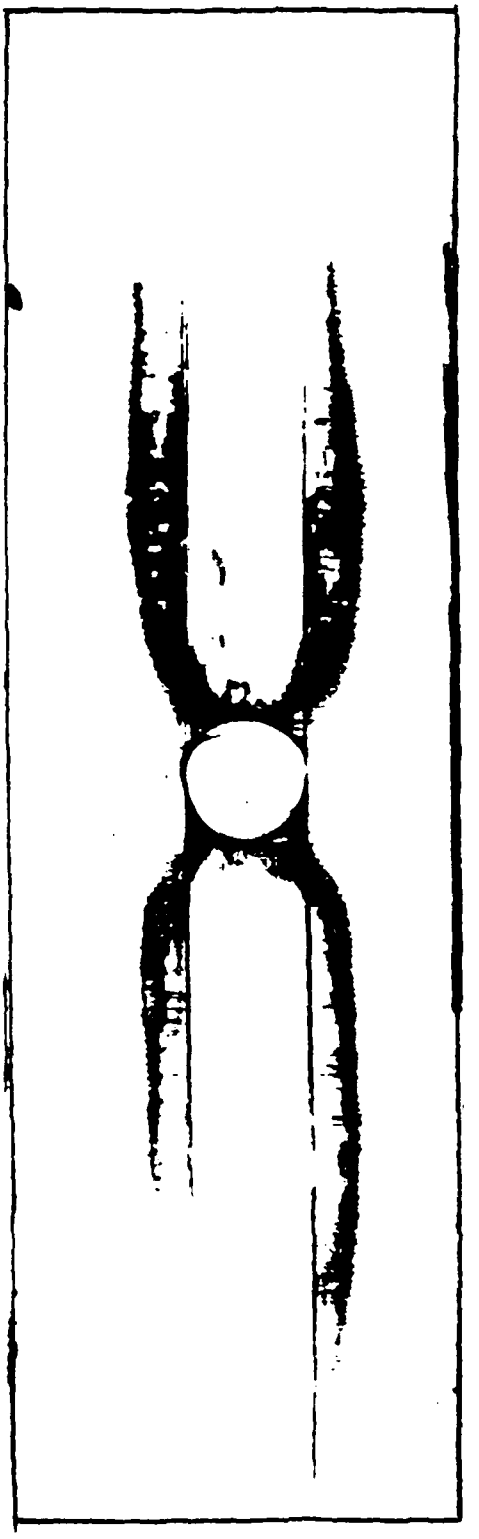

Fig. 1.1 X-radiograph of matric crack development in a notched $[0_2/90_2]_s$ graphite-epoxy laminate loaded in axial tension

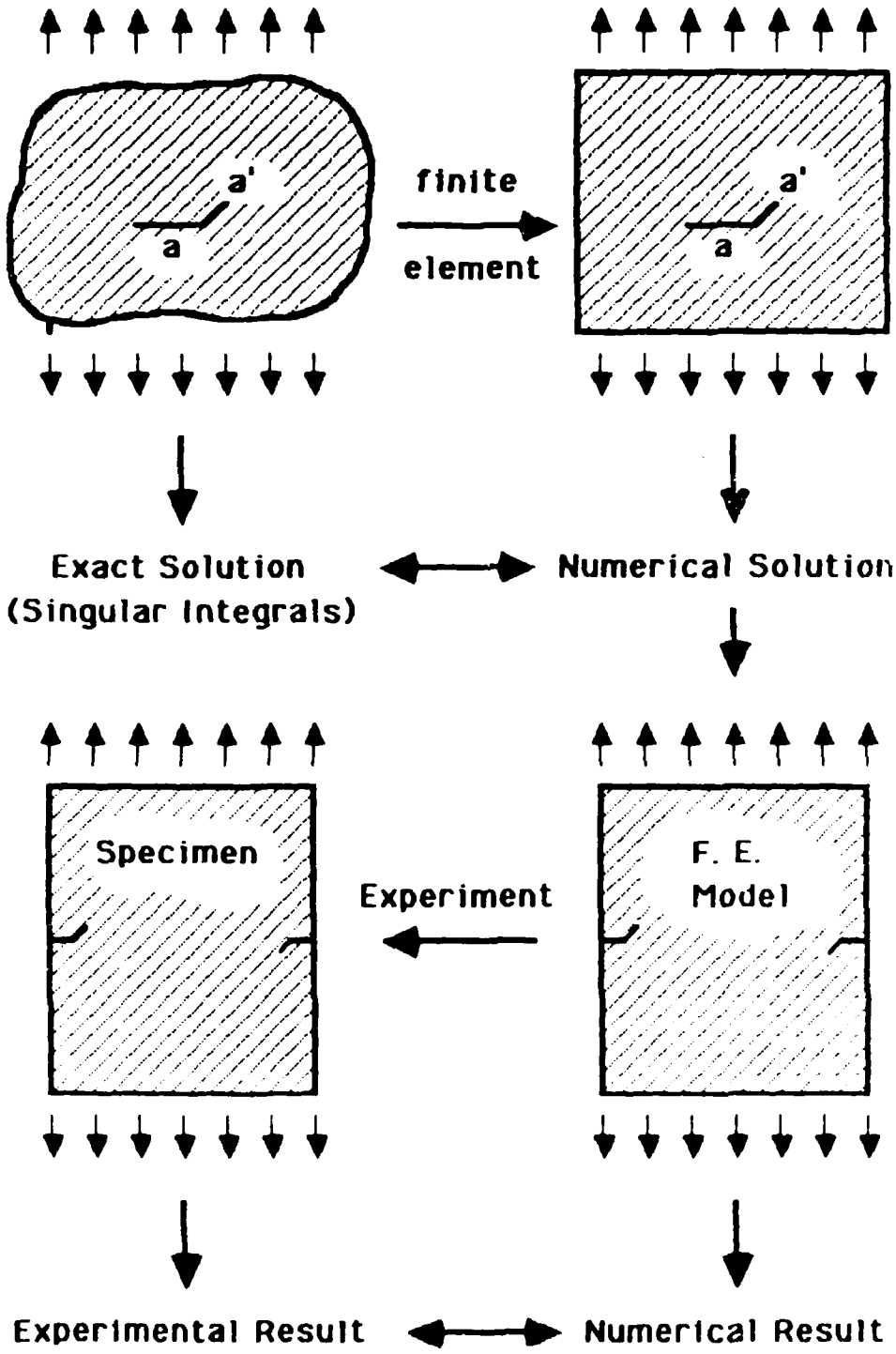

Fig. 1.2 Schematics showing the four analysis steps in the present study

II. MIXED-MODE FRACTURE ANALYSIS MODELS

In this section, we shall consider the problem of a kinked crack in an infinte anisotropic elastic plate which is subjected to a uniform tensile stress field. The problem will be treated first by an exact elasticity formulation and then by a finite element simulation. The purpose of the analytical treatment is to obtain, for the first time, an exact elasticity solution for the posed problem, from which the accuracy of the finite element simulation procedures can be established.

Elasticity Solutions For A Kinked Crack.

Consider the kinked crack shown in Fig. 2.1. The inifinte plate is a representation of the unidirectional laminate with the fibers orientated at an angle θ from the direction of the applied tension. The base of the kinked crack is situated normal to the applied tension, while the kink itself is orientated along the fiber direction. Our objective here is to determine the mixed-mode stress intensity factors K_I and K_{II} and the strain energy release rates G_I and G_{II} at the tip of the base as well as of the kink.

The corresponding problem of a kinked crack in an infinte elastic isotropic plate has been treated by Gupta [8,9] and Chatterjee [10]. In both cases, the singular integral solution scheme was employed. Here, we shall first address the problem of two separate cracks embedded in an orthotropic plate; one is the base and the other is the kink. Initially, these two separate cracks are unconnected. Using the crack surface displacement derivatives as unknowns and the principle of superposition, the problem is then formulated in terms of singular integral equations with Caushy type kernels. The resulting system of equations are solved numerically employing a Gaussian quardrature and the collocation method. The mode I and mode II stress intensity factors are then calculated with the relative angle, relative distance and relative size of the

two cracks as parameters.

Next, by letting the right tip of the base and the lower-left tip of the kink touch each other it thus becomes one kinked crack. At this configuration, the singular integral equations are still valid; but some of the kernels become singular at the point of connection. By imposing the condition that the surfaces at the connecting point are now free of stress, the problem reduces to that posed in Fig. 2.1. The details of the analysis, including the mathematical derivations and solution procedures, are presented in Appendix A.

Some interesting results have been obtained for a number of cases. Consider first the case of two separate cracks where the base crack and the kink do not touch each other. Their interaction in terms of fracture parameters can be investigated by varying their orientation angle, relative length, relative distance and the degree of anisotropy of the medium.

For example, Fig. 2.2 shows the mixed-mode stress intensity factors at the two approaching tips b and c, as a function of their relative distance, h, for an isotropic plate in which the two cracks are of equal size (2") and with an angle $\alpha = 30^0$ (see insert in Fig. 2.2). The interaction between the two approaching cracks is clearly illustrated by the dependence of the stress intensity factors on the relative distance h. In fact, a singular behavior is exhibited when the two cracks touch each other. It is shown mathematically that the crack tip singularity at this configuration is different from being 1/2, see Appendix A.

The corresponding problem for an orthotropic plate (mimicking a graphite-epoxy UD laminate) is shown in Fig. 2.3. The crack interaction behavior is essentially identical to that shown in Fig. 2.2.

With a fixed distance h, the interaction is expected to vary with the kink angle α. Fig. 2.4 shows the case of an isotropic plate in which two cracks of equal size (2") maintain a fixed distance h =0.1". Here, the stress intensity

factors at the extreme crack tips (points a and d) are plotted against the angle α. The corresponding plot for an orthotropic plate is shown in Fig. 2.5. Again, the interaction behaviors of these two cases in terms of fracture parameters are essentially similar.

Next, consider the problem in which the two cracks of equal size (2") touch each other at the kink point and thus become a kinked crack. Fig. 2.6 shows the case of an isotropic plate, where the mixed-mode stress intensity factors at the extreme tips (points a and d) are plotted against the kink angle α. The corresponding plot for an orthotropic plate is shown in Fig. 2.7. The general features in these two cases displayed in terms of the stress intensity factors are also similar.

As was noted earlier, one problem of practical interest is when the length of the kink, a', is shortened as to approach zero. In the limit, the behavior of the crack is still that of a kinked crack. This problem is relevant to the case of a crack which is situated in an orthotropic plate, not aligned in any one principal direction, but will propagate in one of the principal directions (e.g. the fiber direction). The mixed-mode stress intensity factors at the initiation point of the kink can be obtained by this solution procedure.

Fig. 2.8 shows, for an isotropic plate, the change of the mixed-mode stress intensity factors at the kinked crack tips (points a and d) as the length of the kink (L_2) is shortened to zero. Here, the base crack has a length of $L_1 = 2"$ and the kink angle is set at $\alpha = 30^0$. The corresponding plot for an orthotropic plate is shown in Fig. 2.9.

At this point, it should be mentioned that the stress intensity factors obtained for all cases relative to isotropic plate closely agrees with those reported previously, even though our solution technique is different. Table 2.1 shows a comparison between the present results and those obtained by Gupta [9] and Chatterjee [10] for a kinked crack having the base and the kink of equal

size, and kink angles of 30^0, 45^0 and 60^0. Thus, our results for the isotropic plate can be trusted as being exact.

There are no other solutions for the orthotropic plate to compare with our results, however. Since the isotropic plate represent a limiting case of the orthotropic plate in our solution, it is believed that our results for the orthotropic plate can also be trusted as being exact.

Finally, the mixed-mode strain energy release rates G_I and G_{II} at the kinked crack tips will be calculated from the solutions of the elastic stress field which depends on the solutions of the crack tip stress intensity factors. The details of the calculation are again presented in Appendix A.

Fig. 2.10 shows, for the isotropic case, the mixed-mode strain energy release rates G_I and G_{II} and the total $G_T=G_I+G_{II}$ at the tip of the kink (point d) as a function of the length of the kink (L_2). Here, the base crack length L_1 = 1" and the kink angle $\alpha = 30^0$. The corresponding plot for the orthotropic case is shown in Fig. 2.11.

Fig. 2.12 is a plot of the strain energy release rates G_I, G_{II} and G_T, for an isotropic plate, as a function of the kink angle, α. In this case, the length of the kink is made small (L_2 = 0.1") compared to the length of the base (L_1 = 1"). The corresponding plot for an orthotropic plate is shown in Fig. 2.13.

A more detailed parametric study on the mixed-mode stress intensity factors and the strain energy release rates at the kink tip in both isotropic and orthtropic plates is contained in [11,12].

Finite Element Simulations.

The problems, treated above based on exact elasticity formulation, will now be simulated by means of a finite element model. The finite element procedure employed has been developed for a previous NADC study on matrix cracking analysis in multidirectional laminates [13]. Hence, the details of this

work will not be presented here.

The simulated model is illustrated in Fig. 2.14, where a finite-width rectangular plate containing a kinked crack is considered. To simulate an infinite plate, the length and the width of the plate are made very large compared to the size of the kinked crack. In this particular simulation, the width W of the plate was 10 times the length of the base crack; and the length to width ratio of the plate was set at 3 to 1.

With these provisions, the boundary effects on the finite element results for the mixed-mode stress intensity factors and the strain energy release rates are minimized. Generally, the computed stress intensity factors are more sensitive to the finite element shape and mesh size in the crack region than the computed strain energy release rates. In particular, the total strain energy release rate $G_T = G_I + G_{II}$ agrees most closely with the elasticity solutions. Thus, by tuning the finite element shape and mesh near the kinked crack, the accuracy of the finite element results can be optimized.

For the case of an isotropic plate where the kink is made small compared to the base ($L_2/L_1 = 0.1$), a comparison is made between the finite element solutions and the elasticity solutions for the kink tip strain energy release rates.. Figs. 2.15, 16 and 17 show, respectively, the kink tip strain energy release rates G_I, G_{II} and G_T as functions of the kink angle, α. The corresponding comparisons for a kinked crack in an orthotropic plate are displayed in Figs. 2.18, 19 and 20. The close agreement between the finite element results and the elasticity results establishes the accuracy of the numerical procedure.

The finite element method will be used to simulate the test specimens used in the experimental study, since an elasticity solution for those specimen configurations is not available.

TABLE 2.1

Stress Intensity Factors (normalized by σ_0) at Kinked Crack Tips.

(Isotropic Plate with $L_1 = L_2$)

kink angle	K/σ_0	Present Solution	Gupta [9]	Chatterjee [10]
30^0	$K_1(a)$	1.3421	1.3559	1.3508
	$K_2(a)$	0.0328	0.0327	0.0325
	$K_1(d)$	1.0949	1.0873	1.0830
	$K_2(d)$	0.6855	0.6833	0.6804
45^0	$K_1(a)$	1.2732	1.2902	1.2887
	$K_2(a)$	0.0217	0.0211	0.0208
	$K_1(d)$	0.7546	0.7463	0.7438
	$K_2(d)$	0.8450	0.8405	0.8377
60^0	$K_1(a)$	1.2082	1.2221	1.2194
	$K_2(a)$	-0.0108	-0.0109	-0.0116
	$K_1(d)$	0.3941	0.3900	0.3822
	$K_2(d)$	0.8350	0.8319	0.8292

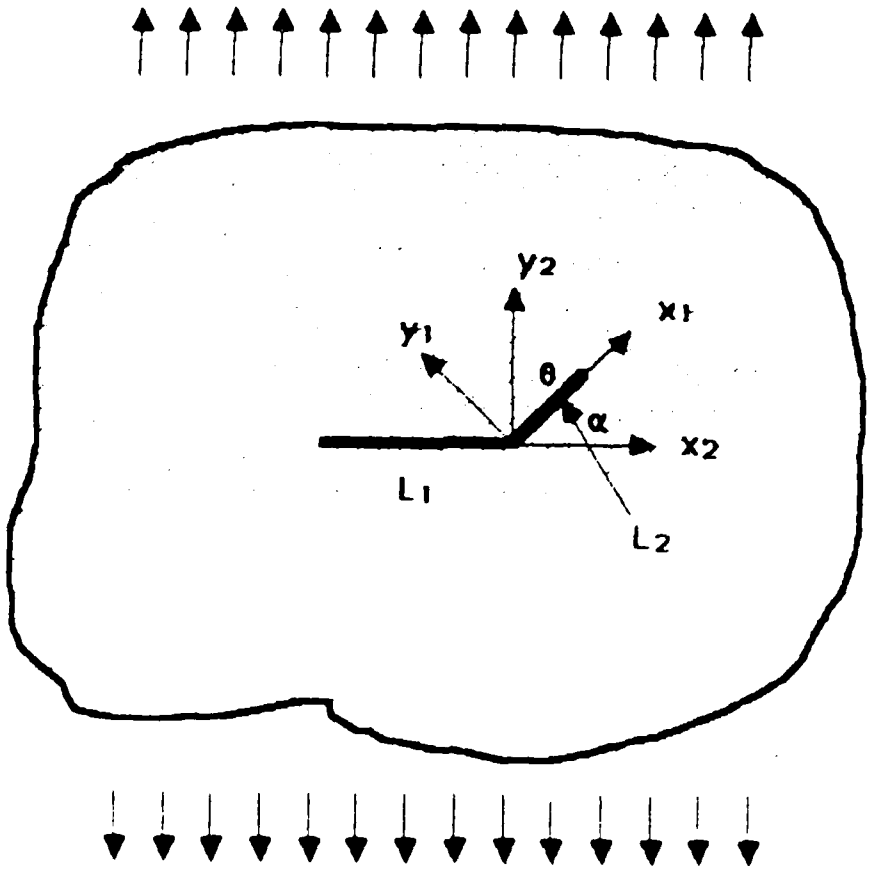

Fig. 2.1 Geometry and reference frames for a kinked crack in an infinte orthotropic plate.

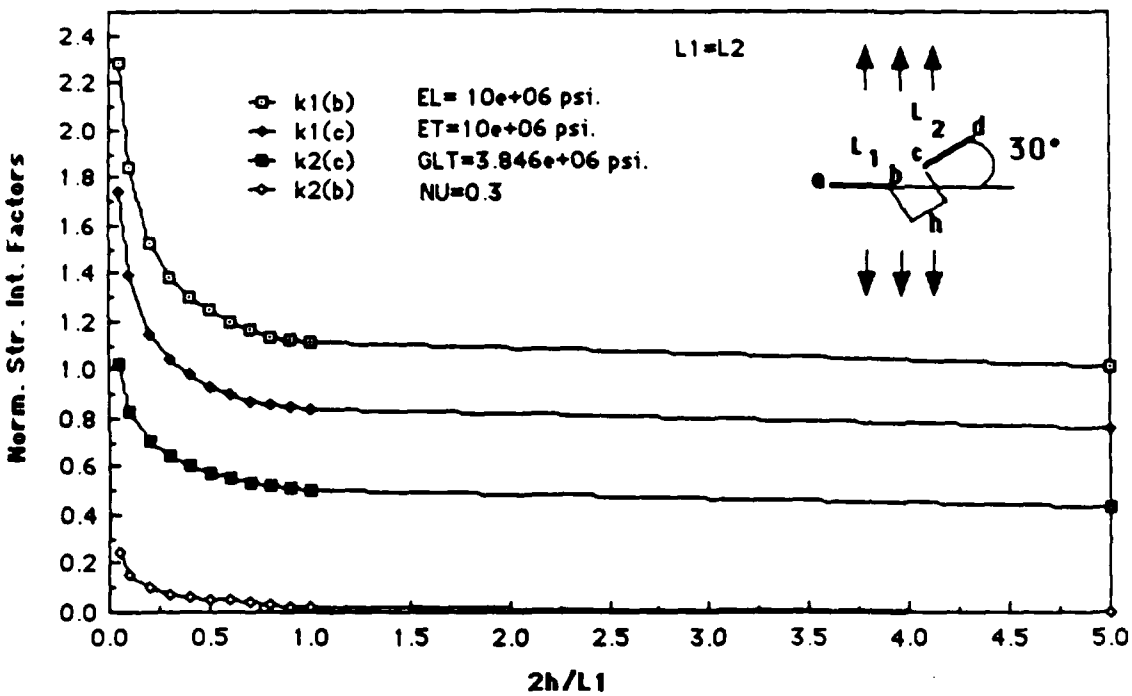

Fig. 2.2 Interaction of two cracks as a function of their relative distance, h. Isotropic case with $\alpha = 30^0$.

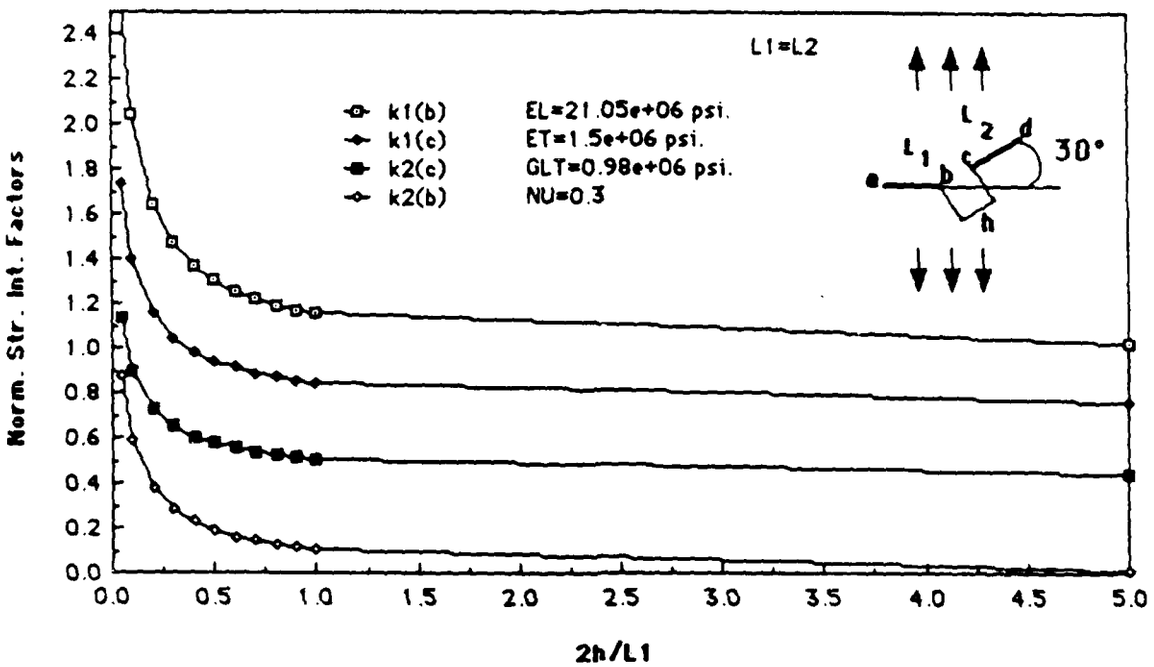

Fig. 2.3 Interaction of two cracks as a function of their relative distance, h. Orthotropic case with $\alpha = 30^0$.

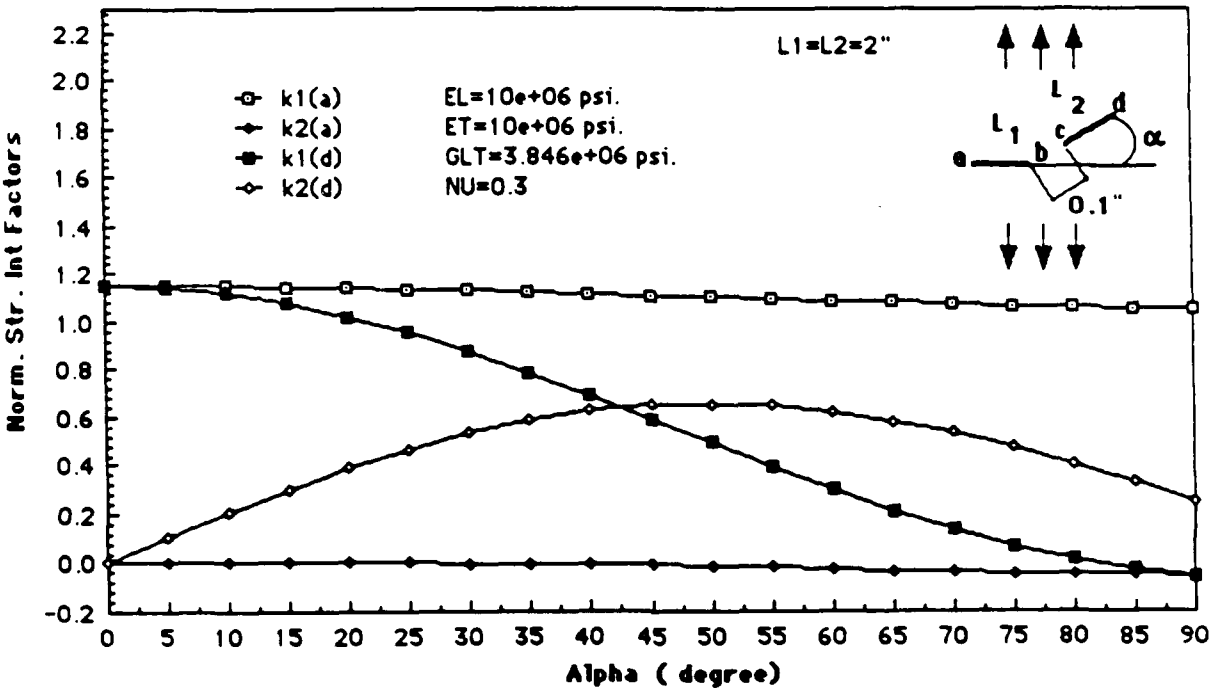

Fig. 2.4 Interaction of two cracks as a function of the kink angle, α. Isotropic case with $2h/L_1 = 0.1$.

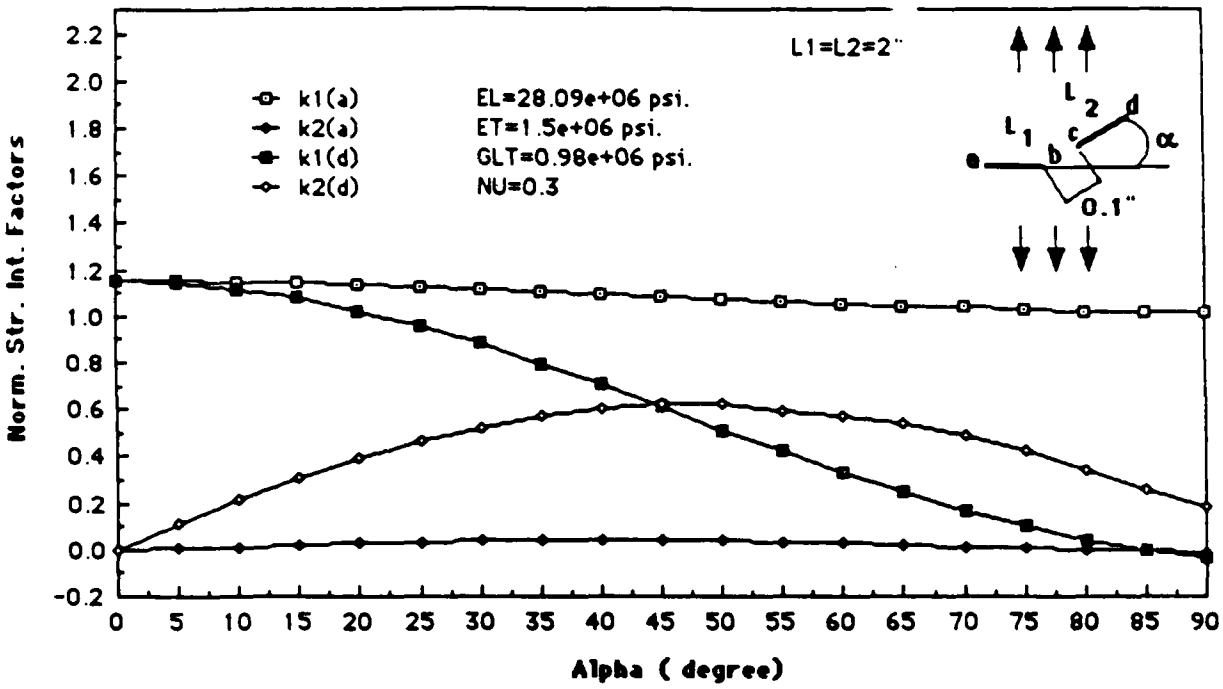

Fig. 2.5 Interaction of two cracks as a function of the kink angle, α.

Orthotropic case with $2h/L_1 = 0.1$.

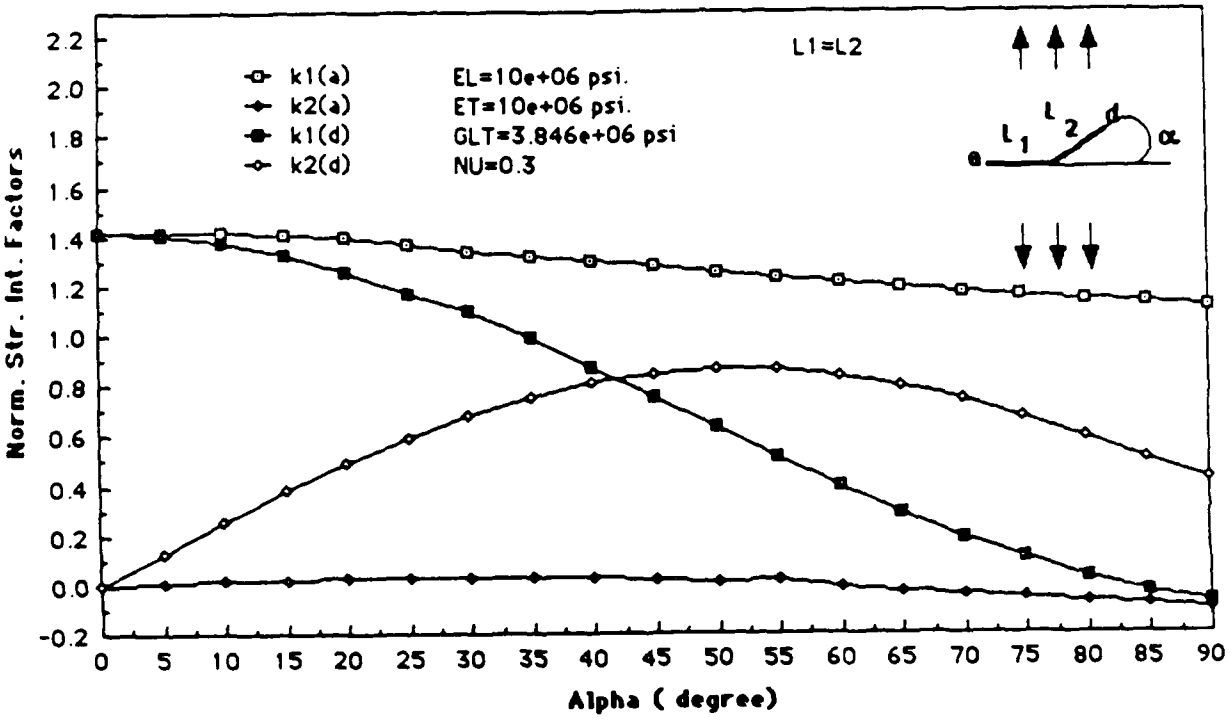

Fig. 2.6 Stress intensity factors (normalized by $\sigma_0\sqrt{L/2}$) at the kink tip as a function of kink angle, α. Isotropic case with $L_1 = L_2$.

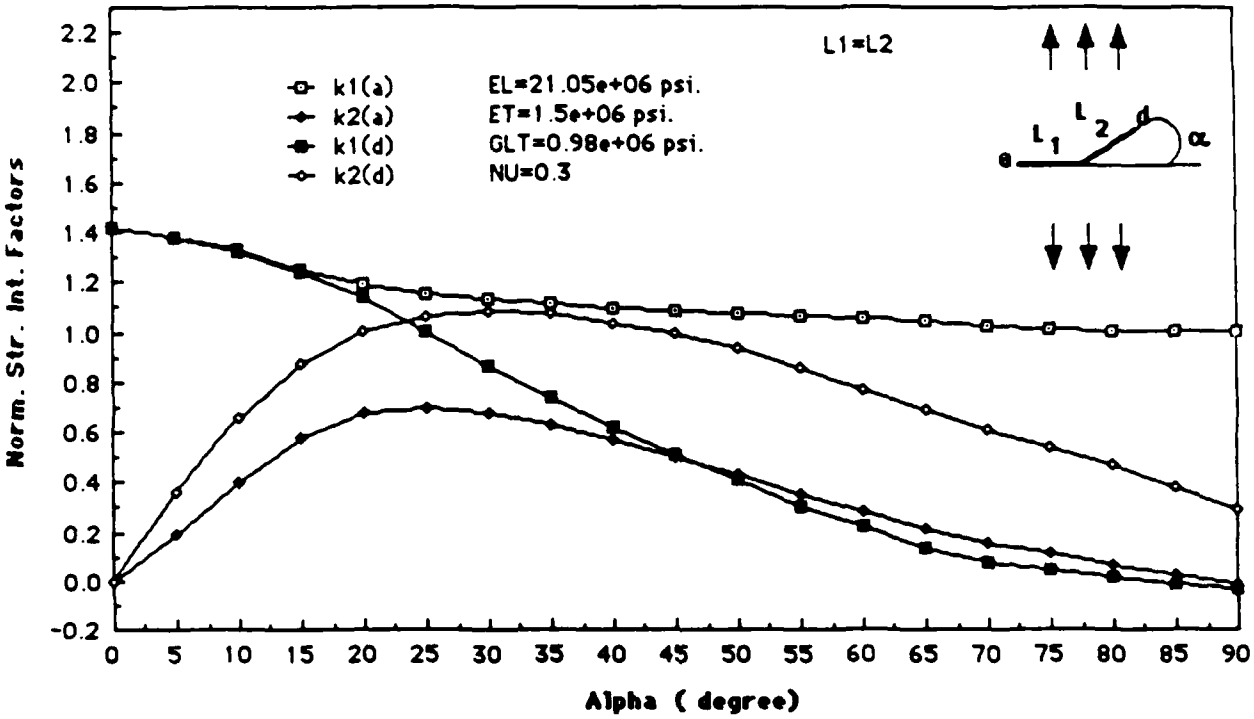

Fig. 2.7 Stress intensity factors (normalized by $\sigma_0\sqrt{L/2}$) at the kink tip as a function of kink angle, α. Orthotropic case with $L_1 = L_2$.

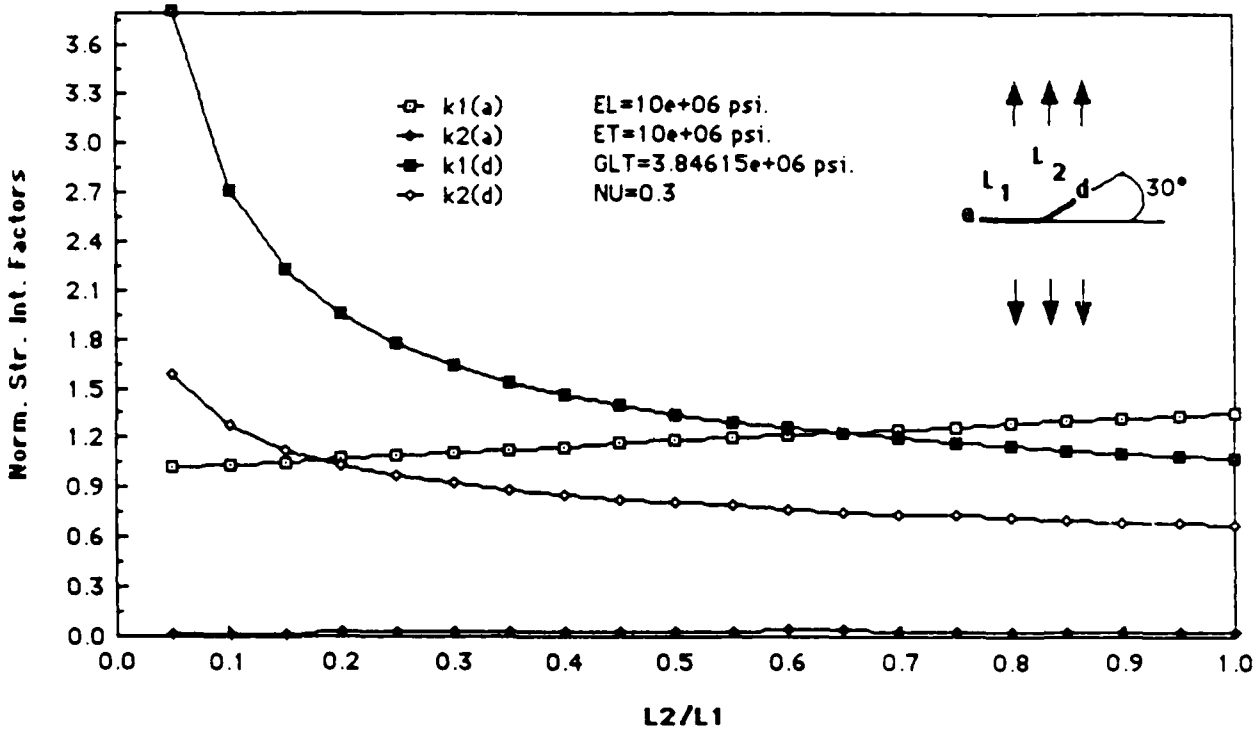

Fig. 2.8 Stress intensity factors (normalized by $\sigma_0\sqrt{L/2}$) at the kink tip as a function of kink length, L_2. Isotropic case with $\alpha = 30^0$.

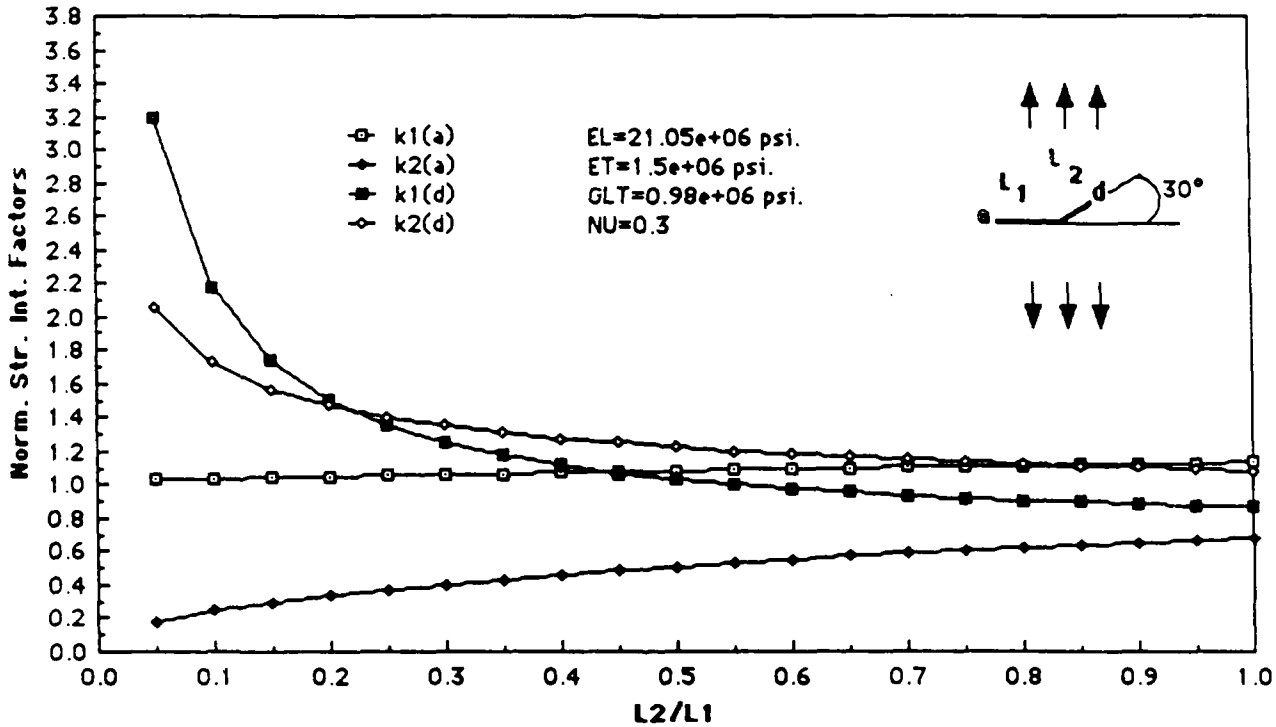

Fig. 2.9 Stress intensity factors (normalized by $\sigma_0\sqrt{L/2}$) at the kink tip as a function of kink length, L_2. Orthotropic case with $\alpha = 30^0$.

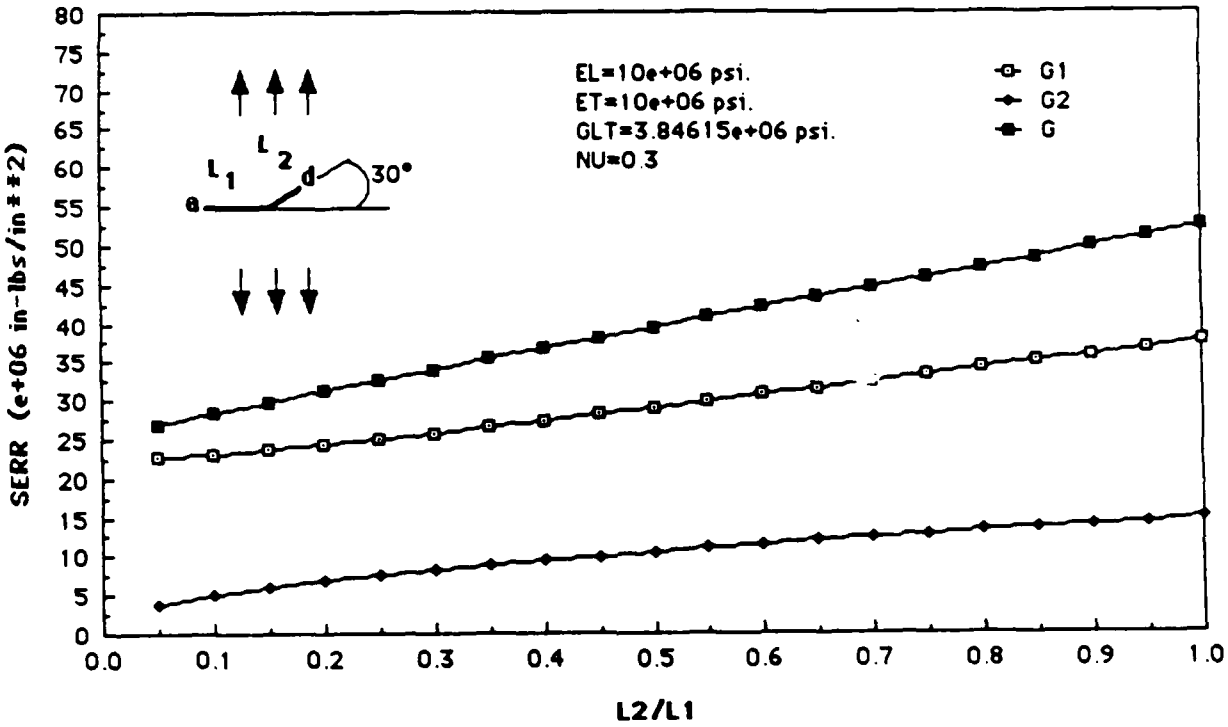

Fig. 2.10 Strain energy release rates (under e_x = 1) at the kink tip as a function of kink length, L_2. Isotropic case with $\alpha = 30^0$.

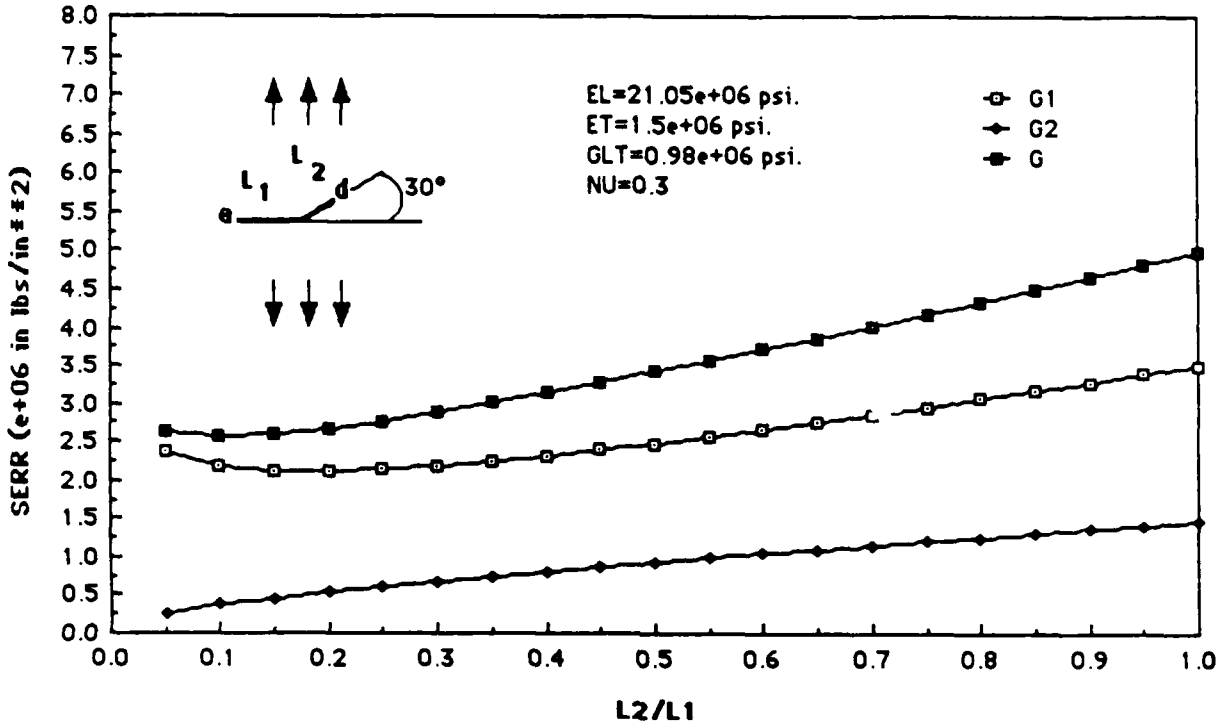

Fig. 2.11 Strain energy release rates (under $e_x = 1$) at the kink tip as a function of kink length, L_2. Orthotropic case with $\alpha = 30^0$.

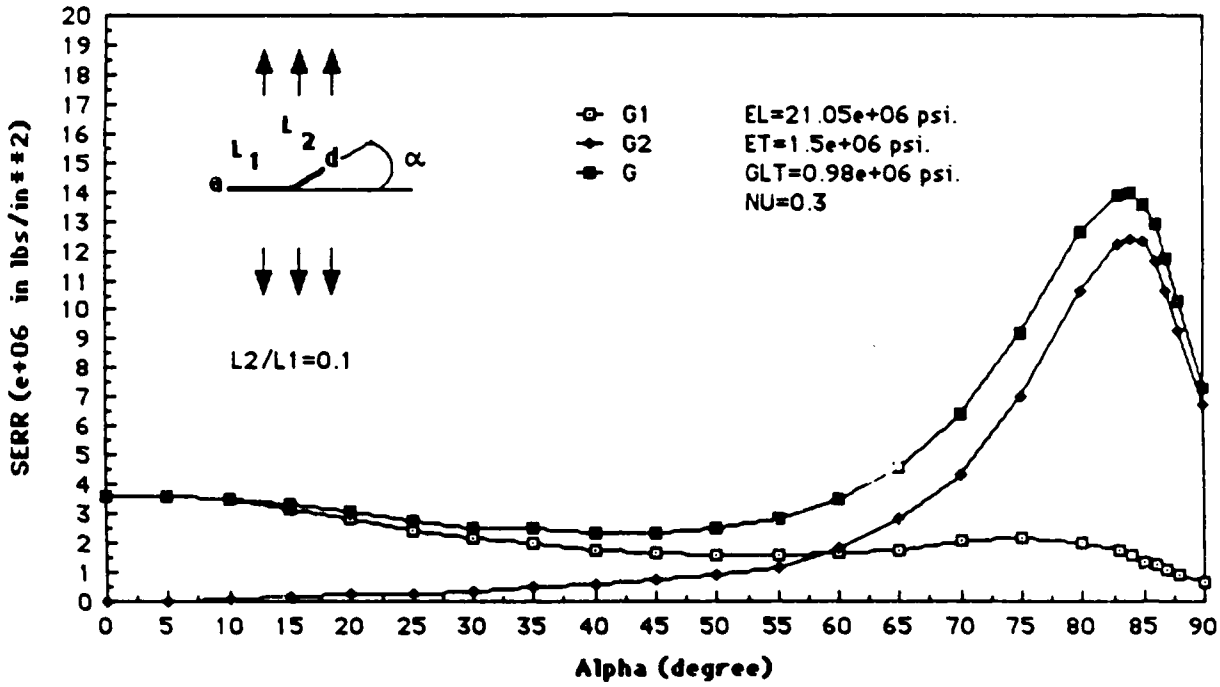

Fig. 2.12 Strain energy release rates (under e_x = 1) at the kink tip as a function of kink angle, α. Isotropic case with L_2/L_1 = 0.1.

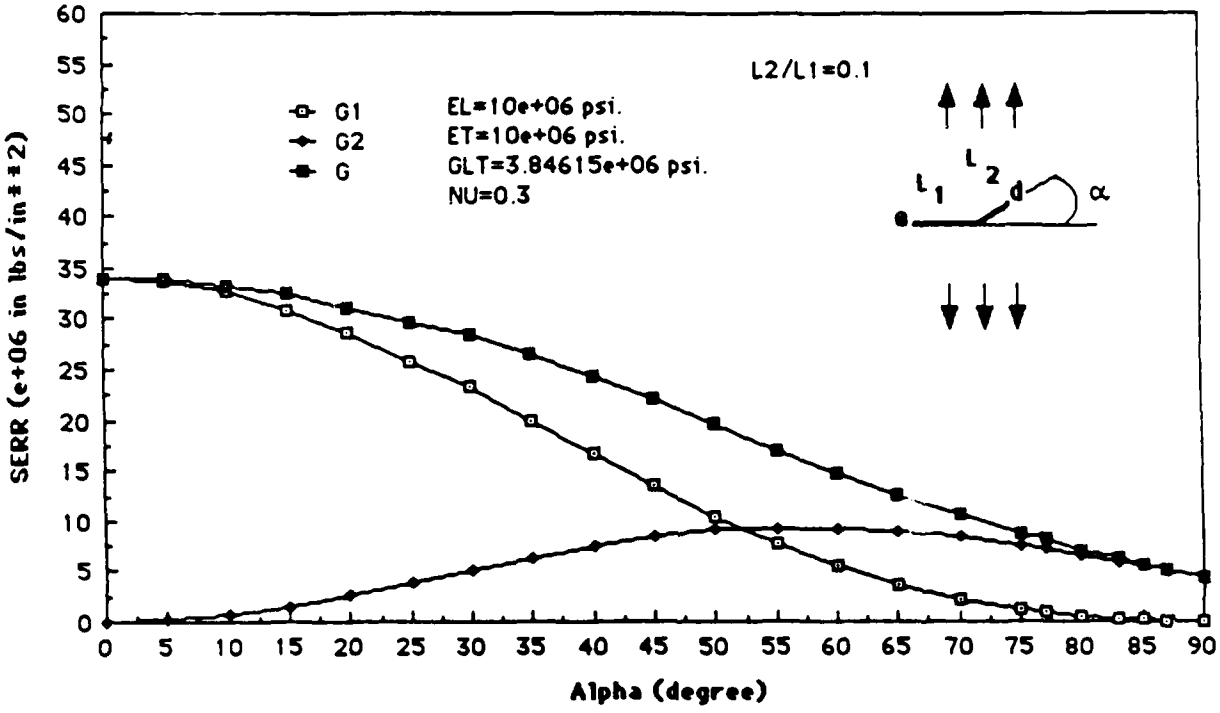

Fig. 2.13 Strain energy release rates (under e_x = 1) at the kink tip as a function of kink angle, α. Orthotropic case with L_2/L_1 = 0.1.

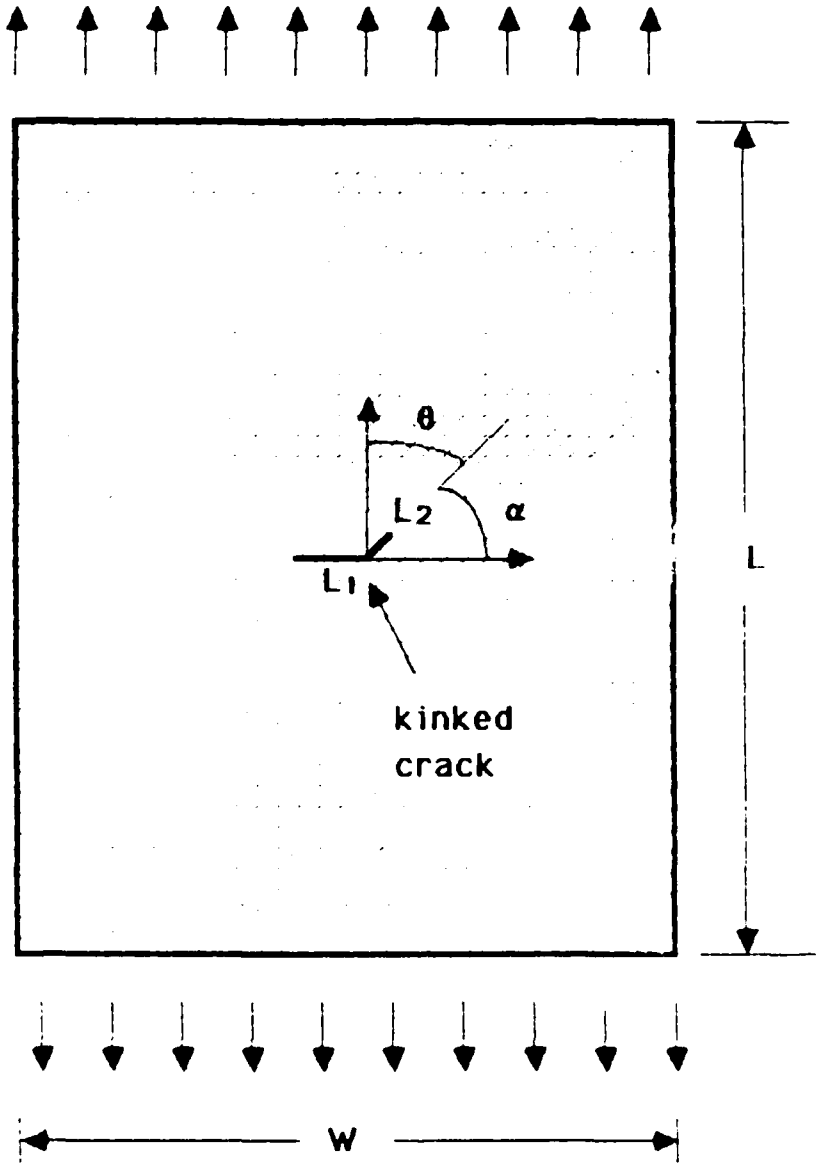

Fig. 2.14 Finite element model for a kinked crack in an infinite plate.

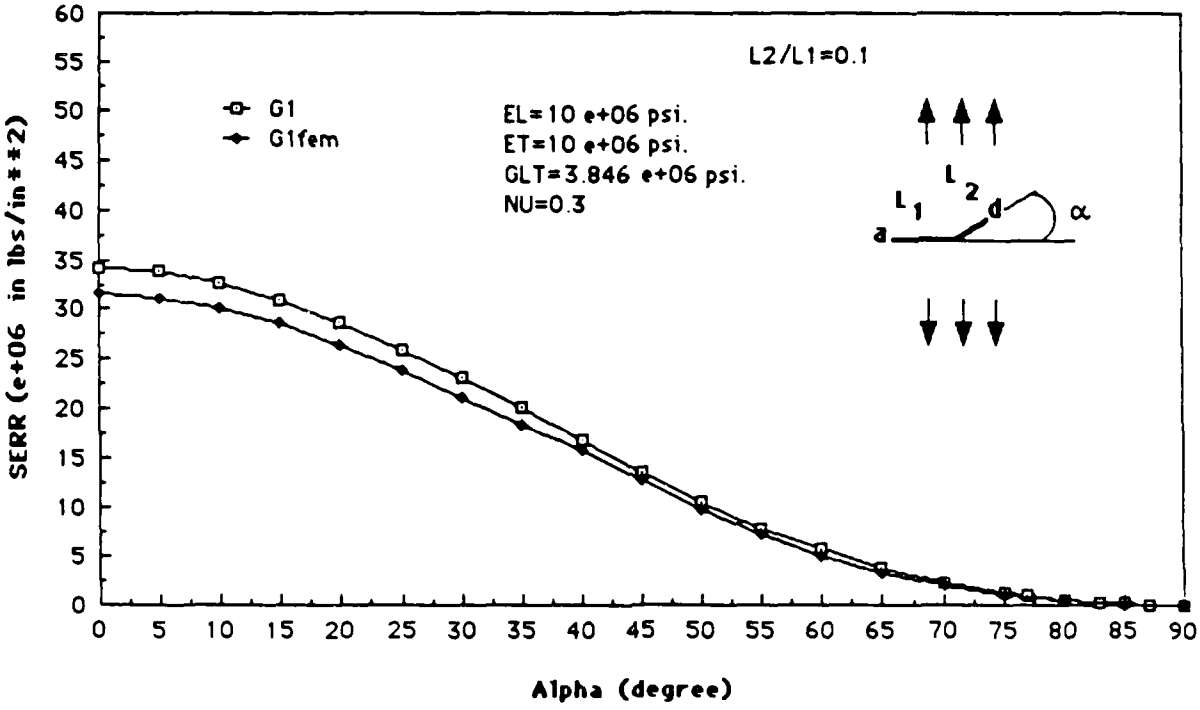

Fig. 2.15 Mode-I strain energy release rate (under e_x=1) at the kink tip as a function of kink angle, α, by elasticity and finite element methods. Isotropic case with L_2/L_1 = 0.1.

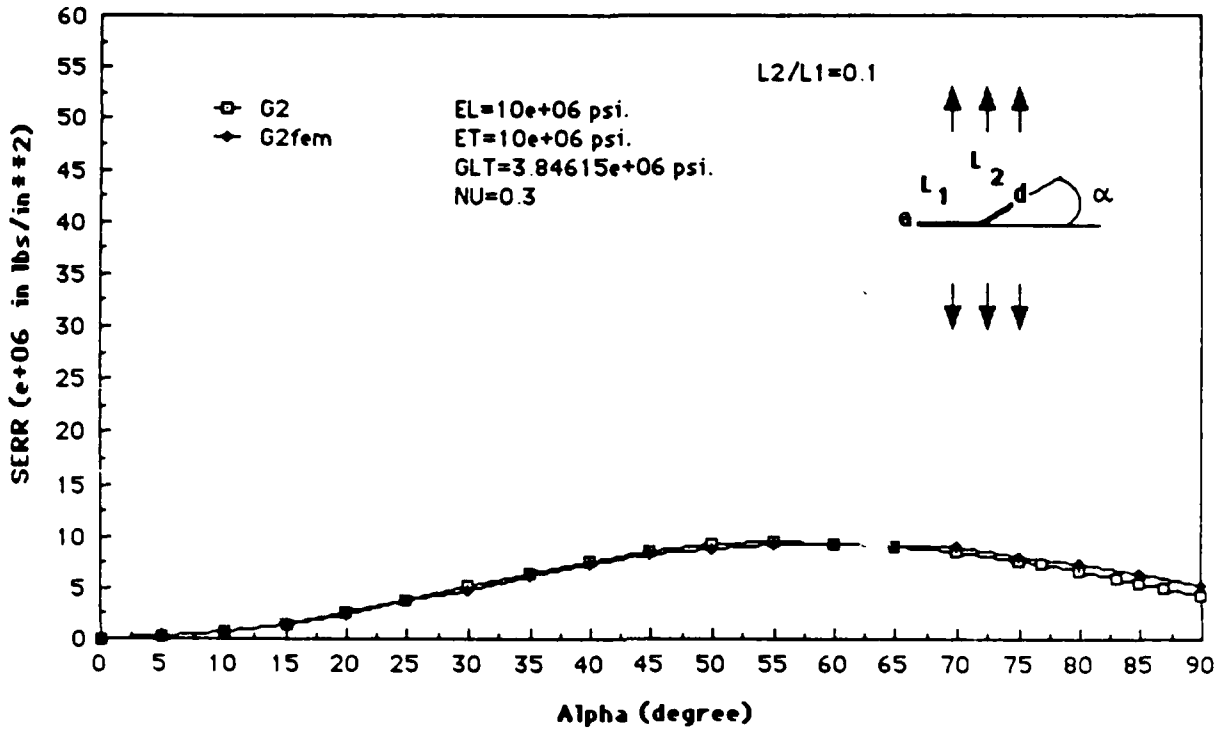

Fig. 2.16 Mode-II strain energy release rate (under e_x=1) at the kink tip as a function of kink angle, α, by elasticity and finite element methods. Isotropic case with L_2/L_1 = 0.1.

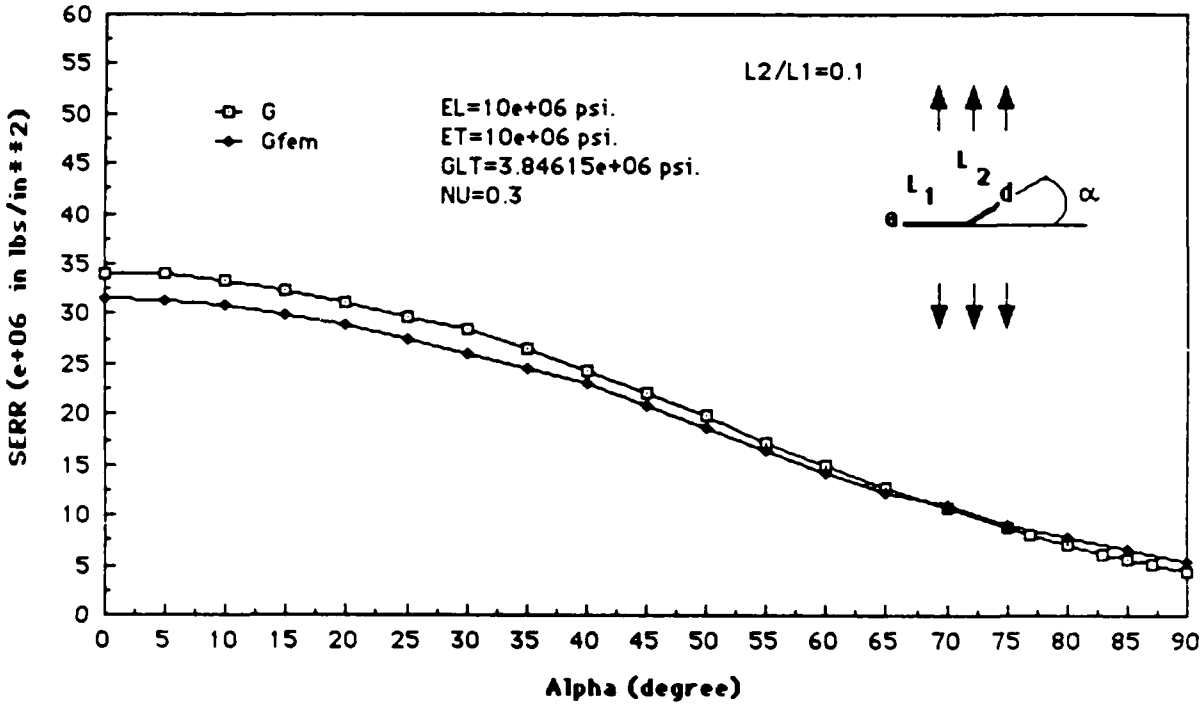

Fig. 2.17 Total strain energy release rate (under ϵ_x=1) at the kink tip as a function of kink angle, α, by elasticity and finite element methods. Isotropic case with L_2/L_1 = 0.1.

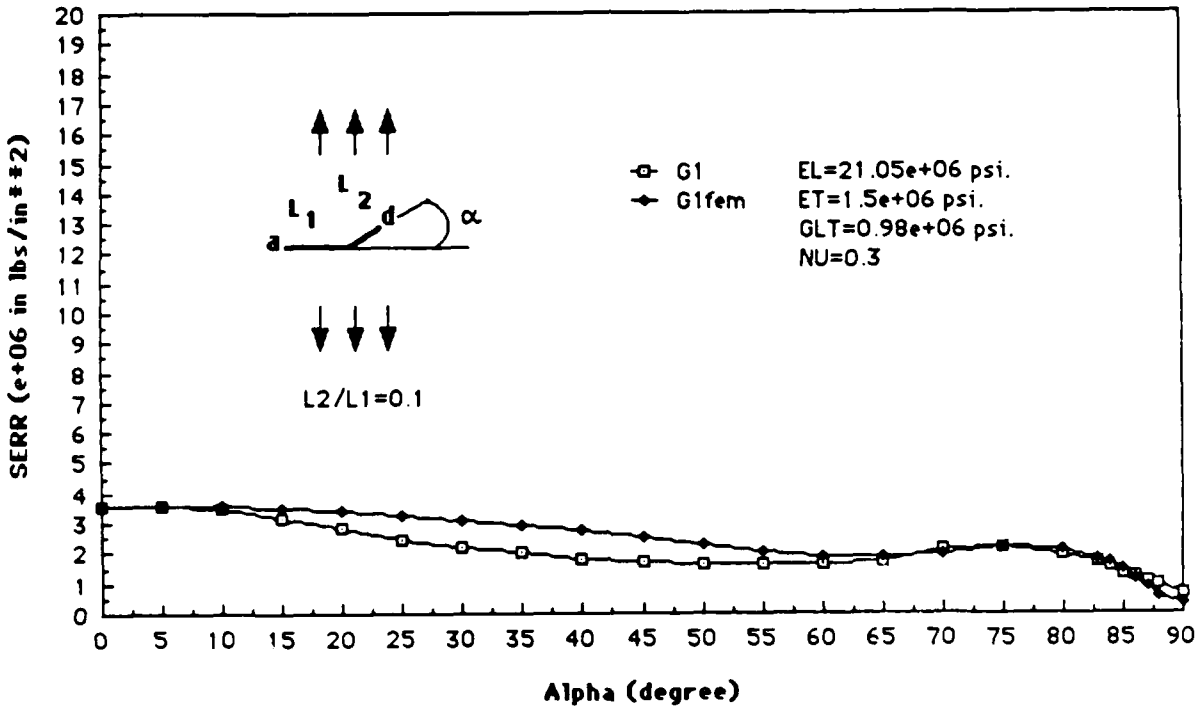

Fig. 2.18 Mode-I strain energy release rate (under e_x=1) at the kink tip as a function of kink angle, α, by elasticity and finite element methods. Orthotropic case with L_2/L_1 = 0.1.

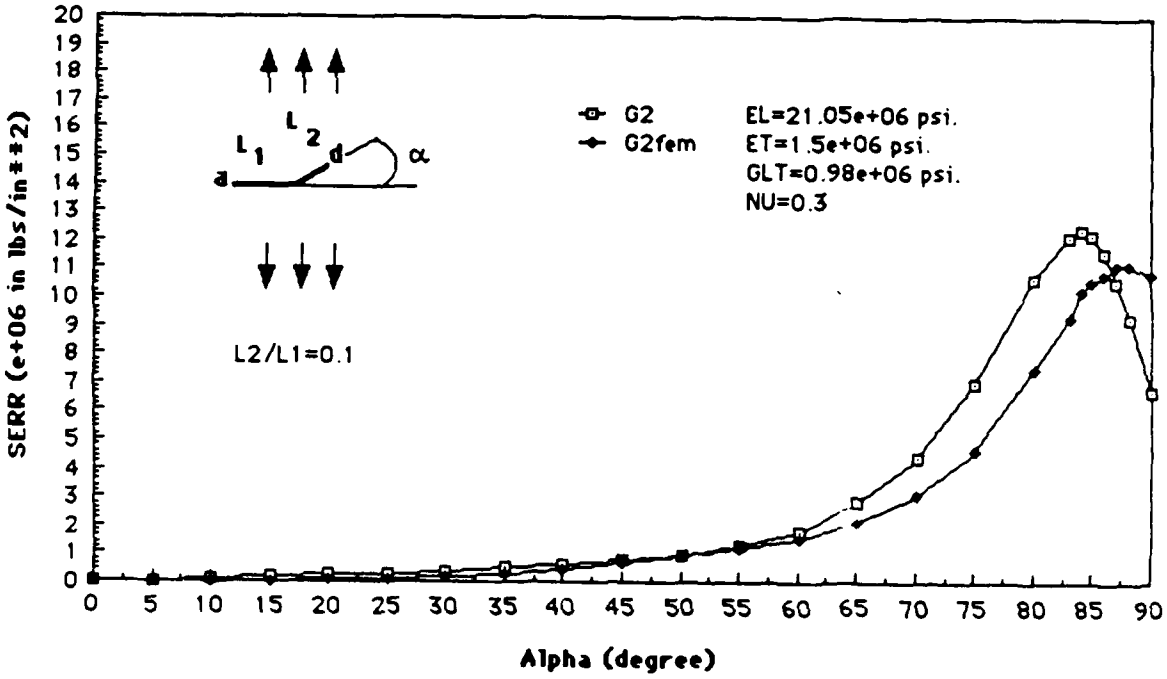

Fig. 2.19 Mode-II strain energy release rate (under e_x=1) at the kink tip as a function of kink angle, α, by elasticity and finite element methods. Orthotropic case with L_2/L_1 = 0.1.

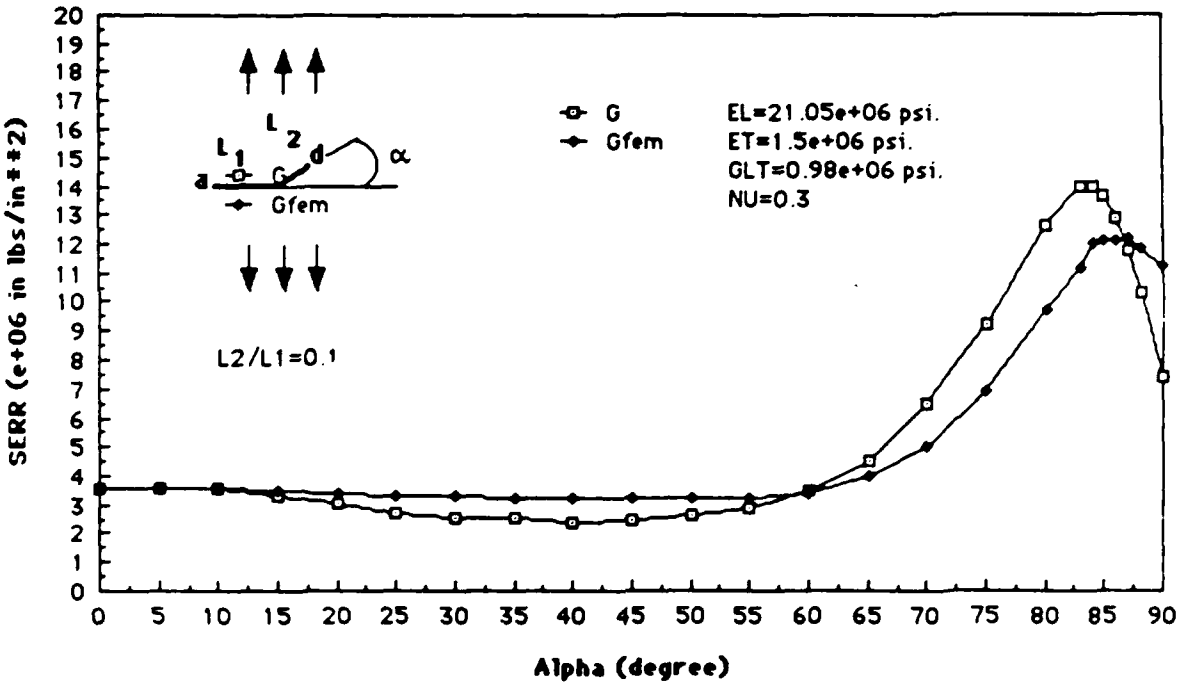

Fig. 2.20 Total strain energy release rate (under $e_x = 1$) at the kink tip as a function of kink angle, α, by elasticity and finite element methods. Orthotropic case with $L_2/L_1 = 0.1$.

III. EXPERIMENT AND RESULTS

Material and Specimens.

Hercules AS4-3501-06 graphite-epoxy unidirectional tape was used to fabricate 8-ply unidirectioal (UD) laminates. Off-axis tensile coupons 9" long and 1" wide were machined from these laminates. End-tabs 1.5" long were bonded to specimens yielding a 6-inch test section.

Two sets of coupons were prepared for test: Unnotched and double-side notched. The set of unnotched coupons were strain-gaged and tension tested to provide the basic unidirectional ply elastic constants. Coupons with the following off-axis angles were tested:

$$\theta = 0^0, 5^0, 10^0, 15^0, 20^0, 25^0 \text{ and } 90^0.$$

In addition, a set of $[\pm 45_2]s$ laminate coupons was also tested to determine the shear modulus G_{LT} of the unidirectional ply.

The set of double side-notched coupons were tested for mixed-mode fracture. Fig. 3.1 depicts the geometry of the double side-notched specimens. Initially, the side-notches were cut with a 8-mil diamond saw to depth, a, as shown. Under the applied tensile stress σ_0, a kink crack, denoted by a', is expected to initiate from the side-notch tip and propagate in the fiber direction. The propagation of the kink crack then provides the desired mixed-mode fracture condition.

Since the mixed-mode fracture behavior at the notch tip is influenced by the off-axis angle θ as well as the depth of the initial side-notch, these parameters were varied during the experiment as follows:

$$\theta = 0^0, 5^0, 10^0, 15^0, 20^0, 25^0 \text{ and } 90^0$$

$$a = 0.1", 0.125", 0.15" \text{ and } 0.175".$$

Thus, a total of 28 mixed-mode fracture conditions were created during this set of tests. Three to four specimen replicates were tested for each

fracture condition, with the exception of one side-notch case (a=0.15) where only one specimen was available for some of the off-axis angles,

Test Method and Test Data.

All specimens were tested under room temperture condition in a close-loop Instron tester with a load-control rate of 4000 lbs/min. Tests of 0^0, 90^0 and $[\pm 45_2]_s$ unnotched coupons were used to determine the following averaged ply properties:

$$E_L = 21.0 \text{ msi} \quad E_T = 1.5 \text{ msi} \quad G_{LT} = 0.98 \text{ msi} \quad \nu_{LT} = 0.3$$

The axial moduli E_x of the unnotched off-axis coupons were also measured. Their averaged values are listed below:

θ	0^0	5^0	10^0	15^0	20^0	25^0	90^0
E_x (msi)	21.0	18.4	13.5	9.4	6.7	5.0	1.5

The critical load at the onset of the kink crack was recorded for side-notched coupons. Post-test SEM examination of the fractured surface near the kink point was conducted to determine the fractured surface morphology under 500x to 1000x magnification.

Fig. 3.2 shows the experimental plot of critical stress versus the off-axis angle θ at the onset of the kink crack in those specimens having side-notches 0.1" deep. In this plot, the average critical axial strains were calculated using

$$(e_x)_{cr} = (\sigma_x)_{cr}/E_{xn} \qquad (1)$$

where E_{xn} is the axial modulus of the notched coupon. E_{xn} was not measured during the experiment. Value used in (1) was calculated by the finite element routine. Table 3.1 lists the values of E_{xn} for all the mixed-mode fracture test cases conducted in this study.

Figs. 3.3 and 3.4 show the critical onset stresses for specimens having

notch depth a = 0.125" and 0.175", respectively. The case for a = 0.15" is not shown because of insufficient numbers of test specimens.

It is seen from Figs. 3.2 to 3.4 that the onset stress, $(\sigma_x)_{cr}$, for kink crack initiation and propagation decreases sharply with the off-axis angle θ, but only slightly with notch depth. On the other hand, the onset strain, $(e_x)_{cr}$, appears to be insensitive to the off-axis angle but sensitive to notch depth.

Post-test SEM examination of the fractured surfaces revealed extensive fiber breaking near the kink. Fig. 3.5 presents a typical SEM for each off-axis specimen tested ($\theta = 0^0$, 5^0, 10^0, 15^0, 20^0, 25^0 and 90^0). Fiber breaks are visible in all cases. This phenomenon is caused by fiber nesting near the notch region and fiber bridging accross the cracking path, an indication of strong adhesion between the matrix and fibers.

Finite Element Simulation.

Using the finite element routine discussed in Section 2, the initiation and propagation of the experimental mixed-mode kinked crack conditions can be simulated. Referring to the off-axis unidirectionally reinforced composite coupon shown in Fig. 3.1, let the coupon be loaded by the far-field strain $e_x = 1$. The resulting stress field will be highly concentrated near each of the side-notches. Assume that the notch tip stresses will cause a kink crack to start from the notch tip and that the kink will propagate stably in the direction of the fibers. Of interest is when the length of the kink a' is small. The mixed-mode strain energy release rates G_I and G_{II} at the kink tip are assumed to control the behavior of the small kink propagation. The values of G_I and G_{II} are calculated by the finite element routine via a crack-closure technique [13]. These are conveniently expressed in terms of the applied far-field strain in the form:

$$G_I = C_I(e_x)^2 \qquad G_{II} = C_{II}(e_x)^2 \tag{2}$$

where C_I and C_{II} are numerical coefficients from the calculation.

The values of and the ratio for G_I and G_{II} (or C_I and C_{II}) can vary dramatically depending on the off-axis angle and the side-notch depth. Fig. 3.6 shows two families of plots for the coefficients C_I and C_{II} with the side-notch depth, a, as a parameter and the off-axis angle, θ, as a dependent variable. Note that the kink is highly mixed in fracture modes for off-axis angles up to 20^0. Beyond 25^0, the fracture of the kink is dominanted by mode-I. The mixed mode ratio, defined here as G_{II}/G_I and shown in Fig. 3.7, is found to depend principally on the off-axis angle θ. It is almost independent on the initial side-notch depth a.

Critical Strain Energy Release Rates at Onset of Kink.

The critical stress $(\sigma_x)_{cr}$ at the onset of the kink was measured experimentally. The corresponding critical strain $(e_x)_{cr}$ can be calculated by mean of equation (1). These results were shown earlier in Figs. 3.2, 3.3 and 3.4 for the cases of a = 0.1", 0.125" and 0.175", respectively. Thus, by using equation (2) and the values of C_I and C_{II} shown in Fig. 3.6 we can calculate the critical strain energy release rates G_I, G_{II} and $G_T = G_I + G_{II}$ for each of these cases.

Fig. 3.8 shows the calculated critical strain energy release rates G_{IC} and G_{TC} for a = 0.1" as a function of the off-axis angle θ. If we disregard the experimental scatter which is relatively small, the plot shows the total strain energy release rate, G_{TC}, to be constant for all angles, dispite variations in the mixed-mode fracture condition. The averaged G_{TC} in this case is about 1.8 in-lb/in^2.

Fig. 3.9 shows the calculated strain energy release rates for the case of

a = 0.125". Again, the behavior of G_{Tc} is the same. Here, the averaged G_{Tc} is about 1.7 in-lb/in^2. The calculated G_{Tc} for the case of a = 0.175" is almost identical to that calculated for the a = 0.125 case, see Fig. 3.10.

Fig. 3.11 is a mixed-mode interaction diagram plotted from all the mixed-mode fracture test cases, including some from specimens of a=0.15". These data show some degree of scatter, but the interaction diagram strongly suggests that a criterion based on the total strain energy release rate G_{Tc} would be acceptable. This conclusion is based on the mixed-mode fracture data which consisted of nearly uniformly distributed data points in the G_{II}/G_I ratio range from 0 to 2.5. This range had not been achieved in any of the referenced previous works.

Most available data for graphite-epoxy composite critical strain energy release rates are limitted to G_{Ic}. Genrally, the measured values for G_{Ic} lie in the range between 0.7 to 1.5 in-lb/in^2, depending on the material system used. In this study, G_{Ic} was found to be of the order of 1.75 in-lb/in^2. This seems high compared to most other accepted values. Recall that in all our mixed-mode fracture test cases, fiber breakage or fiber bridging occurred in the wake of cracking, which could account for the higher measured values for G_{Ic} and G_{Tc}.

TABLE 3.1

Effective Axial Modulus, E_x, (in msi) for Test Specimens

Off-axis angle	Notch depth, inch			
θ	0.100	0.125	0.150	0.175
0^0	20.6	20.4	20.1	19.8
5^0	18.1	17.8	17.7	17.4
10^0	13.3	13.2	13.0	12.9
15^0	9.3	9.2	9.1	9.1
20^0	6.7	6.6	6.6	6.5
25^0	5.0	5.0	4.9	4.9
90^0	1.5	1.5	1.5	1.5

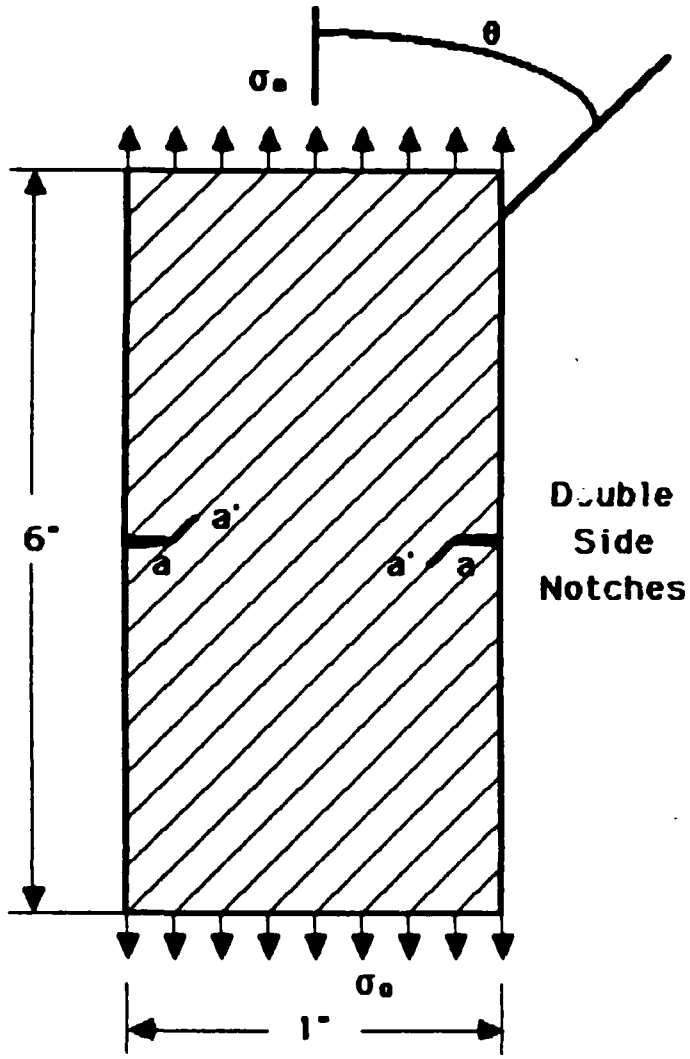

Fig. 3.1 Net section of the tested specimen geometry

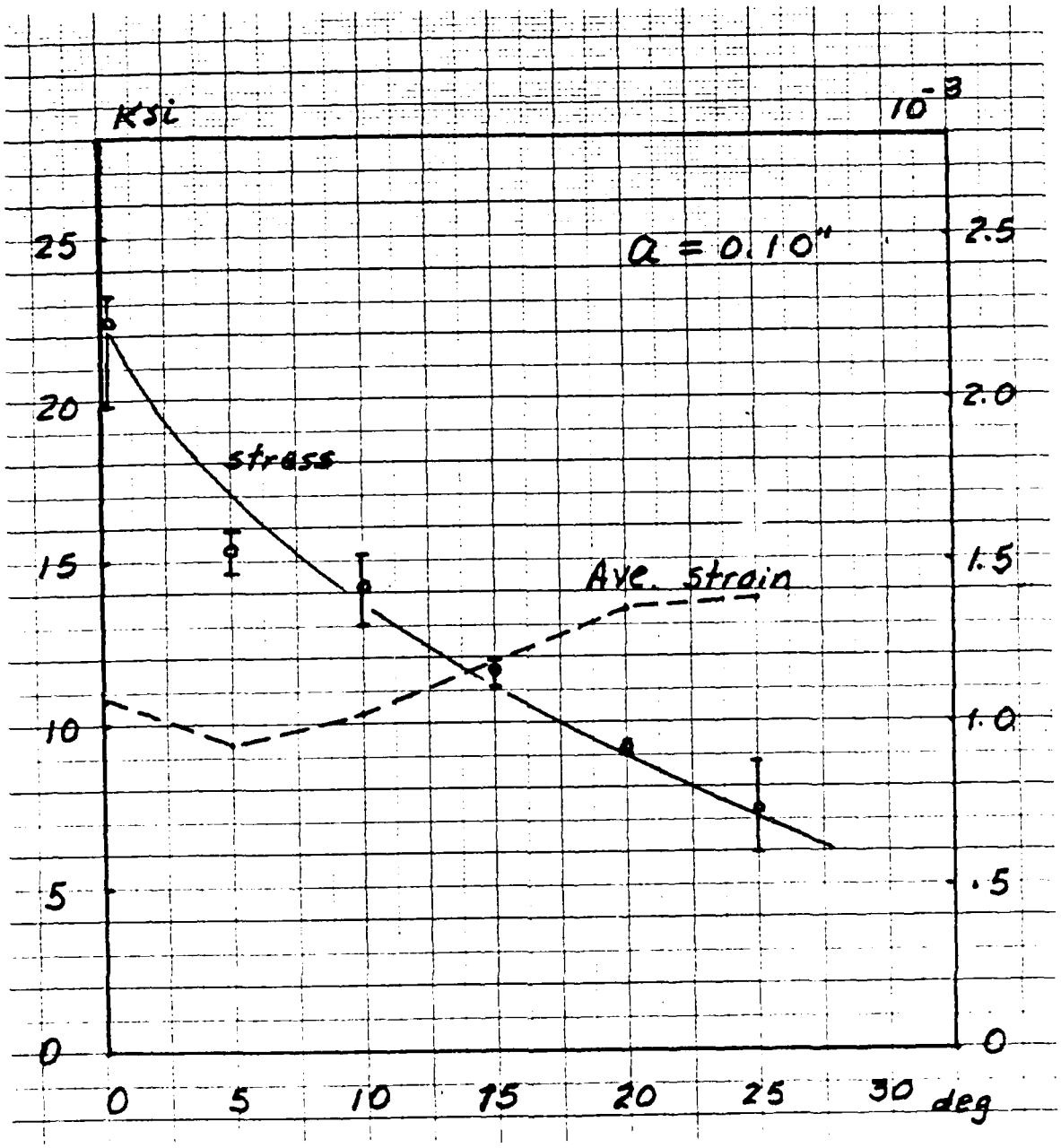

Fig. 3.2 Critical stress and strain at onset of kinked crack. a = 0.1"

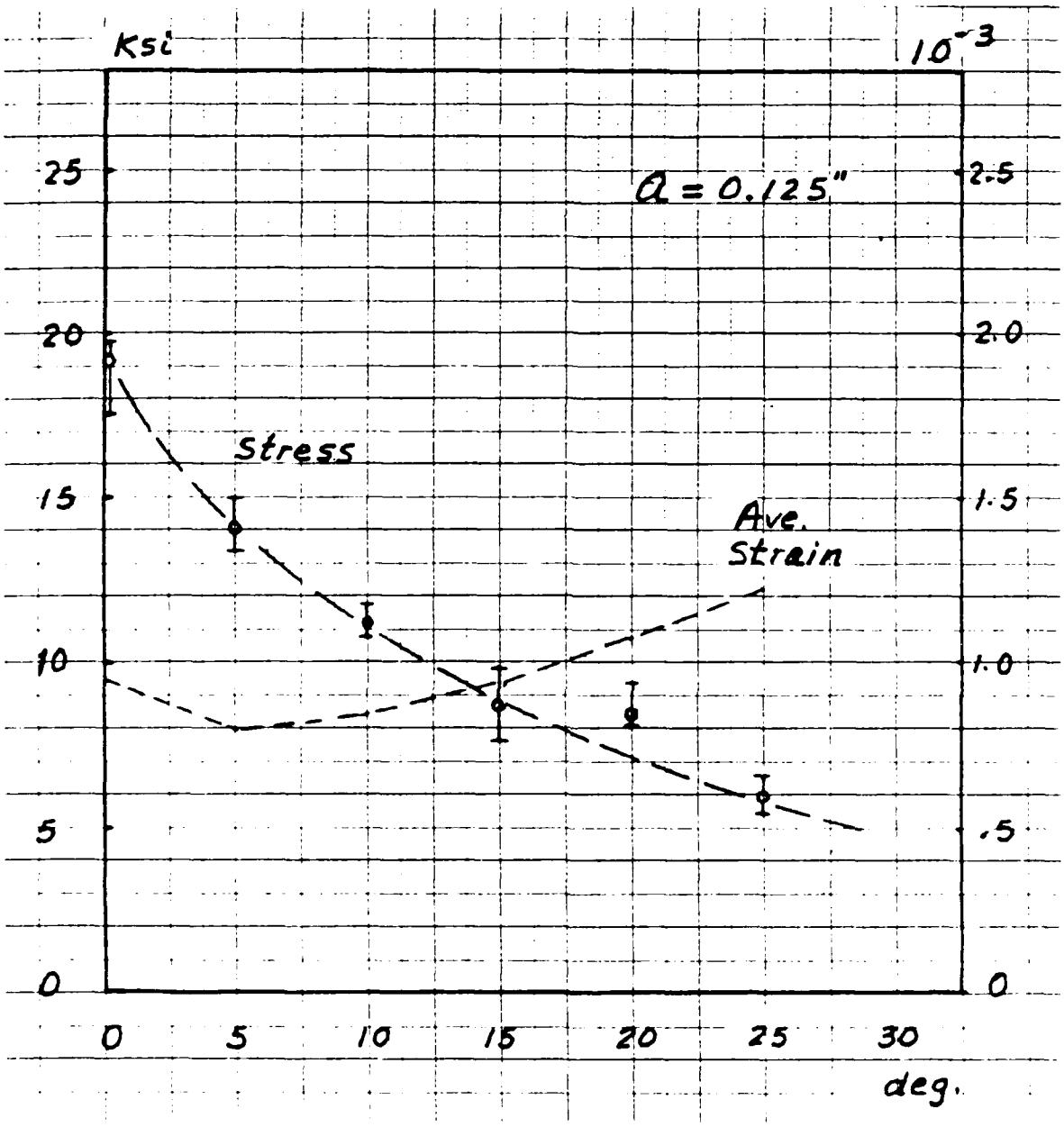

Fig. 3.3 Critical stress and strain at onset of kinked crack, a = 0.125"

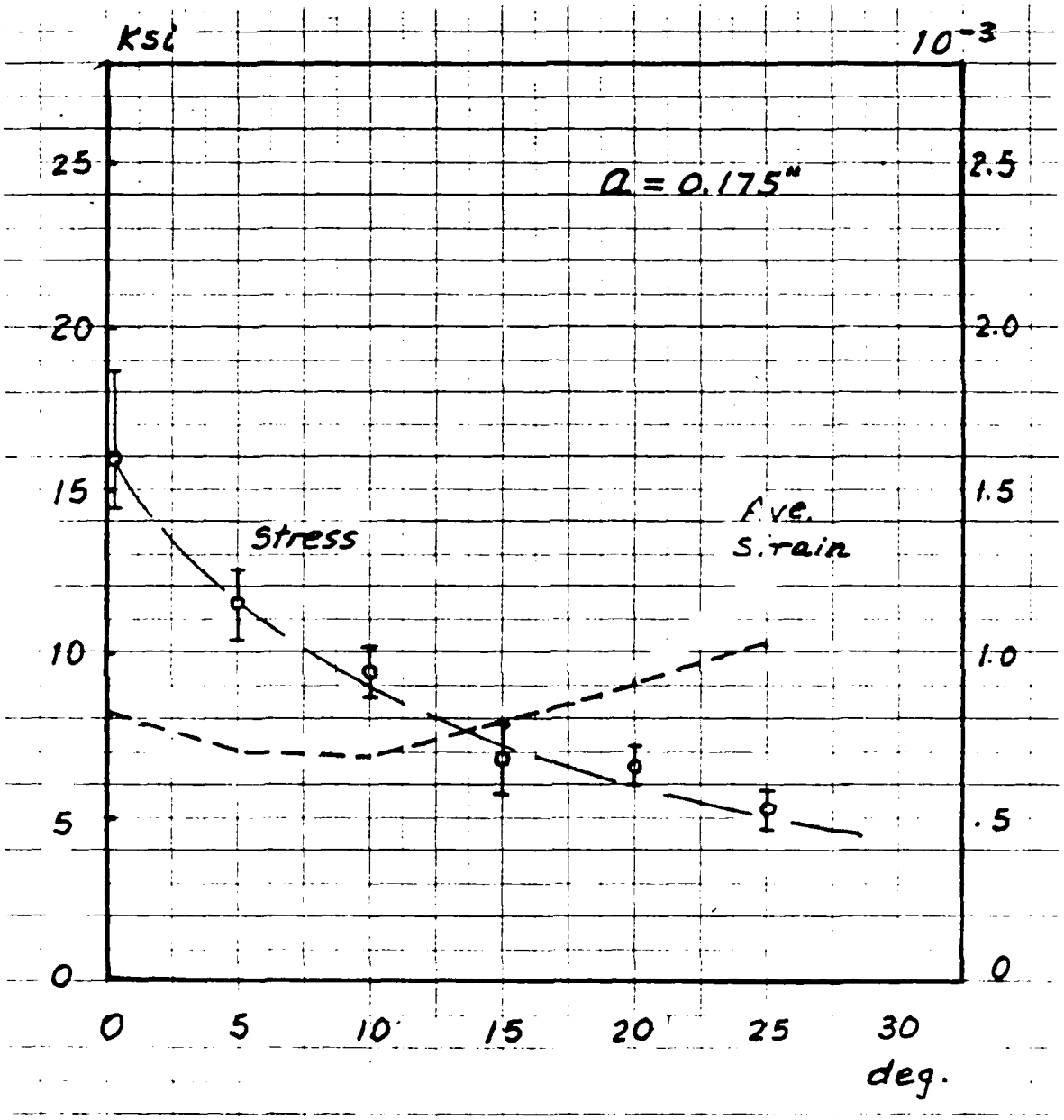

Fig. 3.4 Critical stress and strain at onset of kinked crack. a = 0.175"

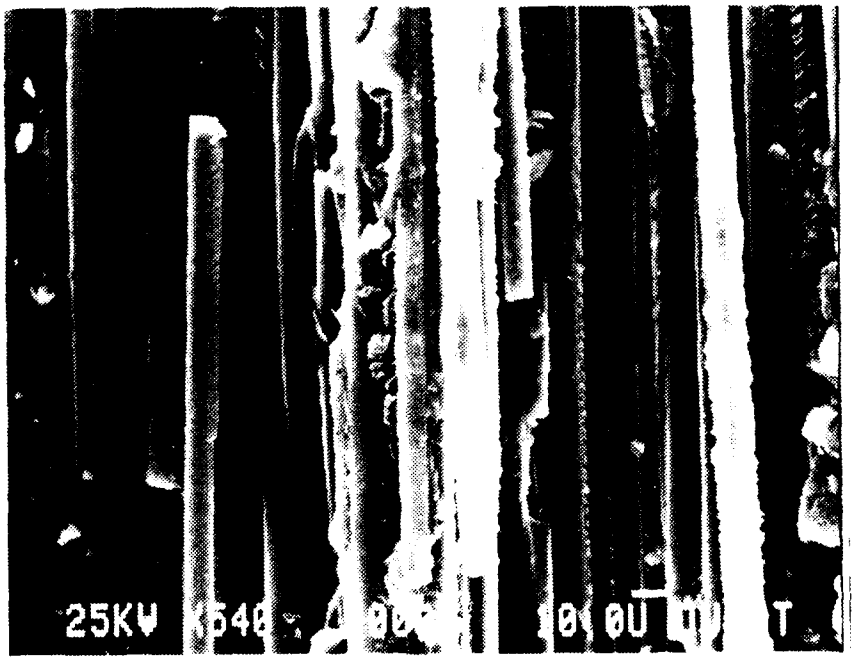

Fig. 3.5 Photomicrograph of fractured surface near kink point. A specimen of $\theta=0^0$, a = 0.15" (above); and a specimen of $\theta = 5^0$, a = 0.1" (below).

Fig 3.5 (continued) Photomicrograph of fractured surface near kink point

A specimen of $\theta = 10^0$, a = 0.125" (above), and a specimen of

$\theta = 15^0$, a = 0.125".

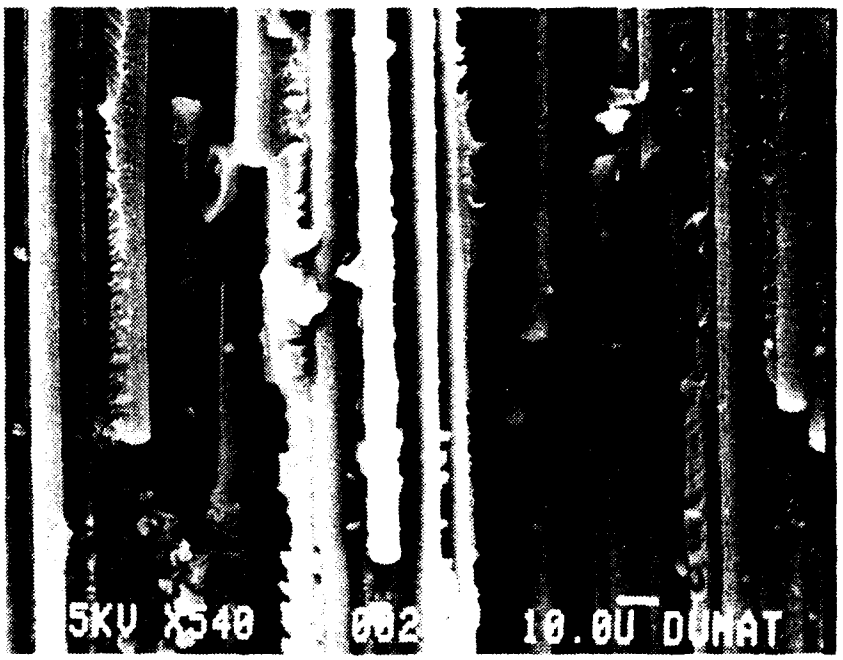

Fig 35 (continued) Photomicrograph of fractured surface near kink point A specimen of $\theta = 20^0$, a = 0.1" (above), and a specimen of $\theta = 25^0$, a = 0.175" (below)

Fig. 3.5 (continued) Photomicrograph of fractured surface near kink point

A specimen of $\theta = 90^0$, $a = 0.1''$

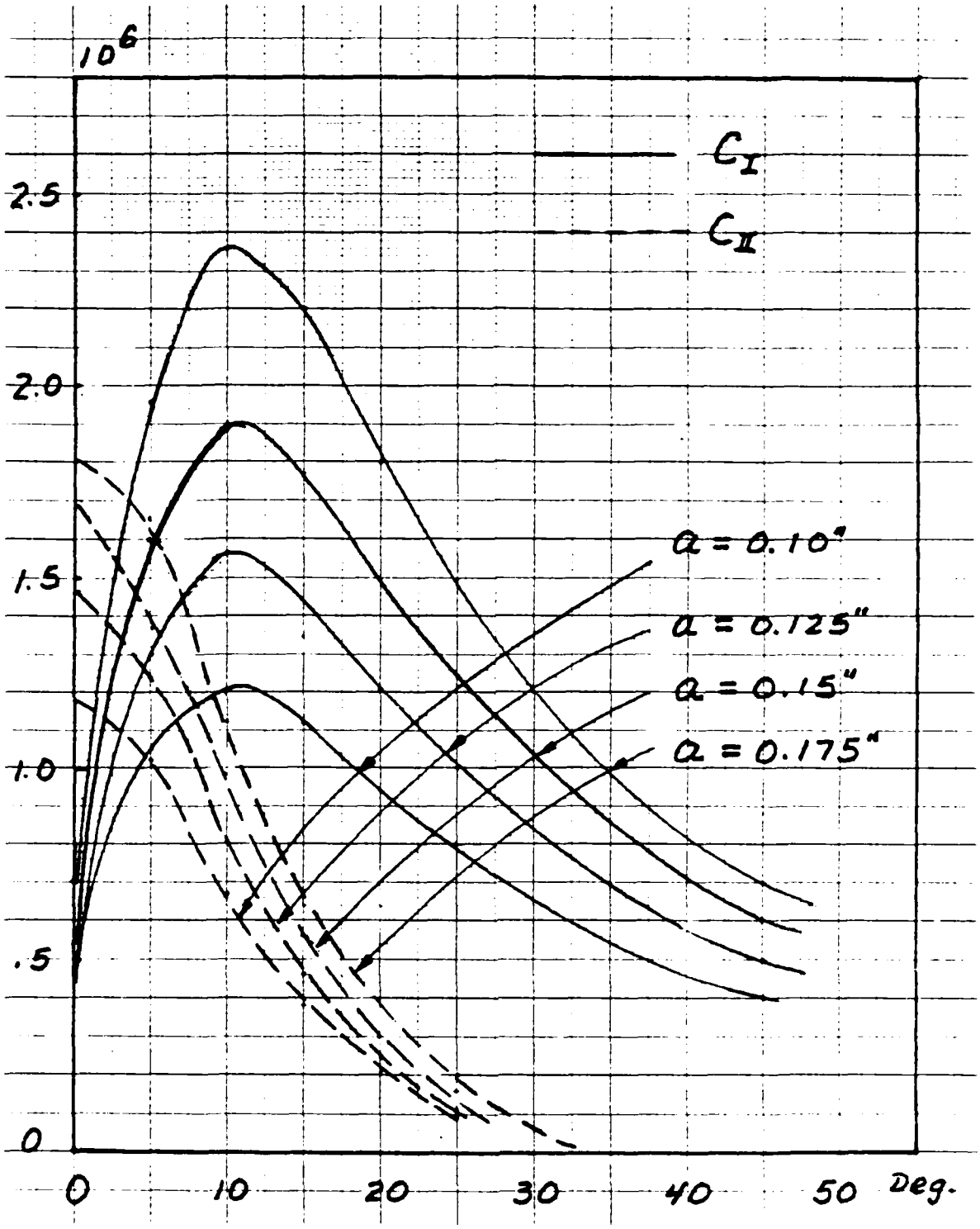

Fig. 3.6 Mode-I and Mode-II strain energy release rate coefficients as function of off-axis angle θ.

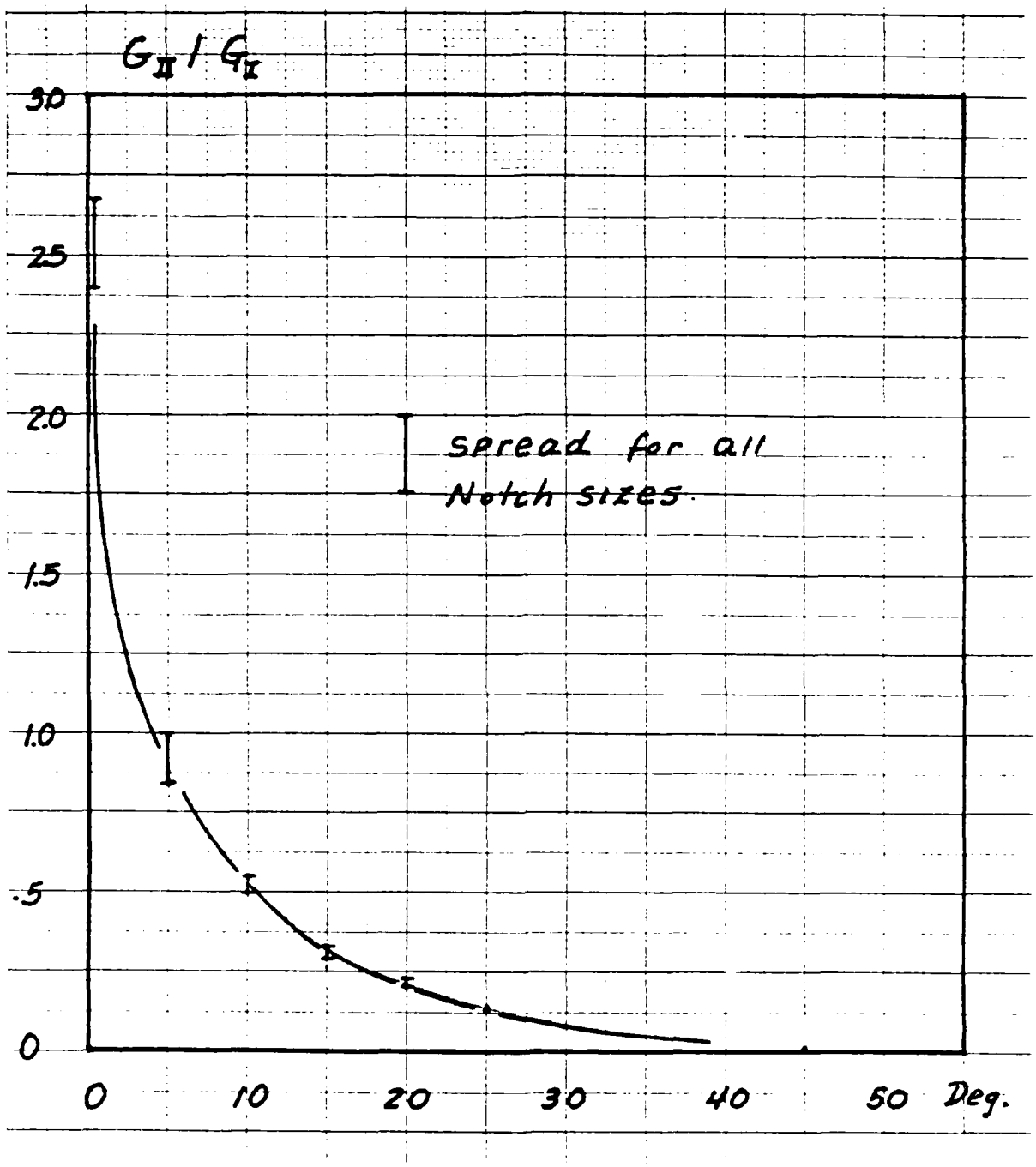

Fig. 3.7 Mode-II to Mode-I strain energy release rate ratio as function of off-axis angle θ.

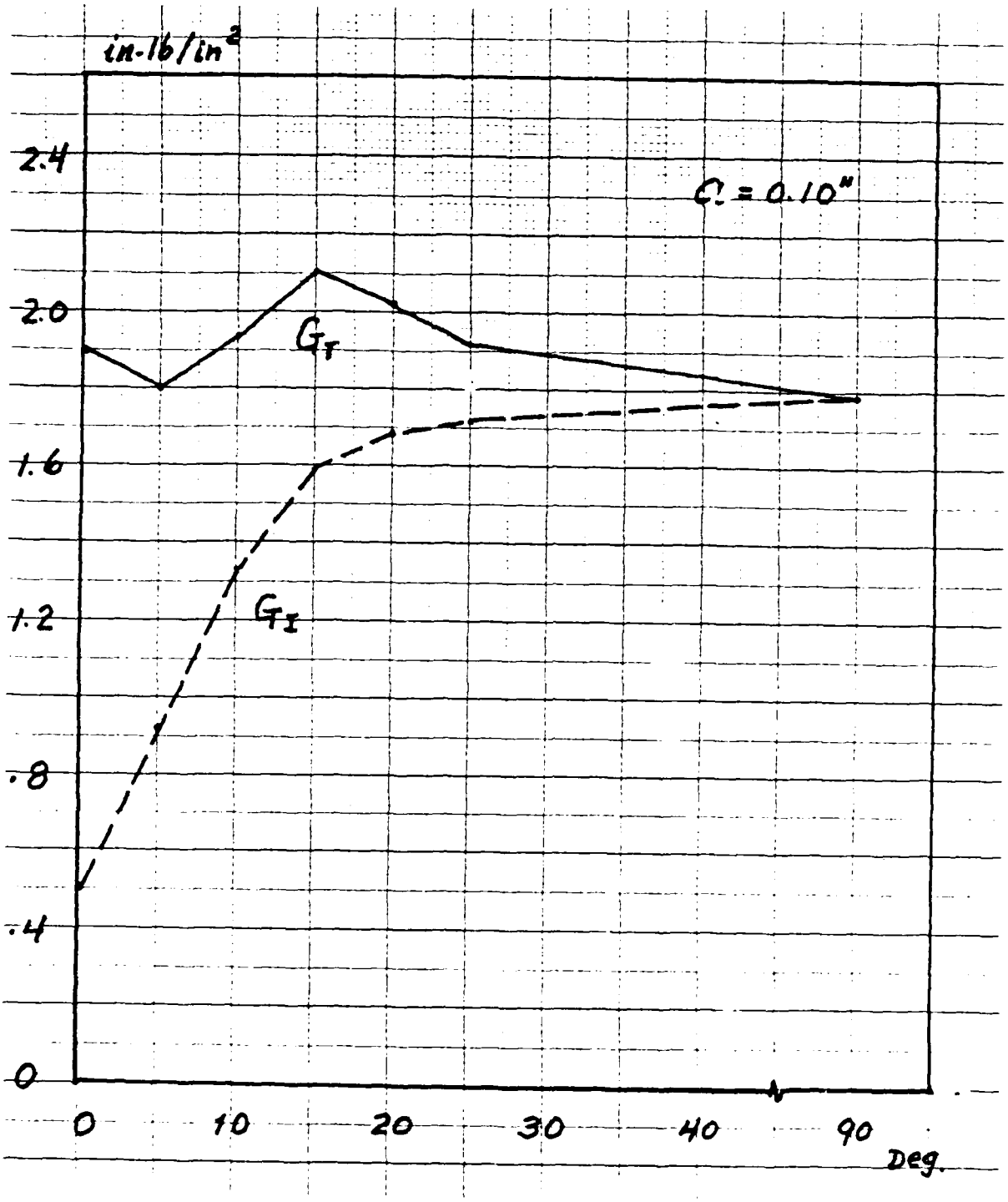

Fig. 3.8 Critical strain energy release Rates, G_{IC} and G_T, for a = 0.1"

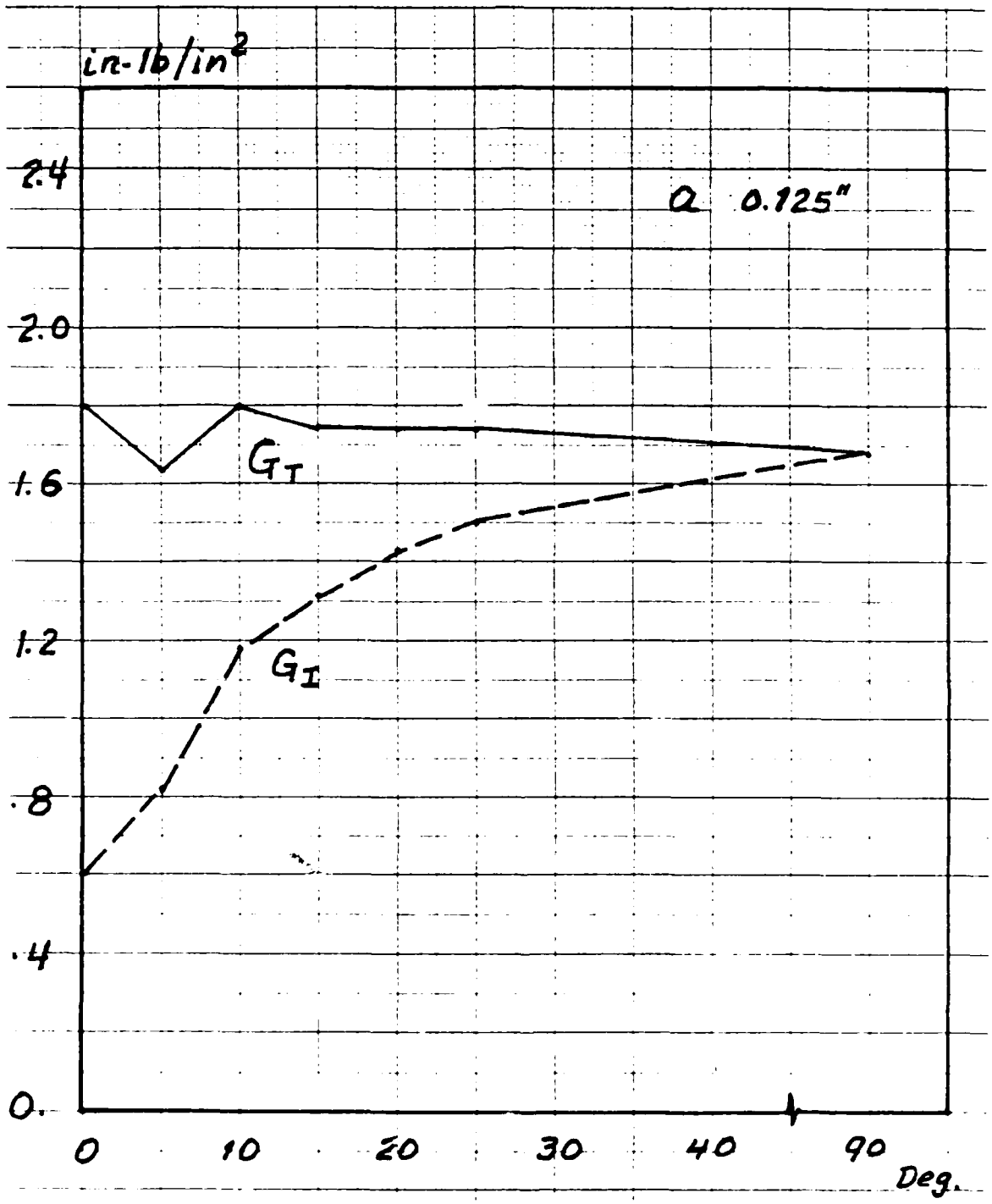

Fig. 3.9 Critical strain energy release Rates, G_{IC} and G_T, for a = 0.125"

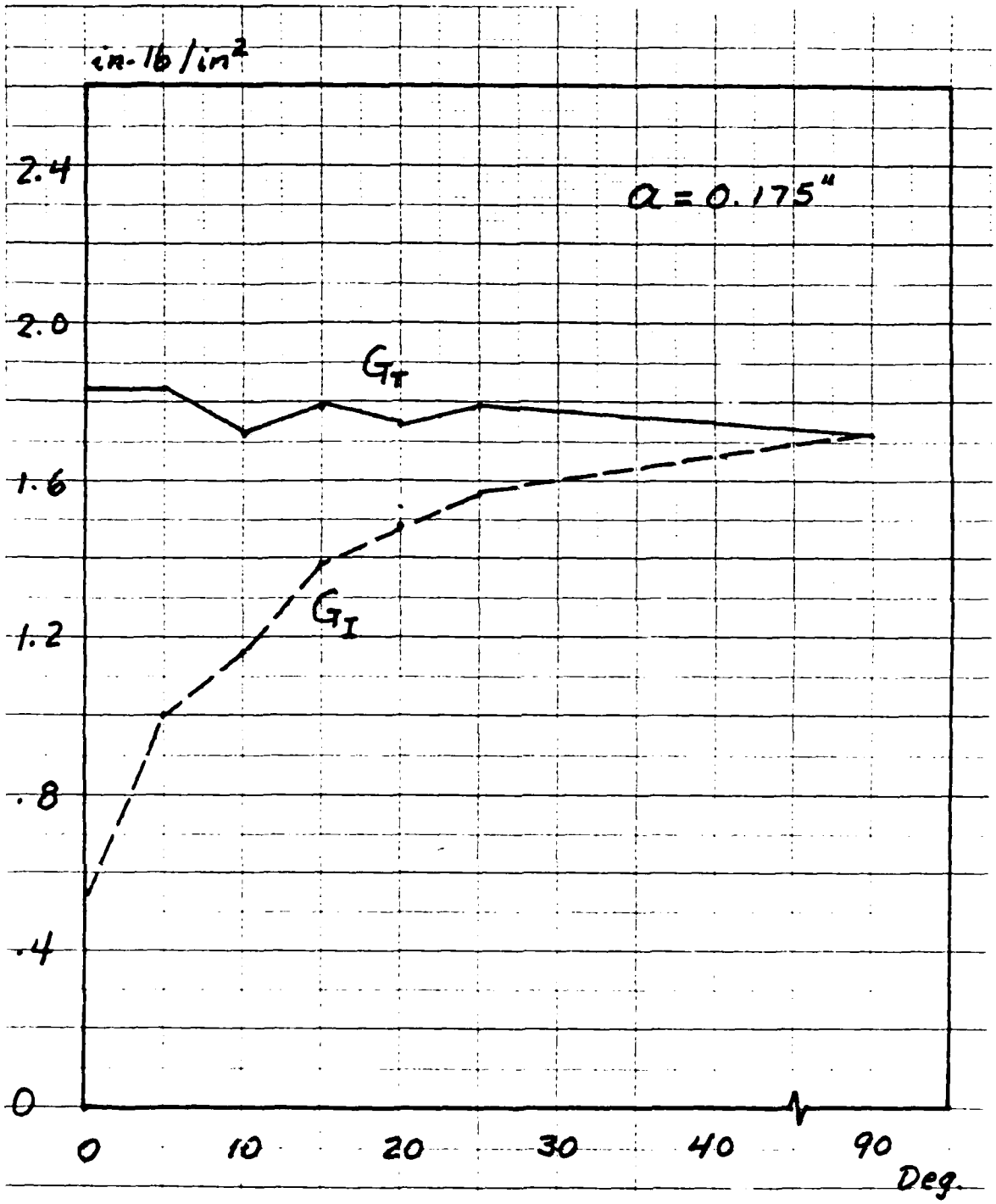

Fig. 3.10 Critical strain energy release Rates, G_{IC} and G_T, for a = 0.175"

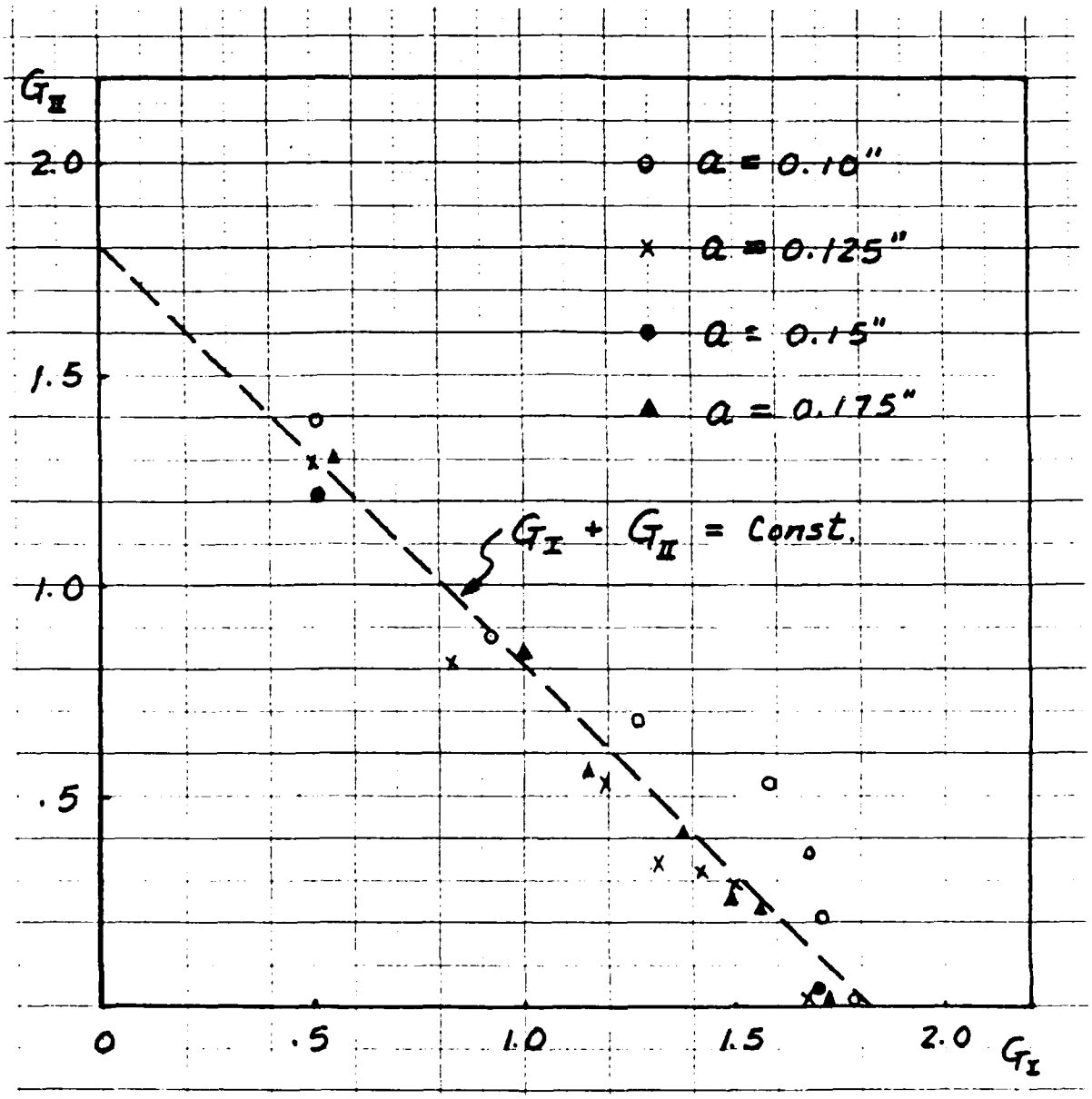

Fig. 3.11 Interaction diagram of mixed-mode strain energy release rate data from all test cases.

IV. CONCLUDING REMARKS

In this report, an effort was made to study the mixed-mode fracture behavior of a kinked matrix crack in graphite-epoxy composite materials. Previous efforts in determining fracture quantities, such as the stress intensity factors or the strain energy release rates, have been based on either crude analytical models (e.g. simple beam theory) or finite element simulations whose numerical accuracy could not be adjudicated.

In this study, the fracture quantities K and G were obtained both by solving the problem of an infinte orthotropic plate containing a kinked crack exactly and by a finite element routine. A comparison between the exact and the numerical solutions allows the finite element shape and mesh size to be optimized to obtain the best results for this class of problems.

Having done so, the finite element routine is then used to simulate a similar class of mixed-mode kink crack in notched finite plates, the specific problem being the off-axis unidirectional tensile coupon with double side-notches. The finite element analysis must be employed because the complex geometry of the test specimen would render an exact solution impossible.

In the experiment, we have designed a specimen which is simple to test and is versatile in geometrical variations. This provided some 28 mixed-mode fracture conditions covering a wider range of G_{II}/G_I ratios (from 0 to 2.5) than previously investigated. Thus, a more definitive conclusion can be reached regarding mixed-mode matrix crack propagation. Specifically, the test results suggest that the total strain energy release rate G_{TC} is a good criterion for mixed-mode matrix fracture in AS4-3501-06 graphite-epoxy composite.

REFERENCE

[1] A. S. D. Wang, N. N. Kishore and C. A. Li, "On Crack Development in Graphite-Epoxy $[0_2/90_n]_s$ Laminates Under Uniaxial Tension," Journal of Composite Science and Technology, Vol. 23, 1985. pp. 1-31.

[2] A. S. D. Wang, "Fracture Analysis of Matrix Cracking in Laminated Composites," NADC-TR-85118-60, 1985.

[3] D. J. Wilkins, J. R. Eisenmann, R. A. Camin, W. S. Margolis and R. A. Benson, "Characterizing Delamination Growth in Graphite Epoxy," in Damage in Composite Materials, ASTM STP-775, 1982. pp. 168-183.

[4] R. L. Ramkumar and J. D. Whitcomb, "Characterization of Mode-I and Mixed-Mode Delamination Growth in T300/5208 Graphite-epoxy," in Delamination and Debonding of Materials, ASTM STP-876, 1985. pp. 315-335.

[5] W. L. Bradley and R. N. Cohen, "Matrix Deformation and Fracture in Graphite Reinforced Epoxies," in Delamination and Debonding of Materials, ASTM STP-876, 1985. pp. 389-410.

[6] A. S. D. Wang, N. N. Kishore and W. W. Feng, "On Mixed-Mode Fracture in Off-Axis Unidirectional Graphite-Epoxy Composites," in Progress in Science and Engineering of Composites, Japan Society for Composite Materials, Vol. 1, 1982. pp. 599-606.

[7] A. J. Russell and K. N. Street, "Moisture and Temperature Effects on the Mixed-Mode Delamination Fracture of Unidirectional Graphite-Epoxy," in Delamination and Debonding of Materials, ASTM STP-876, 1985. pp. 349-370.

[8] R. Badaliance and G. D. Gupta, "Growth Characteristics of Two Interacting Cracks," Engineering Fracture Mechanics, Vol. 8, 1976. pp. 341-353.

[9] G. D. Gupta, "Strain Energy Release Rate For Mixed-Mode Crack Problems," ASME Paper #76-WA-PVP-7, 1977.

[10] S. N. Chatterjee, "The Stress Field in the Neighborhood of A Branched Crack in an Infinte Elastic Sheet," Int. Journal of Solids and Structures, Vol. 11, 1975. pp. 521-538.

[11] W. Binienda, A. S. D. Wang and F. Delale, "Fracture of a Kinked Crack in

Uniaxial Fiber Reinforced Composites," to be presented at the 1987 ASME WAM, Boston.

[12] W. Binienda, F. Delale and A. S. D. Wang, "Strain Energy Release Rates for Cracked Uniaxial Fiber Reinforced Composites," in press

[13] A. S. D. Wang, N. N. Kishore and C. A. Li, "A Three-dimensional Finite Element Analysis of Delamination Growth in Composite Laminates: Part 2 The Finite Element Code and User's Manual," NADC-TR-84018-60, 1984.

APPENDIX A

EXACT SOLUTION OF A KINKED CRACK IN AN ORTHOTROPIC PLATE

APPENDIX TABLE OF CONTENTS

EXACT SOLUTION OF A KINKED CRACK IN AN ORTHOTROPIC PLATE

	Introduction.	1
I	Formulation of the problem of the crack along x_1.	6
II	Formulation of the problem of the crack along x_2.	14
III	Generation of integral equations.	24
IV	Method of solution - set of Cauchy type integral equations.	42
V	Stress intensity factors.	43
VI	Skew crack configuration $x_b=x_c=0$.	
	Introduction.	46
	Singularity order for a kink crack problem.	49
VII	Stress intensity factors for a skew crack case.	64
VIII	Normalized stress intensity factors.	66
IX	Strain energy release rate for x_d.	66
	Appendix references	79

EXACT SOLUTION OF A KINKED CRACK IN AN ORTHOTROPIC PLATE.

Introduction.

This appendix is concerned with fracture analysis of a kinked crack in an infinite elastic orthotropic plate. It is assumed that the plate contains a through-thickness crack of initial length L_1, which makes an angle θ with one of the principal direction of orthotropy. When the plate is subjected to a far-field uniform tensile stress normal to the crack, the crack will kink and propagate self-similarly in the θ direction. The result is a kinked crack propagating in mixed modes, with the degree of modal mixture dependent on the angle θ and the ratio between the length of the kink, L_2, and the length of the main crack, L_1.

To determine the parameters relevant to mixed-mode fracture at the tips of the kinked crack, the problem is formulated in terms of singular integral equations with generalized Cauchy kernels. The resulting system of equations are then cast in a form suitable for numerical solution by a Gaussian quadrature and the collocation method. Analytical expressions for the stress intensity factors, k_1 and k_2, and the strain energy release rate, G_I and G_{II}, at the tip of the kinked crack are also obtained in terms of solution variables.

The problem is solved in the following manner. First, we consider an infinite plate that contains two separate cracks as shown in Figure 1. Here, two sets of reference frames are used to describe the two-crack geometry. Let the applied far-field stress σ_0 be in

the y_2-direction, the base crack of length L_1 be on the x_2-axis, while the kink crack of length L_2 be on x_1-axis. The kink angle θ refers to the angle between x_1 and x_2. The two cracks will become one kinked crack if their approaching tips meet at the common origin of the two reference frames. That is when x_b and x_c become zero in Figure 1.

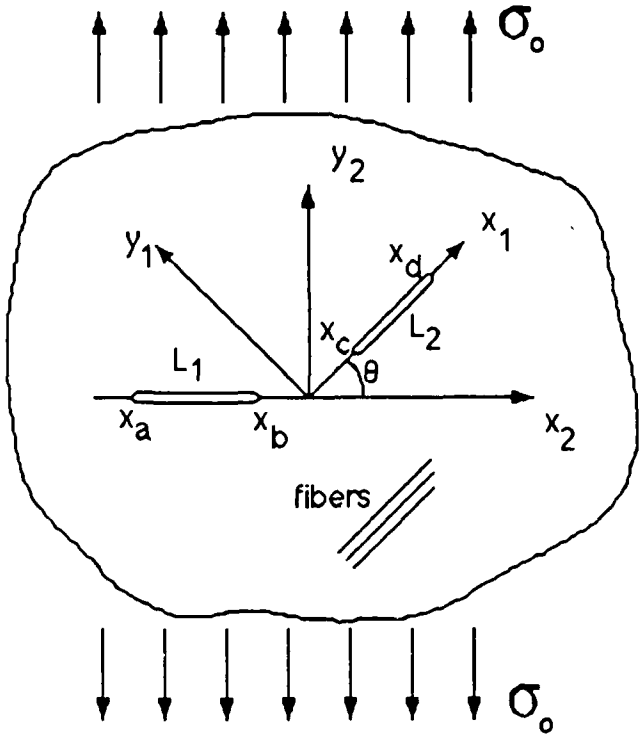

Figure 1. Two-Crack Configuration in an Infinite Plate Under Uniaxial Tension.

The two-crack problem can be represented by the superposition of three individual parts, shown in Figure 2. The first part is the plate without any crack under the external stress σ_0. The second part is the plate with only the base crack of length L_1 loaded by uniform normal stress acting on the crack surfaces. The crack surface normal stress is equal and opposite the stress that exists at the same location in the first part of the problem. The third part is the plate with only the inclined (kink) crack of

length L_2. Similarly, on the surfaces of the crack uniform n. ma and shear stresses are applied with their respective magnitude and sign equal and opposite to that existing at the same location in the first problem. The last two parts of the problem are known as the perturbation problems.

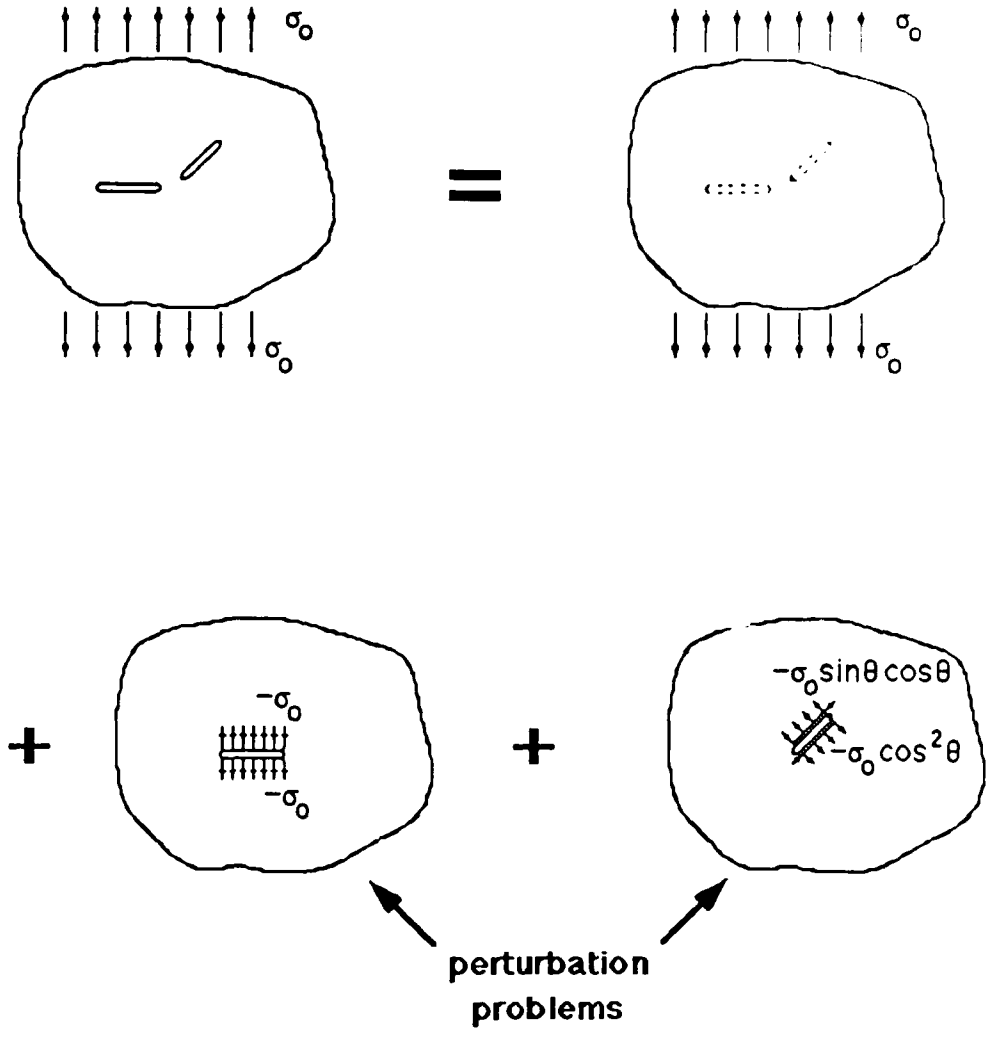

Figure 2. Method of Solution of the Crack Problem by Superposition of a Plate without the Cracks Under Uniaxial Tension and Perturbation Problems Under Negative Stress Imposed onto Crack Surface.

Since the solution to the first part of the problem is trivial, we are interested in solving the two perturbation problems.

Section I treats the perturbation problem in which the inclined (kink) crack lies along the principal axis (selected as the fiber direction) x_1. The problem of the base crack situated along x_2-axis is treated in Section II.

Superposition of the two-part solution for the two-crack problem is treated in Section III, where a set of singular integral equations are formulated. In Section IV, we descretize the singular integral equations suitable for solution by a numerical collocation method. Expression for the stress intensity factors that exist at the four tips of the two separate cracks are formulated in Section V.

The original problem of a kinked crack is treated in Section VI by employing the stress field solution of the two-crack problem obtained earlier. Here, we let the two approaching tips to meet at the common origin of the x_1-y_1 and x_2-y_2 frames. In the limit however, some of the kernels in the singular integral equations become singular themselves. Conditions compatible to the new situation are then formulated, and the resulting system of singular integral equations is obtained.

These equations can be discretized in a form suitable for solution by a similar collocation method. Expressions for the kink tip stress intensity factors are thus obtained. This is presented in Section VII. The definition of the normalized stress intensity factors is given in Section VIII.

Finally, expressions for the mixed-mode strain energy release rates are formulated in Section IX.

I. Formulation of the problem of the crack along x_1.

For the inclined crack, which is situated along the principal direction x_1, the stress field is governed by the biharmonic equation:

$$a_{22}\frac{\partial^4 F_1}{\partial x_1^4} + (2a_{22} + a_{66})\frac{\partial^4 F_1}{\partial x_1^2 \partial y_1^2} + a_{11}\frac{\partial^4 F_1}{\partial y_1^4} = 0 \tag{1.1}$$

or

$$\frac{\partial^4 F_1}{\partial x_1^4} + \beta_2 \frac{\partial^4 F_1}{\partial x_1^2 \partial y_1^2} + \beta_1 \frac{\partial^4 F_1}{\partial y_1^4} = 0 \tag{1.2}$$

where

$$\beta_1 = \frac{a_{11}}{a_{22}} \; ; \qquad \beta_2 = \frac{2a_{12} + a_{66}}{a_{22}} \; ; \tag{1.3}$$

and

$$a_{11} = \frac{1}{E_{LL}} \; ; \quad a_{12} = -\frac{\nu_{LT}}{E_{LL}} \; ; \quad a_{22} = \frac{1}{E_{TT}} \; ; \quad a_{66} = \frac{1}{G_{LT}}$$

E_{LL}, E_{TT}, G_{LT} and ν_{LT} are the engineering elastic constants for the orthotropic material in its principal frame.

Using Fourier transformation the stress function is defined as:

$$F_1(x_1, y_1) = \frac{1}{2\pi}\int_{-\infty}^{+\infty} \Phi_1(s, y_1)\, e^{-i s x_1} ds \tag{1.4}$$

Substituting (1.4) into (1.2), we reduce the 4-th order Partial Differential Equation (PDE) to 4-th order Ordinary Differential Equation (ODE) with constant coefficients as follows:

$$\beta_1 \frac{d^4 \Phi_1}{dy_1^4} - \beta_2 s^2 \frac{d^2 \Phi_1}{dy_1^2} + s^4 \Phi_1 = 0 \tag{1.5}$$

The solution of (1.5) may be written in the form:

$$\Phi_1(s,y_1) = A(s)\, e^{-\omega_1 s y_1} + B(s)\, e^{-\omega_2 s y_1} + C(s)\, e^{\omega_1 s y_1} + D(s)\, e^{\omega_2 s y_1} \tag{1.6}$$

where ω_1, ω_2 are the roots of characteristic equation

$$\beta_1 \omega^4 - \beta_2 \omega^2 + 1 = 0 \tag{1.7}$$

where it is assumed that $\mathrm{Re}(\omega_1) > 0$ and $\mathrm{Re}(\omega_2) > 0$.

By taking the exponetial behavior function for $s \to \infty$ the stress function becomes:

$$F_1(x_1,y_1^+) = \frac{1}{2\pi} \int_{-\infty}^{+\infty} [\, A\, e^{-\omega_1 |s| y_1} + B\, e^{-\omega_2 |s| y_1}]\, e^{-isx_1}\, ds \tag{1.8}$$

$$F_1(x_1,y_1^-) = \frac{1}{2\pi} \int_{-\infty}^{+\infty} [\, C\, e^{\omega_1 |s| y_1} + D\, e^{\omega_2 |s| y_1}]\, e^{-isx_1}\, ds \tag{1.9}$$

where A,B,C,D are functions of Fourier parameter "s" to be determined by the boundary conditions. Note that superscript of y_1 "+" stands for positive y_1 and "-" for negative y_1.

It is known that stresses are the same on positive and negative face of the crack. This can be stated in the following mathematical form:

$$F_1(x_1,0^+) = F_1(x_1,0^-) \tag{1.10}$$

$$\frac{\partial}{\partial y_1} F_1(x_1,0^+) = \frac{\partial}{\partial y_1} F_1(x_1,0^-) \tag{1.11}$$

Then, the stress function becomes:

$$F_1(x_1,y_1^+) = \frac{1}{2\pi}\int_{-\infty}^{+\infty} [\, A\, e^{-\omega_1|s|y_1} + B\, e^{-\omega_2|s|y_1}]\, e^{-isx_1}\, ds \tag{1.12}$$

$$F_1(x_1,y_1^-) = \frac{1}{2\pi}\int_{-\infty}^{+\infty} [(A\, c_1 + B\, c_2)\, e^{\omega_1|s|y_1} + (A\, c_3 - B\, c_1)\, e^{\omega_2|s|y_1}]\, e^{-isx_1}\, ds \tag{1.13}$$

where

$$c_1 = -\frac{\omega_1+\omega_2}{\omega_1-\omega_2} \quad (1.13a) \qquad c_2 = -\frac{2\omega_2}{\omega_1-\omega_2} \quad (1.13b) \qquad c_3 = \frac{2\omega_1}{\omega_1-\omega_2} \quad (1.13c)$$

Thus, the crack surface stresses can be obtained from the stress function:

$$\sigma^{(+)}_{x_1x_1} = \frac{1}{2\pi}\int_{-\infty}^{+\infty} s^2\, [\, A\omega_1^2 e^{-\omega_1|s|y_1} + B\omega_2^2 e^{-\omega_2|s|y_1}]\, e^{-isx_1}\, ds \tag{1.14}$$

$$\sigma^{(-)}_{x_1x_1} = \frac{1}{2\pi}\int_{-\infty}^{+\infty} s^2\, [\, \omega_1^2(Ac_1 + Bc_2)e^{\omega_1|s|y_1} + \omega_2^2(Ac_3 - Bc_1)e^{\omega_2|s|y_1}]\, e^{-isx_1}\, ds \tag{1.15}$$

$$\sigma^{(+)}_{y_1y_1} = \frac{-1}{2\pi}\int_{-\infty}^{+\infty} s^2\, [\, Ae^{-\omega_1|s|y_1} + Be^{-\omega_2|s|y_1}]\, e^{-isx_1}\, ds \tag{1.16}$$

$$\sigma^{(-)}_{y_1y_1} = \frac{-1}{2\pi}\int_{-\infty}^{+\infty} s^2\, [(Ac_1 + Bc_2)e^{\omega_1|s|y_1} + (Ac_3 - Bc_1)e^{\omega_2|s|y_1}]\, e^{-isx_1}\, ds \tag{1.17}$$

$$\sigma^{(+)}_{y_1y_1} = \frac{-1}{2\pi}\int_{-\infty}^{+\infty} s^2\, [\, Ae^{-\omega_1|s|y_1} + Be^{-\omega_2|s|y_1}]\, e^{-isx_1}\, ds \tag{1.18}$$

$$\sigma^{(-)}_{y_1y_1} = \frac{-1}{2\pi}\int_{-\infty}^{+\infty} s^2\, [(Ac_1 + Bc_2)e^{\omega_1|s|y_1} + (Ac_3 - Bc_1)e^{\omega_2|s|y_1}]\, e^{-isx_1}\, ds \tag{1.19}$$

A more convenient form for the above can be obtained in terms of the crack surface displacement derivatives as unknowns :

$$f_1(x_1) = \frac{\partial}{\partial x_1}[\, u(x_1,0^+) - u(x_1,0^-)] \tag{1.20}$$

for $x_c < x_1 < x_d$

$$f_2(x_1) = \frac{\partial}{\partial x_1}[\, v(x_1,0^+) - v(x_1,0^-)] \tag{1.21}$$

where u and v are shear and normal crack surface displacements respectively.

To relate the displacements and their derivatives, the material stress-strain relation (Hooke's Law) is applied :

$$\varepsilon_{x_1x_1} = a_{11}\sigma_{x_1x_1} + a_{12}\sigma_{y_1y_1} \tag{1.22}$$

$$\varepsilon_{y_1y_1} = a_{12}\sigma_{x_1x_1} + a_{22}\sigma_{y_1y_1} \tag{1.23}$$

Upon substitution of the expressions for stresses (1.14-1.17,, we obtain from (1.22), the surface strains:

$$\varepsilon^{(+)}_{x_1x_1} = \frac{1}{2\pi}\int_{-\infty}^{+\infty} s^2\Big\{a_{11}[\, A\omega_1^2 e^{-\omega_1|s|y_1^+} + B\omega_2^2 e^{-\omega_2|s|y_1^+}]$$

$$- a_{12}[\, Ae^{-\omega_1|s|y_1^+} + Be^{-\omega_2|s|y_1^+}]\Big\}e^{-isx_1}ds$$

$$\varepsilon^{(-)}_{x_1x_1} = \frac{1}{2\pi}\int_{-\infty}^{+\infty} s^2\Big\{a_{11}[(Ac_1 + Bc_2)\omega_1^2 e^{\omega_1|s|y_1^-} + (Ac_3 - Bc_1)\omega_2^2 e^{\omega_2|s|y_1^-}]$$

$$- a_{12}[(Ac_1 + Bc_2)e^{\omega_1|s|y_1^-} + (Ac_3 - Bc_1)\, e^{\omega_2|s|y_1^-}]\Big\}e^{-isx_1}ds$$

or

$$\varepsilon^{(+)}_{x_1x_1} = \frac{1}{2\pi}\int_{-\infty}^{+\infty} s^2[\, A(a_{11}\omega_1^2 - a_{12})\, e^{-\omega_1|s|y_1^+} + B(a_{11}\omega_2^2 - a_{12})\, e^{-\omega_2|s|y_1^+}]\, e^{-isx_1}\, ds \tag{1.24}$$

$$\varepsilon^{(-)}_{x_1x_1} = \frac{1}{2\pi}\int_{-\infty}^{+\infty} s^2[(Ac_1 + Bc_2)(a_{11}\omega_1^2 - a_{12})\, e^{\omega_1|s|y_1^-}$$

$$+ (Ac_3 - Bc_1)(a_{11}\omega_2^2 - a_{12})\, e^{\omega_2|s|y_1^-}]\, e^{-isx_1}\, ds \tag{1.25}$$

Then, the surface displacement derivatives in (1.20) become,

$$f_1(x_1) = \lim_{y_1 \to 0} [\, \varepsilon^{(+)}_{x_1x_1} - \varepsilon^{(-)}_{x_1x_1}] \tag{1.26}$$

Similarly, by substituting (1.14-1.17) into (1.23) we obtain:

$$\varepsilon^{(+)}_{y_1y_1} = \frac{1}{2\pi}\int_{-\infty}^{+\infty} s^2\, [A(a_{12}\omega_1^2 - a_{22})\, e^{-\omega_1|s|y_1^+} + B(a_{12}\omega_2^2 - a_{22})\, e^{-\omega_2|s|y_1^+}]\, e^{-isx_1}\, ds$$

$$\varepsilon^{(-)}_{y_1y_1} = \frac{1}{2\pi}\int_{-\infty}^{+\infty} s^2\, [(Ac_1 + Bc_2)(a_{12}\omega_1^2 - a_{22})\, e^{\omega_1|s|y_1^-}$$

$$+ (Ac_3 - Bc_1)(a_{12}\omega_2^2 - a_{22})\, e^{\omega_2|s|y_1^-}]\, e^{-isx_1}\, ds$$

By integrating the expressions for ε_{y1y1} with respect to y_1, an expression for the normal displacement v can be obtained:

$$v^+ = \frac{1}{2\pi}\int_{-\infty}^{+\infty} s^2 [\, \frac{A(a_{12}\omega_1^2 - a_{22})}{-\omega_1|s|}\, e^{-\omega_1|s|y_1^+} + \frac{B(a_{12}\omega_2^2 - a_{22})}{-\omega_2|s|}\, e^{-\omega_2|s|y_1^+}\,]\, e^{-isx_1}\, ds$$

$$v^- = \frac{1}{2\pi}\int_{-\infty}^{+\infty} s^2 [\, \frac{(Ac_1 + Bc_2)(a_{12}\omega_1^2 - a_{22})}{\omega_1|s|}\, e^{\omega_1|s|y_1^-}$$

$$+ \frac{(Ac_3 - Bc_1)(a_{12}\omega_2^2 - a_{22})}{\omega_2|s|}\, e^{\omega_2|s|y_1^-}\,]\, e^{-isx_1}\, ds$$

Now we differentiate v with respect to x_1 and obtain

$$\frac{\partial v^+}{\partial x_1} = \frac{1}{2\pi}\int_{-\infty}^{+\infty} \frac{i s^3}{|s|}\left[\frac{A(a_{12}\omega_1^2 - a_{22})}{\omega_1} e^{-\omega_1|s|y_1^+}\right.$$

$$\left. + \frac{B(a_{12}\omega_2^2 - a_{22})}{\omega_2} e^{-\omega_2|s|y_1^+}\right] e^{-isx_1}\, ds \tag{1.27}$$

$$\frac{\partial v^-}{\partial x_1} = \frac{-1}{2\pi}\int_{-\infty}^{+\infty} \frac{i s^3}{|s|}\left[\frac{(Ac_1 + Bc_2)(a_{12}\omega_1^2 - a_{22})}{\omega_1} e^{\omega_1|s|y_1^-}\right.$$

$$\left. + \frac{(Ac_3 - Bc_1)(a_{12}\omega_2^2 - a_{22})}{\omega_2} e^{\omega_2|s|y_1^-}\right] e^{-isx_1}\, ds \tag{1.28}$$

Substituting (1.24) and (1.25) into (1.26), and (1.27-1.28) into (1.21), we obtain:

$$f_1(x_1) = \lim_{y_1\to 0} \frac{1}{2\pi}\int_{-\infty}^{+\infty} s^2 \Big\{[A e^{-\omega_1|s|y_1^+} - (Ac_1 + Bc_2) e^{\omega_1|s|y_1^-}](a_{11}\omega_1^2 - a_{12}) +$$

$$+ [B e^{-\omega_2|s|y_1^+} - (Ac_3 - Bc_1) e^{\omega_2|s|y_1^-}](a_{11}\omega_2^2 - a_{12})\Big\} e^{-isx_1}\, ds \tag{1.29}$$

$$f_2(x_1) = \lim_{y_1\to 0} \frac{1}{2\pi}\int_{-\infty}^{+\infty} \frac{i s^3}{|s|}\Big\{ \frac{A e^{-\omega_1|s|y_1^+} + (Ac_1 + Bc_2) e^{\omega_1|s|y_1^-}}{\omega_1}(a_{12}\omega_1^2 - a_{22}) +$$

$$+ \frac{B e^{-\omega_2|s|y_1^+} + (Ac_3 - Bc_1) e^{\omega_2|s|y_1^-}}{\omega_2}(a_{12}\omega_2^2 - a_{22})\Big\} e^{-isx_1}\, ds \tag{1.30}$$

or

$$f_1(x_1) = \frac{1}{2\pi}\int_{-\infty}^{+\infty} s^2 [(A - Ac_1 - Bc_2)(a_{11}\omega_1^2 - a_{12})$$

$$+ (B - Ac_3 + Bc_1)(a_{11}\omega_2^2 - a_{12})] e^{-isx_1}\, ds \tag{1.31}$$

$$f_2(x_1) = \frac{1}{2\pi}\int_{-\infty}^{+\infty} \frac{i s^3}{|s|}\Big[\frac{(A + Ac_1 + Bc_2)(a_{12}\omega_1^2 - a_{22})}{\omega_1}$$

$$+ \frac{(B + Ac_3 - Bc_1)(a_{12}\omega_2^2 - a_{22})}{\omega_2}\Big] e^{-isx_1}\, ds \qquad (1.32)$$

Upon substitution in (1.31-1.32) for c_1, c_2, c_3 from (1.13 a-c), the following is obtained:

$$f_1(x_1) = \frac{1}{2\pi}\int_{-\infty}^{+\infty} 2s^2 a_{11}(A\omega_1 + B\omega_2)(\omega_1 + \omega_2)\, e^{-isx_1}\, ds \qquad (1.33)$$

$$f_2(x_1) = \frac{-1}{2\pi}\int_{-\infty}^{+\infty} 2\,\frac{i s^3}{|s|}\, a_{22}(A + B)\,\frac{\omega_1 + \omega_2}{\omega_1\omega_2}\, e^{-isx_1}\, ds \qquad (1.34)$$

The inverse Fourier transformation of (1.33) and (1.34) gives:

$$A\omega_1 + B\omega_2 = \frac{1}{2a_{11}(\omega_1 + \omega_2)\, s^2}\int_{x_c}^{x_d} f_1(t_1)\, e^{ist_1}\, dt_1$$

$$A + B = \frac{|s|}{i s^3}\,\frac{\omega_1\omega_2}{2a_{22}(\omega_1 + \omega_2)}\int_{x_c}^{x_d} f_2(t_1)\, e^{ist_1}\, dt_1$$

with A and B taking the forms:

$$A = \frac{1}{s^2}\,\frac{1}{2a_{11}(\omega_1^2 - \omega_2^2)}\int_{x_c}^{x_d} f_1(t_1)\, e^{ist_1}\, dt_1 + \frac{|s|}{i s^3}\,\frac{\omega_1\omega_2^2}{2a_{22}(\omega_1^2 - \omega_2^2)}\int_{x_c}^{x_d} f_2(t_1)\, e^{ist_1}\, dt_1 \qquad (1.35)$$

$$B = \frac{-1}{s^2}\,\frac{1}{2a_{11}(\omega_1^2 - \omega_2^2)}\int_{x_c}^{x_d} f_1(t_1)\, e^{ist_1}\, dt_1 - \frac{|s|}{i s^3}\,\frac{\omega_1\omega_2^2}{2a_{22}(\omega_1^2 - \omega_2^2)}\int_{x_c}^{x_d} f_2(t_1)\, e^{ist_1}\, dt_1 \qquad (1.36)$$

Equations (1.35) and (1.36) can be substituted in (1.14), (1.16), (1.18) such that the

crack surface stresses are expressed in terms of f_1, f_2. After integrating with respect to "s" and applying:

$$\omega_1^2\omega_2^2 = \frac{a_{22}}{a_{11}}$$

these stresses of the perturbed problem are obtained as:

$$\sigma_{x_1x_1} = \frac{1}{2\pi(\omega_1^2 - \omega_2^2)a_{11}} \int_{x_c}^{x_d} \left\{ \frac{f_1(t_1)\,\omega_1^3 y_1 + f_2(t_1)(t_1 - x_1)\,\omega_1}{\omega_1^2 y_1^2 + (t_1 - x_1)^2} - \frac{f_1(t_1)\,\omega_2^3 y_1 + f_2(t_1)(t_1 - x_1)\,\omega_2}{\omega_1^2 y_1^2 + (t_1 - x_1)^2} \right\} dt_1 \tag{1.37}$$

$$\sigma_{y_1y_1} = \frac{-1}{2\pi(\omega_1^2 - \omega_2^2)a_{11}} \int_{x_c}^{x_d} \left\{ \frac{f_1(t_1)\,\omega_1 y_1 + f_2(t_1)\dfrac{t_1 - x_1}{\omega_1}}{\omega_1^2 y_1^2 + (t_1 - x_1)^2} - \frac{f_1(t_1)\,\omega_2 y_1 + f_2(t_1)\dfrac{t_1 - x_1}{\omega_2}}{\omega_1^2 y_1^2 + (t_1 - x_1)^2} \right\} dt_1 \tag{1.38}$$

$$\tau_{x_1y_1} = \frac{1}{2\pi(\omega_1^2 - \omega_2^2)a_{11}} \int_{x_c}^{x_d} \left\{ \frac{f_1(t_1)\,\omega_1(t_1 - x_1) - f_2(t_1)\,\omega_1 y_1}{\omega_1^2 y_1^2 + (t_1 - x_1)^2} - \frac{f_1(t_1)\,\omega_2(t_1 - x_1) - f_2(t_1)\,\omega_2 y_1}{\omega_1^2 y_1^2 + (t_1 - x_1)^2} \right\} dt_1 \tag{1.39}$$

II. Formulation of the problem of the crack along x_2.

For the horizontal crack, which is situated in the x_2-y_2 frame and is making the angle θ with the direction of fibers, the governing field equation is a general biharmonic equation for anisotropic materials in the form:

$$b_{22}\frac{\partial^4 F_2}{\partial x_2^4} - 2b_{26}\frac{\partial^4 F_2}{\partial x_2^3 \partial y_2} + (2b_{12}+b_{66})\frac{\partial^4 F_2}{\partial x_2^2 \partial y_2^2} - 2b_{16}\frac{\partial^4 F_2}{\partial x_2 \partial y_2^3} + b_{11}\frac{\partial^4 F_2}{\partial y_2^4} = 0 \qquad (2.1)$$

where

$$b_{11} = a_{11}\cos^4\theta + (2a_{12}+a_{66})\sin^2\theta\cos^2\theta + a_{22}\sin^4\theta$$

$$b_{22} = a_{11}\sin^4\theta + (2a_{12}+a_{66})\sin^2\theta\cos^2\theta + a_{22}\cos^4\theta$$

$$b_{12} = a_{12} + (a_{11}+a_{22}-2a_{12}-a_{66})\sin^2\theta\cos^2\theta$$

$$b_{66} = a_{66} + (a_{11}+a_{22}-2a_{12}-a_{66})\sin^2\theta\cos^2\theta$$

$$b_{16} = [a_{22}\sin^2\theta - a_{11}\cos^2\theta + \frac{1}{2}(2a_{12}+a_{66})\cos 2\theta]\sin 2\theta$$

$$b_{26} = [a_{22}\cos^2\theta - a_{11}\sin^2\theta - \frac{1}{2}(2a_{12}+a_{66})\cos 2\theta]\sin 2\theta$$

Let's define:

$$\beta_1 = -\frac{2b_{26}}{b_{22}}; \quad \beta_2 = \frac{2b_{12}+b_{66}}{b_{22}}; \quad \beta_3 = -\frac{2b_{16}}{b_{22}}; \quad \beta_4 = \frac{b_{11}}{b_{22}}; \qquad (2.2)$$

and after substitution of (2.2) into (2.1), the 4-th order PDE is reduced as follows:

$$\frac{\partial^4 F_2}{\partial x_2^4} + \beta_1\frac{\partial^4 F_2}{\partial x_2^3 \partial y_2} + \beta_2\frac{\partial^4 F_2}{\partial x_2^2 \partial y_2^2} + \beta_3\frac{\partial^4 F_2}{\partial x_2 \partial y_2^3} + \beta_4\frac{\partial^4 F_2}{\partial y_2^4} = 0 \qquad (2.3)$$

Assume the solution for the stress function F_2 in the following form:

$$F_2(x_2, y_2) = \frac{1}{2\pi} \int_{-\infty}^{+\infty} \sum_{k=1}^{4} C_k(s)\, e^{r_k y_2 s}\, e^{-i x_2 s}\, ds \tag{2.4}$$

then, the following characteristic equation is obtained by substituting (2.4) into (2.3):

$$\beta_4 r^4 - i\beta_3 r^3 - \beta_2 r^2 + i\beta_1 r + 1 = 0 \tag{2.5}$$

The roots of (2.5) are of the general form:

$$\begin{aligned} r_1 &= a + ib\,; \qquad r_2 = c + id\,; \\ r_4 &= -a + ib\,; \qquad r_3 = -c + id\,; \end{aligned} \tag{2.6}$$

where $a,c > 0$ is assumed.

Thus, for $y_2 > 0$, the stress function F_2 can be written as:

$$F_2(x_2, y_2^+) = \frac{1}{2\pi} \left\{ \int_{-\infty}^{0} [\, C_1 e^{(a+ib)y_2 s} + C_3 e^{(c+id)y_2 s} \,]\, e^{-i x_2 s}\, ds \right.$$

$$\left. + \int_{0}^{+\infty} [\, C_2 e^{(-a+ib)y_2 s} + C_4 e^{(-c+id)y_2 s} \,]\, e^{-i x_2 s}\, ds \right\} \tag{2.7}$$

Define new constants as follow:

$$A(s) = \begin{cases} C_1 & \text{if } s < 0 \\ C_2 & \text{if } s > 0 \end{cases} \quad (2.8) \qquad B(s) = \begin{cases} C_3 & \text{if } s < 0 \\ C_4 & \text{if } s > 0 \end{cases} \quad (2.9)$$

then (2.7) becomes:

$$F_2(x_2, y_2^+) = \frac{1}{2\pi} \int_{-\infty}^{+\infty} [\, A e^{-a|s|y_2^* + iby_2^* s} + B e^{-c|s|y_2^* + idy_2^* s} \,]\, e^{-i x_2 s}\, ds \tag{2.10}$$

Similarly, for $y_2 < 0$, we have:

$$F_2(x_2, y_2^-) = \frac{1}{2\pi}\left\{ \int_{-\infty}^{0} [\, C_2\, e^{(-a+ib)y_2 s} + C_4\, e^{(-c+id)y_2 s} \,]\, e^{-ix_2 s}\, ds \right.$$

$$\left. + \int_{0}^{+\infty} [\, C_1\, e^{(a+ib)y_2 s} + C_3\, e^{(c+id)y_2 s} \,]\, e^{-ix_2 s}\, ds \right\} \qquad (2.11)$$

We then define the following constants:

$$C(s) = \begin{cases} C_2 & \text{if } s < 0 \\ C_1 & \text{if } s > 0 \end{cases} \qquad (2.12) \qquad\qquad D(s) = \begin{cases} C_4 & \text{if } s < 0 \\ C_3 & \text{if } s > 0 \end{cases} \qquad (2.13)$$

and (2.11) becomes:

$$F_2(x_2, y_2^-) = \frac{1}{2\pi}\int_{-\infty}^{+\infty} [\, C\, e^{a|s|y_2^- + iby_2^- s} + D\, e^{c|s|y_2^- + idy_2^- s} \,]\, e^{-ix_2 s}\, ds \qquad (2.14)$$

Since the stresses are the same on the positive and negative face of the crack we can state:

$$F_2(x_2, 0^+) = F_2(x_2, 0^-) \qquad (2.15)$$

$$\frac{\partial}{\partial y_2} F_2(x_2, 0^+) = \frac{\partial}{\partial y_2} F_2(x_2, 0^-) \qquad (2.16)$$

Satisfying the above conditions, the stress functions (2.10) and (2.14) become respectively:

$$F_2(x_2, y_2^+) = \frac{1}{2\pi}\int_{-\infty}^{+\infty} [\, A\, e^{-a|s|y_2^+ + iby_2^+ s} + B\, e^{-c|s|y_2^+ + idy_2^+ s} \,]\, e^{-ix_2 s}\, ds \qquad (2.17)$$

$$F_2(x_2, y_2^-) = \frac{1}{2\pi}\int_{-\infty}^{+\infty}[(S_1A + S_2B)\, e^{a|s|y_2^- + iby_2^- s}$$

$$+ \ (S_3A + S_4B)\, e^{c|s|y_2^- + idy_2^- s}\,]\, e^{-ix_2 s}\, ds \qquad (2.18)$$

where

$$S_1 = \frac{|s|\,(c + a) + i\,s\,(d - b)}{|s|\,(c - a) + i\,s\,(d - b)}; \ (2.19a) \qquad S_3 = \frac{-\,2\,a\,|s|}{|s|\,(c - a) + i\,s\,(d - b)}; \ (2.19c)$$

$$S_2 = \frac{2\,c\,|s|}{|s|\,(c - a) + i\,s\,(d - b)}; \ (2.19b) \qquad S_4 = \frac{-|s|\,(c + a) + i\,s\,(d - b)}{|s|\,(c - a) + i\,s\,(d - b)}; \ (2.19d)$$

The second derivatives of the stress function give us the crack surface stresses:

$$\sigma^{(+)}_{x_2x_2} = \frac{1}{2\pi}\int_{-\infty}^{+\infty}[A(-a|s| + ibs)^2 e^{-a|s|y_2^+ + iby_2^+ s}$$

$$+ \ B(-c|s| + ids)^2 e^{-c|s|y_2^+ + idy_2^+ s}\,]\, e^{-ix_2 s}\, ds \qquad (2.20)$$

$$\sigma^{(-)}_{x_2x_2} = \frac{1}{2\pi}\int_{-\infty}^{+\infty}[(S_1A + S_2B)(a|s| + ibs)^2 e^{a|s|y_2^- + iby_2^- s}$$

$$+ \ (S_3A + S_4B)(c|s| + ids)^2 e^{c|s|y_2^- + idy_2^- s}\,]\, e^{-ix_2 s}\, ds \qquad (2.21)$$

$$\sigma^{(+)}_{y_2y_2} = \frac{-1}{2\pi}\int_{-\infty}^{+\infty} s^2\,[A\, e^{-a|s|y_2^+ + iby_2^+ s} + B\, e^{-c|s|y_2^+ + idy_2^+ s}\,]\, e^{-ix_2 s}\, ds \qquad (2.22)$$

$$\sigma^{(-)}_{y_2y_2} = \frac{-1}{2\pi}\int_{-\infty}^{+\infty} s^2\,[\,(S_1A + S_2B)\, e^{a|s|y_2^- + iby_2^- s}$$

$$+ \ (S_3A + S_4B)\, e^{c|s|y_2^- + idy_2^- s}\,]\, e^{-ix_2 s}\, ds \qquad (2.23)$$

$$\tau^{(+)}_{x_2y_2} = \frac{1}{2\pi}\int_{-\infty}^{+\infty} is\,[A(-a|s| + ibs)\,e^{-a|s|y_2^{+}+iby_2^{+}s}$$

$$+ B(-c|s| + ids)\,e^{-c|s|y_2^{+}+idy_2^{+}s}\,]\,e^{-ix_2s}\,ds \qquad (2.24)$$

$$\tau^{(-)}_{x_2y_2} = \frac{1}{2\pi}\int_{-\infty}^{+\infty} is\,[(S_1A + S_2B)(a|s| + ibs)\,e^{a|s|y_2^{-}+iby_2^{-}s}$$

$$+ (S_3A + S_4B)(c|s| + ids)\,e^{c|s|y_2^{-}+idy_2^{-}s}\,]\,e^{-ix_2s}\,ds \qquad (2.25)$$

Similarly, as in Section I, the discontinuity at the crack is expressed as a set of crack surface derivatives:

$$f_3(x_2) = \frac{\partial}{\partial x_2}[\,u(x_2, 0^+) - u(x_2, 0^-)] \qquad (2.26)$$

$$\text{for } x_a < x_2 < x_b$$

$$f_4(x_2) = \frac{\partial}{\partial x_2}[\,v(x_2, 0^+) - v(x_2, 0^-)\,] \qquad (2.27)$$

The stress-strain relations (Hooke's Law) in the x_2-y_2 frame are:

$$\varepsilon_{x_2x_2} = b_{11}\sigma_{x_2x_2} + b_{12}\sigma_{y_2y_2} + b_{16}\tau_{x_2y_2}$$
$$\varepsilon_{y_2y_2} = b_{12}\sigma_{x_2x_2} + b_{22}\sigma_{y_2y_2} + b_{26}\tau_{x_2y_2}$$

Upon substitution of the expressions for stresses (2.20-2.25) into Hooke's Law, the surface strains are obtained. Then, integrating the ε_{y2y2} with respect to y_2, an expression for the normal displacements is obtained, which is differentiated with respect to x_2 and substituted into (2.27). The expression for e_{x2x2} can be directly substituted into (2.26). Finally the following expressions are obtained:

$$f_3(x_2) = \frac{1}{2\pi}\int_{-\infty}^{+\infty} b_{11}\Big\{A\Big[(-a|s|+ibs)^2 - S_1(a|s| + ibs)^2 - S_3(c|s| + ids)^2\Big] +$$

$$B\Big[(-c|s| + ids)^2 - S_2(a|s| + ibs)^2 - S_4(c|s| + ids)^2\Big]\Big\} e^{-ix_2 s}\, ds \qquad (2.28)$$

$$f_4(x_2) = \frac{1}{2\pi}\int_{-\infty}^{+\infty} is^3 b_{22}\Big\{A\Big[\frac{1}{-a|s| + ibs} - \frac{S_1}{a|s| + ibs} - \frac{S_3}{c|s| + ids}\Big] +$$

$$B\Big[\frac{1}{-c|s| + ids} - \frac{S_2}{a|s| + ibs} - \frac{S_4}{s|s| + ids}\Big]\Big\} e^{-ix_2 s}\, ds \qquad (2.29)$$

The inverse Fourier transformation of (2.28-2.29) gives:

$$A\,P_1 + B\,P_2 = \int_{x_a}^{x_b} f_3(t_2)\, e^{ist_2}\, dt_2$$

$$A\,P_3 + B\,P_4 = \int_{x_a}^{x_b} f_4(t_2)\, e^{ist_2}\, dt_2 \qquad (2.30)$$

from which we find that:

$$A = \frac{P_4}{P_1P_4 - P_2P_3}\int_{x_a}^{x_b} f_3(t_2)\, e^{ist_2}\, dt_2 - \frac{P_2}{P_1P_4 - P_2P_3}\frac{1}{is}\int_{x_a}^{x_b} f_4(t_2)\, e^{ist_2}\, dt_2 \qquad (2.31)$$

$$B = \frac{-P_3}{P_1P_4 - P_2P_3}\int_{x_a}^{x_b} f_3(t_2)\, e^{ist_2}\, dt_2 + \frac{P_1}{P_1P_2 - P_2P_3}\frac{1}{is}\int_{x_a}^{x_b} f_4(t_2)\, e^{ist_2}\, dt_2 \qquad (2.32)$$

where

$$P_1 = s^2 Q_1 ; \quad P_2 = s^2 Q_2 ; \quad P_3 = s Q_3 ; \quad P_4 = s Q_4 ;$$

and

$$\begin{aligned} Q_1^+ &= 2b_{11}[a(a+c) - ia(b-d)] \quad \text{for} \quad s>0 \\ Q_1^- &= 2b_{11}[a(a+c) + ia(b-d)] \quad \text{for} \quad s<0 \end{aligned} \tag{2.33}$$

$$\begin{aligned} Q_2^+ &= 2b_{11}[c(a+c) + ia(b-d)] \quad \text{for} \quad s>0 \\ Q_2^- &= 2b_{11}[c(a+c) - ia(b-d)] \quad \text{for} \quad s<0 \end{aligned} \tag{2.34}$$

$$\begin{aligned} Q_3^+ &= \frac{2a[(db - d^2 - c^2 - ac) + i(cb + ad)]}{(a^2+b^2)(c^2+d^2)} b_{22} \quad \text{for} \quad s>0 \\ Q_3^- &= \frac{2a[(d^2 + c^2 - db + ac) + i(cb + ad)]}{(a^2+b^2)(c^2+d^2)} b_{22} \quad \text{for} \quad s<0 \end{aligned} \tag{2.35}$$

$$\begin{aligned} Q_4^+ &= \frac{-2c[(a^2 + b^2 - db + ac) + i(cb + ad)]}{(a^2+b^2)(c^2+d^2)} b_{22} \quad \text{for} \quad s>0 \\ Q_4^- &= \frac{-2c[(db - a^2 - b^2 - ac) + i(cb + ad)]}{(a^2+b^2)(c^2+d^2)} b_{22} \quad \text{for} \quad s<0 \end{aligned} \tag{2.36}$$

Substituting the above for A and B into (2.20), (2.22) and (2.24) the stress field is obtained :

$$\sigma_{x_2x_2} = \frac{1}{2\pi}\int_{x_a}^{x_b}\left[\frac{R_1 f_3(t_2) - R_2 f_4(t_2)}{y_2(a+ib) + i(t_2 - x_2)} + \frac{R_3 f_4(t_2) - R_4 f_3(t_2)}{y_2(c+id) + i(t_2 - x_2)}\right.$$
$$\left. + \frac{R_5 f_3(t_2) - R_6 f_4(t_2)}{y_2(a-ib) - i(t_2 - x_2)} + \frac{R_7 f_4(t_2) - R_8 f_3(t_2)}{y_2(c-id) - i(t_2 - x_2)}\right] dt_2 \tag{2.37}$$

$$\sigma_{y_2y_2} = \frac{1}{2\pi}\int_{x_a}^{x_b}\left[\frac{R_9 f_3(t_2) - R_{10} f_4(t_2)}{y_2(a+ib) + i(t_2 - x_2)} + \frac{R_{11} f_4(t_2) - R_{12} f_3(t_2)}{y_2(c+id) + i(t_2 - x_2)}\right.$$

$$\left. + \frac{R_{13} f_3(t_2) - R_{14} f_4(t_2)}{y_2(a-ib) - i(t_2 - x_2)} + \frac{R_{15} f_4(t_2) - R_{16} f_3(t_2)}{y_2(c-id) - i(t_2 - x_2)}\right] dt_2 \qquad (2.38)$$

$$\tau_{x_2y_2} = \frac{1}{2\pi}\int_{x_a}^{x_b}\left[\frac{R_{17} f_3(t_2) - R_{18} f_4(t_2)}{y_2(a+ib) + i(t_2 - x_2)} + \frac{R_{19} f_4(t_2) - R_{20} f_3(t_2)}{y_2(c+id) + i(t_2 - x_2)}\right.$$

$$\left. + \frac{R_{21} f_3(t_2) - R_{22} f_4(t_2)}{y_2(a-ib) - i(t_2 - x_2)} + \frac{R_{23} f_4(t_2) - R_{24} f_3(t_2)}{y_2(c-id) - i(t_2 - x_2)}\right] dt_2 \qquad (2.39)$$

where R's are coefficients in the form:

$$R_1 = \frac{Q_4^-}{Q_5^-}(a + ib)^2; \qquad R_4 = \frac{Q_3^-}{Q_5^-}(c + id)^2;$$

$$R_2 = -\frac{iQ_2^-}{Q_5^-}(a + ib)^2; \qquad R_5 = \frac{Q_4^+}{Q_5^+}(-a + ib)^2;$$

$$R_3 = -\frac{iQ_1^-}{Q_5^-}(c + id)^2; \qquad R_6 = -\frac{iQ_2^+}{Q_5^+}(-a + ib)^2;$$

$$R_7 = -\frac{iQ_1^+}{Q_5^+}(-c + id)^2; \qquad R_8 = \frac{Q_3^+}{Q_5^+}(-c + id)^2;$$

$$R_9 = -\frac{Q_4^-}{Q_5^-}; \qquad R_{13} = -\frac{Q_4^-}{Q_5^+};$$

$$R_{10} = \frac{iQ_2^-}{Q_5^-}; \qquad R_{14} = \frac{iQ_2^+}{Q_5^+};$$

$$R_{11} = \frac{iQ_1^-}{Q_5^-}; \qquad R_{15} = \frac{iQ_1^+}{Q_5^+};$$

$$R_{12} = -\frac{Q_3^-}{Q_5^-}; \qquad R_{16} = -\frac{Q_3^+}{Q_5^+};$$

$$R_{17} = \frac{iQ_4^-}{Q_5^-}(a + ib); \qquad R_{21} = \frac{iQ_4^+}{Q_5^+}(-a + ib);$$

$$R_{18} = \frac{Q_2^-}{Q_5^-}(a + ib); \qquad R_{22} = \frac{Q_2^+}{Q_5^+}(-a + ib);$$

$$R_{19} = \frac{Q_1^-}{Q_5^-}(c + id); \qquad R_{23} = \frac{Q_1^+}{Q_5^+}(-c + id);$$

$$R_{20} = \frac{iQ_3^-}{Q_5^-}(c + id); \qquad R_{24} = \frac{iQ_3^+}{Q_5^+}(-c + id);$$

Note that the stresses in the first problem (1.37-1.39) can be written in the form analogous to those in the second problem (2.37-2.38):

$$\sigma_{x_1x_1} = \frac{1}{2\pi}\int_{x_c}^{x_d}\left[\frac{T_1 f_1(t_1) - T_2 f_2(t_1)}{y_1\omega_1 + i(t_1 - x_1)} + \frac{T_3 f_2(t_1) - T_4 f_1(t_1)}{y_1\omega_2 + i(t_1 - x_1)}\right.$$

$$\left. + \frac{T_5 f_1(t_1) - T_6 f_2(t_1)}{y_1\omega_1 - i(t_1 - x_1)} + \frac{T_7 f_2(t_1) - T_8 f_1(t_1)}{y_1\omega_2 - i(t_1 - x_1)}\right] dt_1 \qquad (2.40)$$

$$\sigma_{y_1y_1} = \frac{1}{2\pi}\int_{x_c}^{x_d}\left[\frac{T_9 f_1(t_1) - T_{10}f_2(t_1)}{y_1\omega_1 + i(t_1 - x_1)} + \frac{T_{11}f_2(t_1) - T_{12}f_1(t_1)}{y_1\omega_2 + i(t_1 - x_1)}\right.$$

$$\left. + \frac{T_{13}f_1(t_1) - T_{14}f_2(t_1)}{y_1\omega_1 - i(t_1 - x_1)} + \frac{T_{15}f_2(t_1) - T_{16}f_1(t_1)}{y_1\omega_2 - i(t_1 - x_1)}\right]dt_1 \qquad (2.41)$$

$$\tau_{x_1y_1} = \frac{1}{2\pi}\int_{x_c}^{x_d}\left[\frac{T_{17}f_1(t_1) - T_{18}f_2(t_1)}{y_1\omega_1 + i(t_1 - x_1)} + \frac{T_{19}f_2(t_1) - T_{20}f_1(t_1)}{y_1\omega_2 + i(t_1 - x_1)}\right.$$

$$\left. + \frac{T_{21}f_1(t_1) - T_{22}f_2(t_1)}{y_1\omega_1 - i(t_1 - x_1)} + \frac{T_{23}f_2(t_1) - T_{24}f_1(t_1)}{y_1\omega_2 - i(t_1 - x_1)}\right]dt_1 \qquad (2.42)$$

where

$$T_1 = T_5 = \frac{\omega_1^2}{2(\omega_1^2 - \omega_2^2)\,a_{11}}; \qquad T_9 = T_{13} = T_{12} = T_{16} = \frac{-1}{2(\omega_1^2 - \omega_2^2)\,a_{11}};$$

$$-T_2 = T_6 = \frac{i\omega_1}{2(\omega_1^2 - \omega_2^2)\,a_{11}}; \qquad -T_{10} = T_{14} = \frac{-i}{2\omega_1(\omega_1^2 - \omega_2^2)\,a_{11}};$$

$$T_4 = T_8 = \frac{\omega_2^2}{2(\omega_1^2 - \omega_2^2)\,a_{11}}; \qquad -T_{11} = T_{15} = \frac{-i}{2\omega_2(\omega_1^2 - \omega_2^2)\,a_{11}};$$

$$-T_3 = T_7 = \frac{i\omega_2}{2(\omega_1^2 - \omega_2^2)\,a_{11}};$$

$$-T_{17} = T_{21} = \frac{-i\omega_1}{2(\omega_1^2 - \omega_2^2)\,a_{11}}; \qquad -T_{20} = T_{24} = \frac{-i\omega_2}{2(\omega_1^2 - \omega_2^2)\,a_{11}};$$

$$T_{18} = T_{22} = T_{19} = T_{23} = \frac{1}{2(\omega_1^2 - \omega_2^2)\,a_{11}};$$

III. Generation of Integral equations.

By superposition of stresses from the two problems, we obtain solutions for a plate with two cracks. Thus, we proceed with the coordinate transformation in order to express the total stresses in one common coordinate system. If the total stresses are expressed in x_1-y_1 coordinate system, the transformation is given by:

$$x_2 = x_1 \cos\theta - y_1 \sin\theta$$
$$y_2 = x_1 \sin\theta + y_1 \cos\theta \tag{3.1}$$

and the stresses of the second problem, when expressed in x_1-y_1 system are given by:

$$\sigma'_{x_1x_1} = \frac{\sigma_{x_2x_2} + \sigma_{y_2y_2}}{2} + \frac{\sigma_{x_2x_2} - \sigma_{y_2y_2}}{2}\cos 2\theta + \tau_{x_2y_2}\sin 2\theta \tag{3.2}$$

$$\sigma'_{y_1y_1} = \frac{\sigma_{x_2x_2} + \sigma_{y_2y_2}}{2} - \frac{\sigma_{x_2x_2} - \sigma_{y_2y_2}}{2}\cos 2\theta - \tau_{x_2y_2}\sin 2\theta \tag{3.3}$$

$$\tau'_{x_1y_1} = -\frac{\sigma_{x_2x_2} - \sigma_{y_2y_2}}{2}\sin 2\theta + \tau_{x_2y_2}\cos 2\theta \tag{3.4}$$

and the total stresses are given by:

$$\sigma^T_{x_1x_1} = \sigma_{x_1x_1} + \sigma'_{x_1x_1}$$
$$\sigma^T_{y_1y_1} = \sigma_{y_1y_1} + \sigma'_{y_1y_1} \tag{3.4a}$$
$$\tau^T_{x_1y_1} = \tau_{x_1y_1} + \tau'_{x_1y_1}$$

Similarly, if the total stresses are expressed in x_2-y_2 coordinate, the transformation is given by:

$$x_1 = x_2 \cos\theta + y_2 \sin\theta$$
$$y_1 = -x_2 \sin\theta + y_2 \cos\theta \tag{3.5}$$

and the transformed stresses of the first problem, when expressed in x_2-y_2 are given by:

$$\sigma'_{x_2x_2} = \frac{\sigma_{x_1x_1} + \sigma_{y_1y_1}}{2} + \frac{\sigma_{x_1x_1} - \sigma_{y_1y_1}}{2}\cos 2\theta - \tau_{x_1y_1}\sin 2\theta \tag{3.6}$$

$$\sigma'_{y_2y_2} = \frac{\sigma_{x_1x_1} + \sigma_{y_1y_1}}{2} - \frac{\sigma_{x_1x_1} - \sigma_{y_1y_1}}{2}\cos 2\theta + \tau_{x_1y_1}\sin 2\theta \tag{3.7}$$

$$\tau'_{x_2y_2} = \frac{\sigma_{x_1x_1} - \sigma_{y_1y_1}}{2}\sin 2\theta + \tau_{x_1y_1}\cos 2\theta \tag{3.8}$$

Thus, the total stresses in x_2-y_2 system are:

$$\begin{aligned} \sigma^T_{x_2x_2} &= \sigma_{x_2x_2} + \sigma'_{x_2x_2} \\ \sigma^T_{y_2y_2} &= \sigma_{y_2y_2} + \sigma'_{y_2y_2} \\ \tau^T_{x_2y_2} &= \tau_{x_2y_2} + \tau'_{x_2y_2} \end{aligned} \tag{3.8a}$$

Consequently, the transformed stresses of the second problem, when expressed in x_1-y_1 frame, (3.2) to (3.4) have the form:

$$\begin{aligned} \sigma'_{x_1x_1} = \frac{1}{2\pi}\int_{x_a}^{x_c} \Bigg[& \frac{H_1 f_3(t_2) + H_2 f_4(t_2)}{(x_1\sin\theta + y_1\cos\theta)(a + ib) + i(t_2 - x_1\cos\theta + y_1\sin\theta)} \\ & + \frac{H_3 f_3(t_2) + H_4 f_4(t_2)}{(x_1\sin\theta + y_1\cos\theta)(c + id) + i(t_2 - x_1\cos\theta + y_1\sin\theta)} \\ & + \frac{H_5 f_3(t_2) + H_6 f_4(t_2)}{(x_1\sin\theta + y_1\cos\theta)(a - ib) - i(t_2 - x_1\cos\theta + y_1\sin\theta)} \\ & + \frac{H_7 f_3(t_2) + H_8 f_4(t_2)}{(x_1\sin\theta + y_1\cos\theta)(c - id) - i(t_2 - x_1\cos\theta + y_1\sin\theta)} \Bigg] dt_2 \end{aligned} \tag{3.9}$$

where

$$H_1 = \frac{1}{2}[\, R_1 + R_9 + (R_1 - R_9)\cos 2\theta + 2R_{17}\sin 2\theta \,]$$

$$H_2 = -\frac{1}{2}[\, R_2 + R_{10} + (R_2 - R_{10})\cos 2\theta + 2R_{18}\sin 2\theta \,]$$

$$H_3 = -\frac{1}{2}[\, R_4 + R_{12} + (R_4 - R_{12})\cos 2\theta + 2R_{20}\sin 2\theta \,]$$

$$H_4 = \frac{1}{2}[\, R_3 + R_{11} + (R_3 - R_{11})\cos 2\theta + 2R_{19}\sin 2\theta \,]$$

$$H_5 = \frac{1}{2}[\, R_5 + R_{13} + (R_5 - R_{13})\cos 2\theta + 2R_{21}\sin 2\theta \,]$$

$$H_6 = -\frac{1}{2}[\, R_6 + R_{14} + (R_6 - R_{14})\cos 2\theta + 2R_{22}\sin 2\theta \,]$$

$$H_7 = -\frac{1}{2}[\, R_8 + R_{16} + (R_8 - R_{16})\cos 2\theta + 2R_{24}\sin 2\theta \,]$$

$$H_8 = \frac{1}{2}[\, R_7 + R_{15} + (R_7 - R_{15})\cos 2\theta + 2R_{23}\sin 2\theta \,]$$

and

$$\sigma'_{y_1 y_1} = \frac{1}{2\pi}\int_{x_a}^{x_c} \Bigg[\frac{H_9 f_3(t_2) + H_{10} f_4(t_2)}{(x_1\sin\theta + y_1\cos\theta)(a + ib) + i(t_2 - x_1\cos\theta + y_1\sin\theta)}$$

$$+ \frac{H_{11} f_3(t_2) + H_{12} f_4(t_2)}{(x_1\sin\theta + y_1\cos\theta)(c + id) + i(t_2 - x_1\cos\theta + y_1\sin\theta)}$$

$$+ \frac{H_{13} f_3(t_2) + H_{14} f_4(t_2)}{(x_1\sin\theta + y_1\cos\theta)(a - ib) - i(t_2 - x_1\cos\theta + y_1\sin\theta)} \qquad (3.10)$$

$$+ \frac{H_{15} f_3(t_2) + H_{16} f_4(t_2)}{(x_1\sin\theta + y_1\cos\theta)(c - id) - i(t_2 - x_1\cos\theta + y_1\sin\theta)} \Bigg] dt_2$$

where

$$H_9 = \frac{1}{2}[\, R_1 + R_9 - (R_1 - R_9)\cos 2\theta - 2R_{17}\sin 2\theta \,]$$

$$H_{10} = -\frac{1}{2}[\, R_2 + R_{10} - (R_2 - R_{10})\cos 2\theta - 2R_{18}\sin 2\theta \,]$$

$$H_{11} = -\frac{1}{2}[\, R_4 + R_{12} - (R_4 - R_{12})\cos 2\theta - 2R_{20}\sin 2\theta \,]$$

$$H_{12} = \frac{1}{2}[\, R_3 + R_{11} - (R_3 - R_{11})\cos 2\theta - 2R_{19}\sin 2\theta \,]$$

$$H_{13} = \frac{1}{2}[\, R_5 + R_{13} - (R_5 - R_{13})\cos 2\theta - 2R_{21}\sin 2\theta \,]$$

$$H_{14} = -\frac{1}{2}[\, R_6 + R_{14} - (R_6 - R_{14})\cos 2\theta - 2R_{22}\sin 2\theta \,]$$

$$H_{15} = -\frac{1}{2}[\, R_8 + R_{16} - (R_8 - R_{16})\cos 2\theta - 2R_{24}\sin 2\theta \,]$$

$$H_{16} = \frac{1}{2}[\, R_7 + R_{15} + (R_7 - R_{15})\cos 2\theta + 2R_{23}\sin 2\theta \,]$$

and

$$\begin{aligned}
\tau'_{x_1 y_1} = \frac{1}{2\pi}\int_{x_2}^{x_1} \Bigg[& \frac{H_{17} f_3(t_2) + H_{18} f_4(t_2)}{(x_1\sin\theta + y_1\cos\theta)(a + ib) + i(t_2 - x_1\cos\theta + y_1\sin\theta)} \\
& + \frac{H_{19} f_3(t_2) + H_{20} f_4(t_2)}{(x_1\sin\theta + y_1\cos\theta)(c + id) + i(t_2 - x_1\cos\theta + y_1\sin\theta)} \\
& + \frac{H_{21} f_3(t_2) + H_{22} f_4(t_2)}{(x_1\sin\theta + y_1\cos\theta)(a - ib) - i(t_2 - x_1\cos\theta + y_1\sin\theta)} \\
& + \frac{H_{23} f_3(t_2) + H_{24} f_4(t_2)}{(x_1\sin\theta + y_1\cos\theta)(c - id) - i(t_2 - x_1\cos\theta + y_1\sin\theta)} \Bigg] dt_2
\end{aligned} \tag{3.11}$$

where

$$H_{17} = \frac{1}{2}[(R_9 - R_1)\sin 2\theta + 2R_{17}\cos 2\theta]$$

$$H_{18} = \frac{1}{2}[(R_2 - R_{10})\sin 2\theta - 2R_{18}\cos 2\theta]$$

$$H_{19} = \frac{1}{2}[(R_4 - R_{12})\sin 2\theta - 2R_{20}\cos 2\theta]$$

$$H_{20} = \frac{1}{2}[(R_{11} - R_3)\sin 2\theta + 2R_{19}\cos 2\theta]$$

$$H_{21} = \frac{1}{2}[(R_{13} - R_5)\sin 2\theta + 2R_{21}\cos 2\theta]$$

$$H_{22} = \frac{1}{2}[(R_6 - R_{14})\sin 2\theta - 2R_{22}\cos 2\theta]$$

$$H_{23} = \frac{1}{2}[(R_8 - R_{16})\sin 2\theta - 2R_{24}\cos 2\theta]$$

$$H_{24} = \frac{1}{2}[(R_{15} - R_7)\sin 2\theta + 2R_{23}\cos 2\theta]$$

Similarly, the transformed stresses of the first problem, when expressed in x_2-y_2 frame, (3.6) to (3.8) have the form:

$$\begin{aligned}\sigma'_{x_2x_2} = \frac{1}{2\pi}\int_{x_c}^{x_d} \Bigg[& \frac{G_1 f_1(t_1) + G_2 f_2(t_1)}{(-x_2\sin\theta + y_2\cos\theta)\omega_1 + i(t_1 - x_2\cos\theta - y_2\sin\theta)} \\ & + \frac{G_3 f_1(t_1) + G_4 f_2(t_1)}{(-x_2\sin\theta + y_2\cos\theta)\omega_2 + i(t_1 - x_2\cos\theta - y_2\sin\theta)} \\ & + \frac{G_5 f_1(t_1) + G_6 f_2(t_1)}{(-x_2\sin\theta + y_2\cos\theta)\omega_1 - i(t_1 - x_2\cos\theta - y_2\sin\theta)} \\ & + \frac{G_7 f_1(t_1) + G_8 f_2(t_1)}{(-x_2\sin\theta + y_2\cos\theta)\omega_2 - i(t_1 - x_2\cos\theta - y_2\sin\theta)} \Bigg] dt_1\end{aligned} \tag{3.12}$$

where

$$G_1 = \frac{1}{2}[\,T_1 + T_9 + (T_1 - T_9)\cos 2\theta - 2T_{17}\sin 2\theta\,]$$

$$G_2 = -\frac{1}{2}[\,T_2 + T_{10} + (T_2 - T_{10})\cos 2\theta - 2T_{18}\sin 2\theta]$$

$$G_3 = -\frac{1}{2}[\,T_4 + T_{12} + (T_4 - T_{12})\cos 2\theta - 2T_{20}\sin 2\theta\,]$$

$$G_4 = \frac{1}{2}[\,T_3 + T_{11} + (T_3 - T_{11})\cos 2\theta - 2T_{19}\sin 2\theta\,]$$

$$G_5 = \frac{1}{2}[\,T_5 + T_{13} + (T_5 - T_{13})\cos 2\theta - 2T_{21}\sin 2\theta\,]$$

$$G_6 = -\frac{1}{2}[\,T_6 + T_{14} + (T_6 - T_{14})\cos 2\theta - 2T_{22}\sin 2\theta\,]$$

$$G_7 = -\frac{1}{2}[\,T_8 + T_{16} + (T_8 - T_{16})\cos 2\theta - 2T_{24}\sin 2\theta\,]$$

$$G_8 = \frac{1}{2}[T_7 + T_{15} + (T_7 - T_{15})\cos 2\theta - 2T_{23}\sin 2\theta\,]$$

and

$$\sigma'_{y_2y_2} = \frac{1}{2\pi}\int_{x_c}^{x_d}\Bigg[\frac{G_9 f_1(t_1) + G_{10} f_2(t_1)}{(-x_2\sin\theta + y_2\cos\theta)\omega_1 + i(t_1 - x_2\cos\theta - y_2\sin\theta)} + \frac{G_{11} f_1(t_1) + G_{12} f_2(t_1)}{(-x_2\sin\theta + y_2\cos\theta)\omega_2 + i(t_1 - x_2\cos\theta - y_2\sin\theta)} + \frac{G_{13} f_1(t_1) + G_{14} f_2(t_1)}{(-x_2\sin\theta + y_2\cos\theta)\omega_1 - i(t_1 - x_2\cos\theta - y_2\sin\theta)} + \frac{G_{15} f_1(t_1) + G_{16} f_2(t_1)}{(-x_2\sin\theta + y_2\cos\theta)\omega_2 - i(t_1 - x_2\cos\theta - y_2\sin\theta)}\Bigg]\,dt_1 \qquad (3.13)$$

where

$$G_9 = \frac{1}{2}[\,T_1 + T_9 - (T_1 - T_9)\cos 2\theta + 2T_{17}\sin 2\theta\,]$$

$$G_{10} = -\frac{1}{2}[\,T_2 + T_{10} - (T_2 - T_{10})\cos 2\theta + 2T_{18}\sin 2\theta]$$

$$G_{11} = -\frac{1}{2}[\,T_4 + T_{12} - (T_4 - T_{12})\cos 2\theta + 2T_{20}\sin 2\theta\,]$$

$$G_{12} = \frac{1}{2}[\,T_3 + T_{11} - (T_3 - T_{11})\cos 2\theta + 2T_{19}\sin 2\theta\,]$$

$$G_{13} = \frac{1}{2}[\,T_5 + T_{13} - (T_5 - T_{13})\cos 2\theta + 2T_{21}\sin 2\theta\,]$$

$$G_{14} = -\frac{1}{2}[\,T_6 + T_{14} - (T_6 - T_{14})\cos 2\theta + 2T_{22}\sin 2\theta\,]$$

$$G_{15} = -\frac{1}{2}[\,T_8 + T_{16} - (T_8 - T_{16})\cos 2\theta + 2T_{24}\sin 2\theta\,]$$

$$G_{16} = \frac{1}{2}[T_7 + T_{15} - (T_7 - T_{15})\cos 2\theta + 2T_{23}\sin 2\theta\,]$$

and

$$\tau'_{x_2y_2} = \frac{1}{2\pi}\int_{x_c}^{x_d}\Bigg[\frac{G_{17}f_1(t_1) + G_{18}f_2(t_1)}{(-x_2\sin\theta + y_2\cos\theta)\omega_1 + i(t_1 - x_2\cos\theta - y_2\sin\theta)} + \frac{G_{19}f_1(t_1) + G_{20}f_2(t_1)}{(-x_2\sin\theta + y_2\cos\theta)\omega_2 + i(t_1 - x_2\cos\theta - y_2\sin\theta)} + \frac{G_{21}f_1(t_1) + G_{22}f_2(t_1)}{(-x_2\sin\theta + y_2\cos\theta)\omega_1 - i(t_1 - x_2\cos\theta - y_2\sin\theta)} + \frac{G_{23}f_1(t_1) + G_{24}f_2(t_1)}{(-x_2\sin\theta + y_2\cos\theta)\omega_2 - i(t_1 - x_2\cos\theta - y_2\sin\theta)}\Bigg]dt_1 \qquad (3.14)$$

where

$$G_{17} = \frac{1}{2}[(T_1 - T_9)\sin 2\theta + 2T_{17}\cos 2\theta\,]$$

$$G_{18} = \frac{1}{2}[(T_{10} - T_2)\sin 2\theta - 2T_{18}\cos 2\theta\,]$$

$$G_{19} = \frac{1}{2}[(T_{12} - T_4)\sin 2\theta - 2T_{20}\cos 2\theta\,]$$

$$G_{20} = \frac{1}{2}[(T_3 - T_{11})\sin 2\theta + 2T_{19}\cos 2\theta]$$

$$G_{21} = \frac{1}{2}[(T_5 - T_{13})\sin 2\theta + 2T_{21}\cos 2\theta]$$

$$G_{22} = \frac{1}{2}[(T_{14} - T_6)\sin 2\theta - 2T_{22}\cos 2\theta]$$

$$G_{23} = \frac{1}{2}[(T_{16} - T_8)\sin 2\theta - 2T_{24}\cos 2\theta]$$

$$G_{24} = \frac{1}{2}[(T_7 - T_{15})\sin 2\theta + 2T_{23}\cos 2\theta]$$

So, the total stress field for the infinite plate with two cracks is expressed by the stress components either expressed in x_1-y_1 frame:

$$\sigma^T_{x_1x_1} = \frac{1}{2\pi}\int_{x_c}^{x_d}\left[\frac{T_1 f_1(t_1) - T_2 f_2(t_1)}{y_1\omega_1 + i(t_1 - x_1)} + \frac{T_3 f_2(t_1) - T_4 f_1(t_1)}{y_1\omega_2 + i(t_1 - x_1)}\right.$$

$$\left. + \frac{T_5 f_1(t_1) - T_6 f_2(t_1)}{y_1\omega_1 - i(t_1 - x_1)} + \frac{T_7 f_2(t_1) - T_8 f_1(t_1)}{y_1\omega_2 - i(t_1 - x_1)}\right]dt_1$$

$$+ \frac{1}{2\pi}\int_{x_a}^{x_b}\left[\frac{H_1 f_3(t_2) + H_2 f_4(t_2)}{(x_1\sin\theta + y_1\cos\theta)(a + ib) + i(t_2 - x_1\cos\theta + y_1\sin\theta)}\right.$$

$$+ \frac{H_3 f_3(t_2) + H_4 f_4(t_2)}{(x_1\sin\theta + y_1\cos\theta)(c + id) + i(t_2 - x_1\cos\theta + y_1\sin\theta)} \qquad (3.15)$$

$$+ \frac{H_5 f_3(t_2) + H_6 f_4(t_2)}{(x_1\sin\theta + y_1\cos\theta)(a - ib) - i(t_2 - x_1\cos\theta + y_1\sin\theta)}$$

$$\left. + \frac{H_7 f_3(t_2) + H_8 f_4(t_2)}{(x_1\sin\theta + y_1\cos\theta)(c - id) - i(t_2 - x_1\cos\theta + y_1\sin\theta)}\right]dt_2$$

$$\sigma^{T}_{y_1y_1} = \frac{1}{2\pi}\int_{x_c}^{x_d}\left[\frac{T_9 f_1(t_1) - T_{10}f_2(t_1)}{y_1\omega_1 + i(t_1 - x_1)} + \frac{T_{11}f_2(t_1) - T_{12}f_1(t_1)}{y_1\omega_2 + i(t_1 - x_1)}\right.$$

$$\left. + \frac{T_{13}f_1(t_1) - T_{14}f_2(t_1)}{y_1\omega_1 - i(t_1 - x_1)} + \frac{T_{15}f_2(t_1) - T_{16}f_1(t_1)}{y_1\omega_2 - i(t_1 - x_1)}\right]dt_1$$

$$+ \frac{1}{2\pi}\int_{x_a}^{x_b}\left[\frac{H_9 f_3(t_2) + H_{10}f_4(t_2)}{(x_1\sin\theta + y_1\cos\theta)(a + ib) + i(t_2 - x_1\cos\theta + y_1\sin\theta)}\right.$$

$$+ \frac{H_{11}f_3(t_2) + H_{12}f_4(t_2)}{(x_1\sin\theta + y_1\cos\theta)(c + id) + i(t_2 - x_1\cos\theta + y_1\sin\theta)} \qquad (3.16)$$

$$+ \frac{H_{13}f_3(t_2) + H_{14}f_4(t_2)}{(x_1\sin\theta + y_1\cos\theta)(a - ib) - i(t_2 - x_1\cos\theta + y_1\sin\theta)}$$

$$\left. + \frac{H_{15}f_3(t_2) + H_{16}f_4(t_2)}{(x_1\sin\theta + y_1\cos\theta)(c - id) - i(t_2 - x_1\cos\theta + y_1\sin\theta)}\right]dt_2$$

$$
\begin{aligned}
\tau^{T}_{x_1 y_1} = \frac{1}{2\pi}\int_{x_c}^{x_d} \Bigg[& \frac{T_{17}f_1(t_1) - T_{18}f_2(t_1)}{y_1\omega_1 + i(t_1 - x_1)} + \frac{T_{19}f_2(t_1) - T_{20}f_1(t_1)}{y_1\omega_2 + i(t_1 - x_1)} \\
& + \frac{T_{21}f_1(t_1) - T_{22}f_2(t_1)}{y_1\omega_1 - i(t_1 - x_1)} + \frac{T_{23}f_2(t_1) - T_{24}f_1(t_1)}{y_1\omega_2 - i(t_1 - x_1)} \Bigg] dt_1 \\
+ \frac{1}{2\pi}\int_{x_a}^{x_b} \Bigg[& \frac{H_{17}f_3(t_2) + H_{18}f_4(t_2)}{(x_1\sin\theta + y_1\cos\theta)(a + ib) + i(t_2 - x_1\cos\theta + y_1\sin\theta)} \\
& + \frac{H_{19}f_3(t_2) + H_{20}f_4(t_2)}{(x_1\sin\theta + y_1\cos\theta)(c + id) + i(t_2 - x_1\cos\theta + y_1\sin\theta)} \\
& + \frac{H_{21}f_3(t_2) + H_{22}f_4(t_2)}{(x_1\sin\theta + y_1\cos\theta)(a - ib) - i(t_2 - x_1\cos\theta + y_1\sin\theta)} \\
& + \frac{H_{23}f_3(t_2) + H_{24}f_4(t_2)}{(x_1\sin\theta + y_1\cos\theta)(c - id) - i(t_2 - x_1\cos\theta + y_1\sin\theta)} \Bigg] dt_2
\end{aligned}
\tag{3.17}
$$

or the x_2-y_2 frame:

$$\sigma^{T}_{x_2x_2} = \frac{1}{2\pi}\int_{x_a}^{x_b}\left[\frac{R_1 f_3(t_2) - R_2 f_4(t_2)}{y_2(a+ib) + i(t_2 - x_2)} + \frac{R_3 f_4(t_2) - R_4 f_3(t_2)}{y_2(c+id) + i(t_2 - x_2)}\right.$$

$$\left. + \frac{R_5 f_3(t_2) - R_6 f_4(t_2)}{y_2(a-ib) - i(t_2 - x_2)} + \frac{R_7 f_4(t_2) - R_8 f_3(t_2)}{y_2(c-id) - i(t_2 - x_2)}\right] dt_2$$

$$+ \frac{1}{2\pi}\int_{x_c}^{x_d}\left[\frac{G_1 f_1(t_1) + G_2 f_2(t_1)}{(-x_2\sin\theta + y_2\cos\theta)\omega_1 + i(t_1 - x_2\cos\theta - y_2\sin\theta)}\right.$$

$$+ \frac{G_3 f_1(t_1) + G_4 f_2(t_1)}{(-x_2\sin\theta + y_2\cos\theta)\omega_2 + i(t_1 - x_2\cos\theta - y_2\sin\theta)} \tag{3.18}$$

$$+ \frac{G_5 f_1(t_1) + G_6 f_2(t_1)}{(-x_2\sin\theta + y_2\cos\theta)\omega_1 - i(t_1 - x_2\cos\theta - y_2\sin\theta)}$$

$$\left. + \frac{G_7 f_1(t_1) + G_8 f_2(t_1)}{(-x_2\sin\theta + y_2\cos\theta)\omega_2 - i(t_1 - x_2\cos\theta - y_2\sin\theta)}\right] dt_1$$

AD-A191 629 MIXED-MODE FRACTURE OF UNIAXIAL FIBER REINFORCED COMPOSITES(U) DREXEL UNIV PHILADELPHIA PA DEPT OF MECHANICAL ENGINEERING AN.. A S WANG ET AL. APR 87 2/2

UNCLASSIFIED NADC-87133-60 N62269-85-C-0246 F/G 11/4 NL

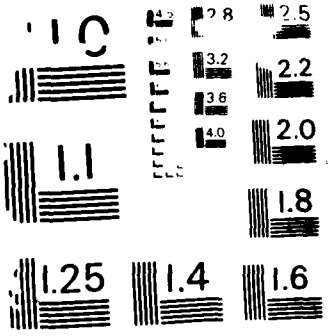

TEST CHART
NATIONAL BUREAU OF STANDARDS - 1963

$$\sigma^{T}_{y_2y_2} = \frac{1}{2\pi}\int_{x_a}^{x_b}\left[\frac{R_9 f_3(t_2) - R_{10} f_4(t_2)}{y_2(a+ib) + i(t_2 - x_2)} + \frac{R_{11} f_4(t_2) - R_{12} f_3(t_2)}{y_2(c+id) + i(t_2 - x_2)}\right.$$

$$\left. + \frac{R_{13} f_3(t_2) - R_{14} f_4(t_2)}{y_2(a-ib) - i(t_2 - x_2)} + \frac{R_{15} f_4(t_2) - R_{16} f_3(t_2)}{y_2(c-id) - i(t_2 - x_2)}\right] dt_2$$

$$+ \frac{1}{2\pi}\int_{x_c}^{x_d}\left[\frac{G_9 f_1(t_1) + G_{10} f_2(t_1)}{(-x_2\sin\theta + y_2\cos\theta)\omega_1 + i(t_1 - x_2\cos\theta - y_2\sin\theta)}\right. \tag{3.19}$$

$$+ \frac{G_{11} f_1(t_1) + G_{12} f_2(t_1)}{(-x_2\sin\theta + y_2\cos\theta)\omega_2 + i(t_1 - x_2\cos\theta - y_2\sin\theta)}$$

$$+ \frac{G_{13} f_1(t_1) + G_{14} f_2(t_1)}{(-x_2\sin\theta + y_2\cos\theta)\omega_1 - i(t_1 - x_2\cos\theta - y_2\sin\theta)}$$

$$\left. + \frac{G_{15} f_1(t_1) + G_{16} f_2(t_1)}{(-x_2\sin\theta + y_2\cos\theta)\omega_2 - i(t_1 - x_2\cos\theta - y_2\sin\theta)}\right] dt_1$$

$$\tau^T_{x_2y_2} = \frac{1}{2\pi}\int_{x_a}^{x_b}\left[\frac{R_{17}f_3(t_2) - R_{18}f_4(t_2)}{y_2(a+ib) + i(t_2 - x_2)} + \frac{R_{19}f_4(t_2) - R_{20}f_3(t_2)}{y_2(c+id) + i(t_2 - x_2)}\right.$$

$$\left. + \frac{R_{21}f_3(t_2) - R_{22}f_4(t_2)}{y_2(a-ib) - i(t_2 - x_2)} + \frac{R_{23}f_4(t_2) - R_{24}f_3(t_2)}{y_2(c-id) - i(t_2 - x_2)}\right] dt_2$$

$$+ \frac{1}{2\pi}\int_{x_c}^{x_d}\left[\frac{G_{17}f_1(t_1) + G_{18}f_2(t_1)}{(-x_2\sin\theta + y_2\cos\theta)\omega_1 + i(t_1 - x_2\cos\theta - y_2\sin\theta)}\right. \tag{3.20}$$

$$+ \frac{G_{19}f_1(t_1) + G_{20}f_2(t_1)}{(-x_2\sin\theta + y_2\cos\theta)\omega_2 + i(t_1 - x_2\cos\theta - y_2\sin\theta)}$$

$$+ \frac{G_{21}f_1(t_1) + G_{22}f_2(t_1)}{(-x_2\sin\theta + y_2\cos\theta)\omega_1 - i(t_1 - x_2\cos\theta - y_2\sin\theta)}$$

$$\left. + \frac{G_{23}f_1(t_1) + G_{24}f_2(t_1)}{(-x_2\sin\theta + y_2\cos\theta)\omega_2 - i(t_1 - x_2\cos\theta - y_2\sin\theta)}\right] dt_1$$

In the stresses (3.15-3.17) or (3.18-3.20), there are four unknown functions f_1, f_2, f_3, f_4 which must be determined from the appropriate boundary conditions for this problem. Since the plate is under uniaxial tension σ_0, for the crack lying on x_2 $(x_a < x_2 < x_b)$ we have:

$$\sigma^T_{y_2y_2} = -\sigma_0 \tag{3.21}$$

$$\tau^T_{x_2y_2} = 0 \tag{3.22}$$

And, for the crack lying on x_1 $(x_c < x_1 < x_d)$ we have:

$$\sigma^T_{y_1y_1} = -\sigma_0\cos^2\theta \tag{3.23}$$

$$\tau^T_{x_1y_1} = -\sigma_0\sin\theta\cos\theta \tag{3.24}$$

applying these four boundaries and normalizing the variables x and t by substituting the following:

$$t_2 = \frac{\tau_2(x_b - x_a)}{2} + \frac{x_b + x_a}{2} \tag{3.25}$$

$$x_2 = \frac{s_2(x_b - x_a)}{2} + \frac{x_b + x_a}{2} \tag{3.26}$$

$$dt_2 = \frac{x_b - x_a}{2} d\tau_2 \qquad -1 < \tau_2, s_2 < 1 \tag{3.27}$$

and

$$t_1 = \frac{\tau_1(x_d - x_c)}{2} + \frac{x_d + x_c}{2} \tag{3.28}$$

$$x_1 = \frac{s_1(x_d - x_c)}{2} + \frac{x_d + x_c}{2} \tag{3.29}$$

$$dt_1 = \frac{x_d - x_c}{2} d\tau_1 \qquad -1 < \tau_1, s_1 < 1 \tag{3.30}$$

a set of Cauchy type singular integral equations is obtained as follows:

$$C_{12} \int_{-1}^{1} \frac{f_2(\tau_1)}{\tau_1 - s_1} d\tau_1 + \int_{-1}^{1} K_{13} f_3(\tau_2)\, d\tau_2 + \int_{-1}^{1} K_{14} f_4(\tau_2)\, d\tau_2 = -\sigma_0 \cos^2\theta \tag{3.31}$$

$$C_{21} \int_{-1}^{1} \frac{f_2(\tau_1)}{\tau_1 - s_1} d\tau_1 + \int_{-1}^{1} K_{23} f_3(\tau_2)\, d\tau_2 + \int_{-1}^{1} K_{24} f_4(\tau_2)\, d\tau_2 = -\sigma_0 \sin\theta \cos\theta \tag{3.32}$$

$$C_{33} \int_{-1}^{1} \frac{f_3(\tau_2)}{\tau_2 - s_2} d\tau_2 + C_{34} \int_{-1}^{1} \frac{f_4(\tau_2)}{\tau_2 - s_2} d\tau_2 + \int_{-1}^{1} K_{31} f_1(\tau_1)\, d\tau_1 + \int_{-1}^{1} K_{32} f_2(\tau_1)\, d\tau_1 = -\sigma_0 \tag{3.33}$$

$$C_{43} \int_{-1}^{1} \frac{f_3(\tau_2)}{\tau_2 - s_2} d\tau_2 + C_{44} \int_{-1}^{1} \frac{f_4(\tau_2)}{\tau_2 - s_2} d\tau_2 + \int_{-1}^{1} K_{41} f_1(\tau_1)\, d\tau_1 + \int_{-1}^{1} K_{42} f_2(\tau_1)\, d\tau_1 = 0 \tag{3.34}$$

which must be solved for the unknown functions f_1, f_2, f_3 and f_4. For single-valuedness of solution it is necessary to use also additional conditions which in this case are going to be equations of the following form:

$$\int_{-1}^{1} f_1(\tau)\,d\tau = 0 \qquad (3.35) \qquad\qquad \int_{-1}^{1} f_2(\tau)\,d\tau = 0 \qquad (3.36)$$

$$\int_{-1}^{1} f_3(\tau)\,d\tau = 0 \qquad (3.37) \qquad\qquad \int_{-1}^{1} f_4(\tau)\,d\tau = 0 \qquad (3.38)$$

The constants C's in (3.31 -3.34) are real numbers and are calculated according to the following expressions:

$$C_{12} = \frac{T_{14} + T_{11} - T_{10} - T_{15}}{2\pi i}; \qquad C_{34} = \frac{R_{11} - R_{10} + R_{14} - R_{15}}{2\pi i};$$

$$C_{21} = \frac{T_{17} - T_{20} - T_{21} + T_{24}}{2\pi i}; \qquad C_{43} = \frac{R_{17} - R_{20} - R_{21} + R_{24}}{2\pi i};$$

$$C_{33} = \frac{R_9 - R_{12} - R_{13} + R_{16}}{2\pi i}; \qquad C_{44} = \frac{R_{19} - R_{18} + R_{22} - R_{23}}{2\pi i};$$

The Cauchy type kernels K_{ij} are defined as follow:

$$K_{13} = \frac{x_b - x_a}{2\pi}\left[\frac{H_9}{[s_1(x_d - x_c) + x_d + x_c][\sin\theta(a + ib) - i\cos\theta] + i[\tau_2(x_b - x_a) + x_b + x_a]}\right.$$

$$+ \frac{H_{11}}{[s_1(x_d - x_c) + x_d + x_c][\sin\theta(c + id) - i\cos\theta] + i[\tau_2(x_b - x_a) + x_b + x_a]}$$

$$+ \frac{H_{13}}{[s_1(x_d - x_c) + x_d + x_c][\sin\theta(a - ib) + i\cos\theta] - i[\tau_2(x_b - x_a) + x_b + x_a]}$$

$$\left. + \frac{H_{15}}{[s_1(x_d - x_c) + x_d + x_c][\sin\theta(c - id) + i\cos\theta] - i[\tau_2(x_b - x_a) + x_b + x_a]}\right]$$

$$K_{14} = \frac{x_b - x_a}{2\pi} \left[\frac{H_{10}}{[s_1(x_d - x_c) + x_d + x_c][\sin\theta(a + ib) - i\cos\theta] + i[\tau_2(x_b - x_a) + x_b + x_a]} \right.$$

$$+ \frac{H_{12}}{[s_1(x_d - x_c) + x_d + x_c][\sin\theta(c + id) - i\cos\theta] + i[\tau_2(x_b - x_a) + x_b + x_a]}$$

$$+ \frac{H_{14}}{[s_1(x_d - x_c) + x_d + x_c][\sin\theta(a - ib) + i\cos\theta] - i[\tau_2(x_b - x_a) + x_b + x_a]}$$

$$\left. + \frac{H_{16}}{[s_1(x_d - x_c) + x_d + x_c][\sin\theta(c - id) + i\cos\theta] - i[\tau_2(x_b - x_a) + x_b + x_a]} \right]$$

$$K_{23} = \frac{x_b - x_a}{2\pi} \left[\frac{H_{17}}{[s_1(x_d - x_c) + x_d + x_c][\sin\theta(a + ib) - i\cos\theta] + i[\tau_2(x_b - x_a) + x_b + x_a]} \right.$$

$$+ \frac{H_{19}}{[s_1(x_d - x_c) + x_d + x_c][\sin\theta(c + id) - i\cos\theta] + i[\tau_2(x_b - x_a) + x_b + x_a]}$$

$$+ \frac{H_{21}}{[s_1(x_d - x_c) + x_d + x_c][\sin\theta(a - ib) + i\cos\theta] - i[\tau_2(x_b - x_a) + x_b + x_a]}$$

$$\left. + \frac{H_{23}}{[s_1(x_d - x_c) + x_d + x_c][\sin\theta(c - id) + i\cos\theta] - i[\tau_2(x_b - x_a) + x_b + x_a]} \right]$$

$$K_{24} = \frac{x_b - x_a}{2\pi} \left[\frac{H_{18}}{[s_1(x_d - x_c) + x_d + x_c][\sin\theta(a + ib) - i\cos\theta] + i[\tau_2(x_b - x_a) + x_b + x_a]} \right.$$

$$+ \frac{H_{20}}{[s_1(x_d - x_c) + x_d + x_c][\sin\theta(c + id) - i\cos\theta] + i[\tau_2(x_b - x_a) + x_b + x_a]}$$

$$+ \frac{H_{22}}{[s_1(x_d - x_c) + x_d + x_c][\sin\theta(a - ib) + i\cos\theta] - i[\tau_2(x_b - x_a) + x_b + x_a]}$$

$$\left. + \frac{H_{24}}{[s_1(x_d - x_c) + x_d + x_c][\sin\theta(c - id) + i\cos\theta] - i[\tau_2(x_b - x_a) + x_b + x_a]} \right]$$

$$K_{31} = \frac{x_d - x_c}{2\pi} \left[\frac{G_9}{-[s_2(x_b - x_a) + x_b + x_a][\sin\theta\,\omega_1 + i\cos\theta] + i[\tau_1(x_d - x_c) + x_d + x_c]} \right.$$

$$+ \frac{G_{11}}{-[s_2(x_b - x_a) + x_b + x_a][\sin\theta\,\omega_2 + i\cos\theta] + i[\tau_1(x_d - x_c) + x_d + x_c]}$$

$$+ \frac{G_{13}}{-[s_2(x_b - x_a) + x_b + x_a][\sin\theta\,\omega_1 - i\cos\theta] - i[\tau_1(x_d - x_c) + x_d + x_c]}$$

$$\left. + \frac{G_{15}}{-[s_2(x_b - x_a) + x_b + x_a][\sin\theta\,\omega_2 - i\cos\theta] - i[\tau_1(x_d - x_c) + x_d + x_c]} \right]$$

$$K_{32} = \frac{x_d - x_c}{2\pi} \left[\frac{G_{10}}{-[s_2(x_b - x_a) + x_b + x_a][\sin\theta\,\omega_1 + i\cos\theta] + i[\tau_1(x_d - x_c) + x_d + x_c]} \right.$$

$$+ \frac{G_{12}}{-[s_2(x_b - x_a) + x_b + x_a][\sin\theta\,\omega_2 + i\cos\theta] + i[\tau_1(x_d - x_c) + x_d + x_c]}$$

$$+ \frac{G_{14}}{-[s_2(x_b - x_a) + x_b + x_a][\sin\theta\,\omega_1 - i\cos\theta] - i[\tau_1(x_d - x_c) + x_d + x_c]}$$

$$\left. + \frac{G_{16}}{-[s_2(x_b - x_a) + x_b + x_a][\sin\theta\,\omega_2 - i\cos\theta] - i[\tau_1(x_d - x_c) + x_d + x_c]} \right]$$

$$K_{41} = \frac{x_d - x_c}{2\pi} \left[\frac{G_{17}}{-[s_2(x_b - x_a) + x_b + x_a][\sin\theta\,\omega_1 + i\cos\theta] + i[\tau_1(x_d - x_c) + x_d + x_c]} \right.$$

$$+ \frac{G_{19}}{-[s_2(x_b - x_a) + x_b + x_a][\sin\theta\,\omega_2 + i\cos\theta] + i[\tau_1(x_d - x_c) + x_d + x_c]}$$

$$+ \frac{G_{21}}{-[s_2(x_b - x_a) + x_b + x_a][\sin\theta\,\omega_1 - i\cos\theta] - i[\tau_1(x_d - x_c) + x_d + x_c]}$$

$$\left. + \frac{G_{23}}{-[s_2(x_b - x_a) + x_b + x_a][\sin\theta\,\omega_2 - i\cos\theta] - i[\tau_1(x_d - x_c) + x_d + x_c]} \right]$$

$$K_{42} = \frac{x_d - x_c}{2\pi} \left[\frac{G_{18}}{-[s_2(x_b - x_a) + x_b + x_a][\sin\theta\,\omega_1 + i\cos\theta] + i[\tau_1(x_d - x_c) + x_d + x_c]} \right.$$

$$+ \frac{G_{20}}{-[s_2(x_b - x_a) + x_b + x_a][\sin\theta\,\omega_2 + i\cos\theta] + i[\tau_1(x_d - x_c) + x_d + x_c]}$$

$$+ \frac{G_{22}}{-[s_2(x_b - x_a) + x_b + x_a][\sin\theta\,\omega_1 - i\cos\theta] - i[\tau_1(x_d - x_c) + x_d + x_c]}$$

$$\left. + \frac{G_{24}}{-[s_2(x_b - x_a) + x_b + x_a][\sin\theta\,\omega_2 - i\cos\theta] - i[\tau_1(x_d - x_c) + x_d + x_c]} \right]$$

IV. Method of solution - set of Cauchy type integral equations.

The set of equations (3.31-3.34) are known as singular Cauchy type integral equations. They can be solved by using Lobatto-Tchebyshev collocation method. In this method, we replace each equation by n linear algebraic equations of the following structure:

$$C_{\alpha\beta}\sum_{k=1}^{n}\frac{F_\beta(\tau_k)\,W_k}{\tau_k - x_j} + \sum_{k=1}^{n} K_{\alpha\beta}\,F_\gamma(\tau_k)\,W_k = p(x_j) \tag{4.1}$$

where $\alpha,\beta = 1,2,3,4$ and

$$\tau_k = \cos\frac{(k-1)\pi}{n-1} \qquad k=1,2,\ldots,n \tag{4.2}$$

$$W_1 = W_n = \frac{\pi}{2(n-1)} \qquad W_r = \frac{\pi}{n-1} \qquad r = 2,3,\ldots,n-1 \tag{4.3}$$

$$x_j = \cos\frac{(2j-1)\pi}{2n-2} \qquad j = 1,2,\ldots,n-1 \tag{4.4}$$

Also, equations (3.35-3.38) are replaced by:

$$\sum_{k=1}^{n} F_\beta(\tau_k)\,W_k = 0 \tag{4.5}$$

Hence, the set of integral equations together with conditions are reduced mathematically to set of 4n algebraic equations with 4n unknowns in the form:

$$[A]\,\{F\} = \{P\} \tag{4.6}$$

where [A] is 4n x 4n matrix of coefficients and { P } is loading function vector. So the solution of the problem is:

$$\{F\} = [A]^{-1}\,\{P\} \tag{4.7}$$

V. Stress intensity factors.

Stress intensity factors at the tips of the crack are defined as follow:

$$k_1(x_a) = \lim_{x_2 \to x_a} \sqrt{2(x_a - x_2)}\ \sigma_{y_2y_2}(x_2, 0) \tag{5.1}$$

$$k_2(x_a) = \lim_{x_2 \to x_a} \sqrt{2(x_a - x_2)}\ \tau_{x_2y_2}(x_2, 0) \tag{5.2}$$

$$k_1(x_b) = \lim_{x_2 \to x_b} \sqrt{2(x_2 - x_b)}\ \sigma_{y_2y_2}(x_2, 0) \tag{5.3}$$

$$k_2(x_b) = \lim_{x_2 \to x_b} \sqrt{2(x_2 - x_b)}\ \tau_{x_2y_2}(x_2, 0) \tag{5.4}$$

$$k_1(x_c) = \lim_{x_1 \to x_c} \sqrt{2(x_c - x_1)}\ \sigma_{y_1y_1}(x_1, 0) \tag{5.5}$$

$$k_2(x_c) = \lim_{x_1 \to x_c} \sqrt{2(x_c - x_1)}\ \tau_{x_1y_1}(x_1, 0) \tag{5.6}$$

$$k_1(x_d) = \lim_{x_1 \to x_d} \sqrt{2(x_1 - x_d)}\ \sigma_{y_1y_1}(x_1, 0) \tag{5.7}$$

$$k_2(x_d) = \lim_{x_1 \to x_d} \sqrt{2(x_1 - x_d)}\ \tau_{x_1y_1}(x_1, 0) \tag{5.8}$$

where the stresses are the total stresses (the superscript T is omitted).

It is also possible to express the stress intensity factors in t rms of a special function evaluated at the ends of the crack ie. $F_\mu(1)$ or $F_\mu(-1)$ (μ=1,2,3,4) by applying the following transformation to the singular part of stress equations.

It is known, [1] and [2], that the singular behavior around the end points of the crack can be expressed by:

$$\frac{1}{\pi}\int_a^b \frac{f(t)}{t-z}\,dt = -F(a)(b-a)^{\alpha}\frac{e^{-\pi i\beta}}{\sin\pi\beta}(z-a)^{\beta} + F(b)(b-a)^{\beta}\frac{1}{\sin\pi\alpha}(z-b)^{\alpha} + 0(z) \qquad (5.9)$$

where α,β are order of singularity at a,b respectively; z is a complex number; 0(z) is a higer order error term which can be neglected. Function F(t) is assumed to be bounded because singular behavior of f(t) is completely determined by the fundamental function w(t). For this class of problems in elasticity the fundamental function is of the form:

$$w(t) = (b-t)^{\alpha}(t-a)^{\beta} \qquad (5.9a)$$

Thus, we can write:

$$f_{\alpha}(t) \cong F_{\alpha}(t)(b-t)^{\alpha}(t-a)^{\beta} \qquad (5.9b)$$

If the singularity at the crack tips is -0.5 and a=-1, b=1 equation (5.9a) can be written as:

$$f_{\alpha}(t) \cong \frac{F_{\alpha}(t)}{\sqrt{t^2-1}} \qquad (5.9c)$$

Using the above equations, it is assumed that, the order of singularity at:

$$\begin{array}{lll} x_a & \text{is} & \beta_2 \\ x_b & \text{is} & \alpha_2 \\ x_c & \text{is} & \beta_1 \\ x_d & \text{is} & \alpha_1 \end{array} \qquad (5.9d)$$

It will be shown in the case of a skewed crack configuration, that the order of singularity at the common point (x_b=x_c=0) is not equal to -0.5, while at x_a and x_d it

remains -0.5.

Applying the transformation (3.26),(3.29) into equations (5.1-5.8) we obtain the stress intensity factor $k_1(x_a)$ as:

$$k_1(x_a) = \lim_{s_2 \to -1} \sqrt{2\left(x_a - s_2 \frac{x_b - x_a}{2} - \frac{x_b + x_a}{2}\right)}\ \sigma_{y_2y_2}(s_2, 0) =$$

$$= \lim_{s_2 \to -1} \sqrt{2\left(-\frac{x_b - x_a}{2}\right)(1 + s_2)}\ \sigma_{y_2y_2}(s_2, 0) = \tag{5.10}$$

$$= \lim_{s_2 \to -1} \sqrt{x_b - x_a}\ \sqrt{(-1)(1 + s_2)}\ \sigma_{y_2y_2}(s_2, 0)$$

All the singular terms in equations (3.31-3.34) are transformed using (5.9). For the case of a=-1 and b=1, the first two terms of (3.31) become:

$$\pi C_{33} \frac{1}{\pi} \int_{-1}^{1} \frac{f_3(\tau_2)}{\tau_2 - s_2} d\tau_2 = \pi C_{33} \left\{ -F_3(-1) \frac{1}{\sqrt{2}} \frac{e^{\frac{i\pi}{2}}}{\sin(-\frac{\pi}{2})} (s_2 + 1)^{-\frac{1}{2}} + F_3(1) \frac{1}{\sqrt{2}} \frac{1}{\sin(-\frac{\pi}{2})} (s_2 - 1)^{-\frac{1}{2}} \right\} \tag{5.11}$$

$$\pi C_{34} \frac{1}{\pi} \int_{-1}^{1} \frac{f_4(\tau_2)}{\tau_2 - s_2} d\tau_2 = \pi C_{34} \left\{ -F_4(-1) \frac{1}{\sqrt{2}} \frac{e^{\frac{i\pi}{2}}}{\sin(-\frac{\pi}{2})} (s_2 + 1)^{-\frac{1}{2}} + F_4(1) \frac{1}{\sqrt{2}} \frac{1}{\sin(-\frac{\pi}{2})} (s_2 - 1)^{-\frac{1}{2}} \right\} \tag{5.12}$$

Finally substituting the sum of (5.11) and (5.12) for $\sigma_{y2y2}(s_2,0)$ into (5.10) we have:

$$k_1(x_a) = \pi \sqrt{\frac{x_b - x_a}{2}} \left[C_{33} F_3(-1) + C_{34} F_4(-1) \right] \tag{5.13}$$

All the other stress intensity factors are obtained in a similar way.

Hence,

$$k_2(x_a) = \pi \sqrt{\frac{x_b - x_a}{2}} \left[C_{43} F_3(-1) + C_{44} F_4(-1) \right] \tag{5.14}$$

$$k_1(x_b) = -\pi \sqrt{\frac{x_b - x_a}{2}} \left[C_{33} F_3(1) + C_{34} F_4(1) \right] \tag{5.15}$$

$$k_2(x_b) = -\pi \sqrt{\frac{x_b - x_a}{2}} \left[C_{43} F_3(1) + C_{44} F_4(1) \right] \tag{5.16}$$

$$k_1(x_c) = \pi \sqrt{\frac{x_d - x_c}{2}} C_{12} F_2(-1) \tag{5.17}$$

$$k_2(x_c) = \pi \sqrt{\frac{x_d - x_c}{2}} C_{21} F_1(-1) \tag{5.18}$$

$$k_1(x_d) = -\pi \sqrt{\frac{x_d - x_c}{2}} C_{12} F_2(1) \tag{5.19}$$

$$k_2(x_d) = -\pi \sqrt{\frac{x_d - x_c}{2}} C_{21} F_1(1) \tag{5.20}$$

VI. Skew Crack Configuration $x_b=x_c=0$.

Introduction.

By setting $x_b=x_c=0$ in equations (3.15-3.20) we have the case of a skewed crack in an infinite plate. The boundary conditions (3.21-3.24) remain the same and equations (3.15-3.30) become:

$$t_2 = (1 - \tau_2)\frac{x_a}{2} \tag{6.1}$$

$$x_2 = (1 - s_2)\frac{x_a}{2} \qquad -1 < \tau_2, s_2 < 1 \tag{6.2}$$

$$dt_2 = -\frac{x_a}{2} d\tau_2 \tag{6.3}$$

$$t_1 = (1 + \tau_1)\frac{x_d}{2} \tag{6.4}$$

$$x_1 = (1 + s_1)\frac{x_d}{2} \qquad -1 < \tau_1, s_1 < 1 \tag{6.5}$$

$$dt_1 = \frac{x_d}{2} d\tau_1 \tag{6.6}$$

Normalizing the integral equations with (6.1-6.6) we obtain again a set of integral equations as (3.31-3.34), however the kernels become singular when t_K and x_j approach the common point (x_b=x_c=0). Thus, a different kind of collocation method has to be employed. Also (3.35-3.38) no longer holds, so another set of constraints must be applied.

If one attempts to use the Lobatto-Tchebyshev collocation method as a rough approximation, then the following conditions can be used:

$$F_1(-1) = 0 \tag{6.7}$$

$$F_2(-1) = 0 \tag{6.8}$$

$$F_3(1) = 0 \tag{6.9}$$

$$F_4(1) = 0 \tag{6.10}$$

since we have to assume that the function f(t) is approximated by F(t), for example:

$$f_3(t) \cong \frac{F_3(t)}{\sqrt{t^2 - 1}}$$

but as it was mention above, in the skew crack case at the common point (x_b=x_c=0) the order of singularity is not -0.5, the proper fundamental function is actually:

$$f_3(t) \cong \frac{F_3^{\bullet}(t)}{\sqrt{t+1}}(t-1)^{\alpha}$$

where $F^{\bullet}$ is new bounded function and α is not -0.5. Considering the above we have:

$$F_3(t) = F_3^{\bullet}(t)\sqrt{t-1}\,(t-1)^{\alpha} \overset{t=1}{\Longrightarrow} F_3(1) = F_3^{\bullet}(1)\cdot 0 = 0$$

ave:

similar arguments (6.8-6.10) can also be proved.

It is better, however, to use the Gauss-Jacobi or Lobatto-Jacobi collocation method, because the general order of singularity β can be applied. In this case, we can use the additional constraint, that the displacements at the common point must be the same, either for the main or for the kink crack:

$$x_d \int_{-1}^{1} f_2(\tau_1)\, d\tau_1 = x_a \int_{-1}^{1} \left[f_3(\tau_2)\sin\theta - f_4(\tau_2)\cos\theta \right] d\tau_2 \tag{6.11}$$

$$x_d \int_{-1}^{1} f_1(\tau_1)\, d\tau_1 = -x_a \int_{-1}^{1} \left[f_3(\tau_2)\cos\theta + f_4(\tau_2)\sin\theta \right] d\tau_2 \tag{6.12}$$

We also need two additional equations and to determine the order of singularity β at the "wedge appex" ie. common point of both cracks (0,0).

Singularity order for a kink crack problem.

Let's start with (3.31) where we set $x_b=x_c=0$. Then, the kernel becomes:

$$K_{13} = \frac{1}{2\pi}\left[\frac{H_9}{(-\frac{x_d}{x_a})(s_1+1)[\sin\theta(a+ib)-i\cos\theta]+i(\tau_2-1)}\right.$$

$$+\frac{H_{11}}{(-\frac{x_d}{x_a})(s_1+1)[\sin\theta(c+id)-i\cos\theta]+i(\tau_2-1)}$$

$$+\frac{H_{13}}{(-\frac{x_d}{x_a})(s_1+1)[\sin\theta(a-ib)+i\cos\theta]-i(\tau_2-1)}$$

$$\left.+\frac{H_{15}}{(-\frac{x_d}{x_a})(s_1+1)[\sin\theta(c-id)+i\cos\theta]-i(\tau_2-1)}\right]$$

or

$$K_{13} = \frac{1}{2}\frac{1}{\pi}\left[\frac{-i\,H_9}{(\tau_2-1)-i\left(-\frac{x_d}{x_a}\right)[\sin\theta(a+ib)-i\cos\theta](s_1+1)}\right.$$

$$+\frac{-i\,H_{11}}{(\tau_2-1)-i\left(-\frac{x_d}{x_a}\right)[\sin\theta(c+id)-i\cos\theta](s_1+1)}$$

$$+\frac{i\,H_{13}}{(\tau_2-1)+i\left(-\frac{x_d}{x_a}\right)[\sin\theta(a-ib)+i\cos\theta](s_1+1)}$$

$$\left.+\frac{i\,H_{15}}{(\tau_2-1)+i\left(-\frac{x_d}{x_a}\right)[\sin\theta(c-id)+i\cos\theta](s_1+1)}\right]$$

Let's define new variables as follow:

$$\rho_2 = \tau_2 - 1 \qquad -2 < \rho_2 < 0 \qquad d\rho_2 = d\tau_2 \tag{6.13}$$

and

$$w_1 = [\cos\theta + i\sin\theta\,(a + ib)]\left(-\frac{x_d}{x_a}\right)(s_1 + 1) \tag{6.14}$$

$$w_2 = [\cos\theta + i\sin\theta\,(c + id)]\left(-\frac{x_d}{x_a}\right)(s_1 + 1) \tag{6.15}$$

$$w_3 = [\cos\theta + i\sin\theta\,(a - ib)]\left(-\frac{x_d}{x_a}\right)(s_1 + 1) \tag{6.16}$$

$$w_4 = [\cos\theta + i\sin\theta\,(c - id)]\left(-\frac{x_d}{x_a}\right)(s_1 + 1) \tag{6.17}$$

Noting structural similarity between K_{13}, K_{14}, K_{23} and K_{24} also substituting (6.13-6.17) in (3.31) and in (3.32) we obtain:

$$\begin{aligned}
&\pi C_{12}\frac{1}{\pi}\int_{-1}^{1}\frac{f_2(\tau_1)}{\tau_1 - s_1}d\tau_1 + \frac{i}{2}\Bigg[- H_9\frac{1}{\pi}\int_{-2}^{0}\frac{f_3(\rho_2)}{\rho_2 - w_1}d\rho_2 \\
&- H_{11}\frac{1}{\pi}\int_{-2}^{0}\frac{f_3(\rho_2)}{\rho_2 - w_2}d\rho_2 + H_{13}\frac{1}{\pi}\int_{-2}^{0}\frac{f_3(\rho_2)}{\rho_2 - w_3}d\rho_2 \\
&+ H_{15}\frac{1}{\pi}\int_{-2}^{0}\frac{f_3(\rho_2)}{\rho_2 - w_4}d\rho_2 - H_{10}\frac{1}{\pi}\int_{-2}^{0}\frac{f_4(\rho_2)}{\rho_2 - w_1}d\rho_2 \\
&- H_{12}\frac{1}{\pi}\int_{-2}^{0}\frac{f_4(\rho_2)}{\rho_2 - w_2}d\rho_2 + H_{14}\frac{1}{\pi}\int_{-2}^{0}\frac{f_4(\rho_2)}{\rho_2 - w_3}d\rho_2 \\
&+ H_{16}\frac{1}{\pi}\int_{-2}^{0}\frac{f_4(\rho_2)}{\rho_2 - w_4}d\rho_2 \Bigg] = -\sigma_0\cos^2\theta
\end{aligned} \tag{6.18}$$

and

$$\pi C_{21}\frac{1}{\pi}\int_{-1}^{1}\frac{f_2(\tau_1)}{\tau_1 - s_1}d\tau_1 + \frac{i}{2}\Bigg[- H_{17}\frac{1}{\pi}\int_{-2}^{0}\frac{f_3(\rho_2)}{\rho_2 - w_1}d\rho_2$$

$$- H_{19}\frac{1}{\pi}\int_{-2}^{0}\frac{f_3(\rho_2)}{\rho_2 - w_2}d\rho_2 + H_{21}\frac{1}{\pi}\int_{-2}^{0}\frac{f_3(\rho_2)}{\rho_2 - w_3}d\rho_2$$

$$+ H_{23}\frac{1}{\pi}\int_{-2}^{0}\frac{f_3(\rho_2)}{\rho_2 - w_4}d\rho_2 - H_{18}\frac{1}{\pi}\int_{-2}^{0}\frac{f_4(\rho_2)}{\rho_2 - w_1}d\rho_2 \tag{6.19}$$

$$- H_{20}\frac{1}{\pi}\int_{-2}^{0}\frac{f_4(\rho_2)}{\rho_2 - w_2}d\rho_2 + H_{22}\frac{1}{\pi}\int_{-2}^{0}\frac{f_4(\rho_2)}{\rho_2 - w_3}d\rho_2$$

$$+ H_{24}\frac{1}{\pi}\int_{-2}^{0}\frac{f_4(\rho_2)}{\rho_2 - w_4}d\rho_2\Bigg] = - \sigma_0 \sin\theta \cos\theta$$

Performing similar operations on (3.33) we obtain:

$$K_{31} = \frac{1}{2\pi}\Bigg[\frac{G_9}{\left(-\frac{X_a}{X_d}\right)(1 - s_2)(\sin\theta\,\omega_1 + i\cos\theta) + i(\tau_1 + 1)}$$

$$+ \frac{G_{11}}{\left(-\frac{X_a}{X_d}\right)(1 - s_2)(\sin\theta\,\omega_2 + i\cos\theta) + i(\tau_1 + 1)}$$

$$+ \frac{G_{13}}{\left(-\frac{X_a}{X_d}\right)(1 - s_2)(\sin\theta\,\omega_1 - i\cos\theta) - i(\tau_1 + 1)}$$

$$+ \frac{G_{15}}{\left(-\frac{X_a}{X_d}\right)(1 - s_2)(\sin\theta\,\omega_2 - i\cos\theta) - i(\tau_1 + 1)}\Bigg]$$

or

$$K_{31} = \frac{1}{2}\frac{1}{\pi}\left[\frac{-iG_9}{(\tau_1+1) - i\left(-\frac{X_a}{X_d}\right)(1-s_2)(\sin\theta\,\omega_1 + i\cos\theta)}\right.$$

$$+\frac{-iG_{11}}{(\tau_1+1) - i\left(-\frac{X_a}{X_d}\right)(1-s_2)(\sin\theta\,\omega_2 + i\cos\theta)}$$

$$+\frac{iG_{13}}{(\tau_1+1) + i\left(-\frac{X_a}{X_d}\right)(1-s_2)(\sin\theta\,\omega_1 - i\cos\theta)}$$

$$\left.+\frac{iG_{15}}{(\tau_1+1) + i\left(-\frac{X_a}{X_d}\right)(1-s_2)(\sin\theta\,\omega_2 - i\cos\theta)}\right]$$

Again defining new variables:

$$\rho_1 = \tau_1 + 1 \qquad d\rho_1 = d\tau_1 \qquad 0 < \rho_1 < 2 \tag{6.20}$$

and

$$z_1 = [\cos\theta - i\sin\theta\,\omega_1]\left(-\frac{X_a}{X_d}\right)(s_2 - 1) \tag{6.21}$$

$$z_2 = [\cos\theta - i\sin\theta\,\omega_2]\left(-\frac{X_a}{X_d}\right)(s_2 - 1) \tag{6.22}$$

$$z_3 = [\cos\theta + i\sin\theta\,\omega_1]\left(-\frac{X_a}{X_d}\right)(s_2 - 1) \tag{6.23}$$

$$z_4 = [\cos\theta + i\sin\theta\,\omega_2]\left(-\frac{X_a}{X_d}\right)(s_2 - 1) \tag{6.25}$$

Substituting (6.20-6.24) into (3.33) and (3.34) we obtain:

$$\pi C_{33}\frac{1}{\pi}\int_{-1}^{1}\frac{f_3(\tau_2)}{\tau_2 - s_2}d\tau_2 + \pi C_{34}\frac{1}{\pi}\int_{-1}^{1}\frac{f_4(\tau_2)}{\tau_2 - s_2}d\tau_2$$

$$+ \frac{i}{2}\Bigg[- G_9\frac{1}{\pi}\int_0^2\frac{f_1(\rho_1)}{\rho_1 - z_1}d\rho_1 - G_{11}\frac{1}{\pi}\int_0^2\frac{f_1(\rho_1)}{\rho_1 - z_2}d\rho_1$$

$$+ G_{13}\frac{1}{\pi}\int_0^2\frac{f_1(\rho_1)}{\rho_1 - z_3}d\rho_1 + G_{15}\frac{1}{\pi}\int_0^2\frac{f_1(\rho_1)}{\rho_1 - z_4}d\rho_1 \tag{6.25}$$

$$- G_{10}\frac{1}{\pi}\int_0^2\frac{f_2(\rho_1)}{\rho_1 - z_1}d\rho_1 - G_{12}\frac{1}{\pi}\int_0^2\frac{f_2(\rho_1)}{\rho_1 - z_2}d\rho_1$$

$$+ G_{14}\frac{1}{\pi}\int_0^2\frac{f_2(\rho_1)}{\rho_1 - z_3}d\rho_1 + G_{16}\frac{1}{\pi}\int_0^2\frac{f_2(\rho_1)}{\rho_1 - z_4}d\rho_1 \Bigg] = -\sigma_0$$

and

$$\pi C_{43}\frac{1}{\pi}\int_{-1}^{1}\frac{f_3(\tau_2)}{\tau_2 - s_2}d\tau_2 + \pi C_{44}\frac{1}{\pi}\int_{-1}^{1}\frac{f_4(\tau_2)}{\tau_2 - s_2}d\tau_2$$

$$+ \frac{i}{2}\Bigg[- G_{17}\frac{1}{\pi}\int_0^2\frac{f_1(\rho_1)}{\rho_1 - z_1}d\rho_1 - G_{19}\frac{1}{\pi}\int_0^2\frac{f_1(\rho_1)}{\rho_1 - z_2}d\rho_1$$

$$+ G_{21}\frac{1}{\pi}\int_0^2\frac{f_1(\rho_1)}{\rho_1 - z_3}d\rho_1 + G_{23}\frac{1}{\pi}\int_0^2\frac{f_1(\rho_1)}{\rho_1 - z_4}d\rho_1 \tag{6.26}$$

$$- G_{18}\frac{1}{\pi}\int_0^2\frac{f_2(\rho_1)}{\rho_1 - z_1}d\rho_1 - G_{20}\frac{1}{\pi}\int_0^2\frac{f_2(\rho_1)}{\rho_1 - z_2}d\rho_1$$

$$+ G_{22}\frac{1}{\pi}\int_0^2\frac{f_2(\rho_1)}{\rho_1 - z_3}d\rho_1 + G_{24}\frac{1}{\pi}\int_0^2\frac{f_2(\rho_1)}{\rho_1 - z_4}d\rho_1 \Bigg] = 0$$

It should be noted that for $s_1 \to -1$ when $-1 < s_1 < 1$ $\mathrm{Re}(w_1,w_2,w_3,w_4) > 0$ and for $s_2 \to 1$ when $-1 < s_2 < 1$ $\mathrm{Re}(z_1,z_2,z_3,z_4) < 0$. So applying (5.9) to (6.18) and noting that terms with f_3 and f_4 are singular only for $\rho_2 = w_i = 0$ or $\tau_2 = 1$ and $s_1 = -1$ we have:

$$
\begin{aligned}
&\pi C_{12}\left[-F_2(-1)\,2^{\alpha_1}\cot\pi\beta_1\,(s_1+1)^{\beta_1} + F_2(1)\,2^{\beta_1}\cot\pi\alpha_1\,(1-s_1)^{\alpha_1}\right] \\
&\quad - \frac{iH_9}{2}\left[F_3(1)\,2^{\beta_2}\frac{1}{\sin\pi\alpha_2}w_1^{\alpha_2} + O(\rho)\right] \\
&\quad - \frac{iH_{11}}{2}\left[F_3(1)\,2^{\beta_2}\frac{1}{\sin\pi\alpha_2}w_2^{\alpha_2} + O(\rho)\right] \\
&\quad + \frac{iH_{13}}{2}\left[F_3(1)\,2^{\beta_2}\frac{1}{\sin\pi\alpha_2}w_3^{\alpha_2} + O(\rho)\right] \\
&\quad + \frac{iH_{15}}{2}\left[F_3(1)\,2^{\beta_2}\frac{1}{\sin\pi\alpha_2}w_4^{\alpha_2} + O(\rho)\right] \\
&\quad - \frac{iH_{10}}{2}\left[F_4(1)\,2^{\beta_2}\frac{1}{\sin\pi\alpha_2}w_1^{\alpha_2} + O(\rho)\right] \\
&\quad - \frac{iH_{12}}{2}\left[F_4(1)\,2^{\beta_2}\frac{1}{\sin\pi\alpha_2}w_2^{\alpha_2} + O(\rho)\right] \\
&\quad + \frac{iH_{14}}{2}\left[F_4(1)\,2^{\beta_2}\frac{1}{\sin\pi\alpha_2}w_3^{\alpha_2} + O(\rho)\right] \\
&\quad + \frac{iH_{16}}{2}\left[F_4(1)\,2^{\beta_2}\frac{1}{\sin\pi\alpha_2}w_4^{\alpha_2} + O(\rho)\right] \cong -\sigma_0\cos^2\theta
\end{aligned}
\tag{6.27}
$$

where $\alpha_1,\alpha_2,\beta_1,\beta_2$ are chosen according to (5.9c).

Analogically from (6.19) we have:

$$
\begin{aligned}
&\pi C_{21}\left[-F_1(-1)\,2^{\alpha_1}\cot\pi\beta_1\,(s_1+1)^{\beta_1} + F_1(1)\,2^{\beta_1}\cot\pi\alpha_1\,(1-s_1)^{\alpha_1}\right] \\
&\quad - \frac{i H_{17}}{2}\left[F_3(1)\,2^{\beta_2}\frac{1}{\sin\pi\alpha_2}w_1^{\alpha_2} + 0(\rho)\right] \\
&\quad - \frac{i H_{19}}{2}\left[F_3(1)\,2^{\beta_2}\frac{1}{\sin\pi\alpha_2}w_2^{\alpha_2} + 0(\rho)\right] \\
&\quad + \frac{i H_{21}}{2}\left[F_3(1)\,2^{\beta_2}\frac{1}{\sin\pi\alpha_2}w_3^{\alpha_2} + 0(\rho)\right] \\
&\quad + \frac{i H_{23}}{2}\left[F_3(1)\,2^{\beta_2}\frac{1}{\sin\pi\alpha_2}w_4^{\alpha_2} + 0(\rho)\right] \\
&\quad - \frac{i H_{18}}{2}\left[F_4(1)\,2^{\beta_2}\frac{1}{\sin\pi\alpha_2}w_1^{\alpha_2} + 0(\rho)\right] \\
&\quad - \frac{i H_{20}}{2}\left[F_4(1)\,2^{\beta_2}\frac{1}{\sin\pi\alpha_2}w_2^{\alpha_2} + 0(\rho)\right] \\
&\quad + \frac{i H_{22}}{2}\left[F_4(1)\,2^{\beta_2}\frac{1}{\sin\pi\alpha_2}w_3^{\alpha_2} + 0(\rho)\right] \\
&\quad + \frac{i H_{24}}{2}\left[F_4(1)\,2^{\beta_2}\frac{1}{\sin\pi\alpha_2}w_4^{\alpha_2} + 0(\rho)\right] \cong -\sigma_0\cos\theta\sin\theta
\end{aligned}
\tag{6.28}
$$

Similar operations with (6.25) and (6.26) when terms with f_1, f_2 are singular at $\rho_1 = z_k = 0$ or $\tau_1 = -1$ and $s_2 = 1$ give us :

$$
\begin{aligned}
&\pi C_{33}\left[-F_3(-1)\,2^{\alpha_2}\cot\pi\beta_2\,(s_2+1)^{\beta_2} + F_3(1)\,2^{\beta_2}\cot\pi\alpha_2\,(1-s_2)^{\alpha_2}\right] \\
&+\ \pi C_{34}\left[-F_4(-1)\,2^{\alpha_2}\cot\pi\beta_2\,(s_2+1)^{\beta_2} + F_4(1)\,2^{\beta_2}\cot\pi\alpha_2\,(1-s_2)^{\alpha_2}\right] \\
&\quad -\frac{iG_9}{2}\left[-F_1(-1)\,2^{\alpha_1}\frac{1}{\sin\pi\beta_1}(-z_1)^{\beta_1} + O(\rho)\right] \\
&\quad -\frac{iG_{11}}{2}\left[-F_1(-1)\,2^{\alpha_1}\frac{1}{\sin\pi\beta_1}(-z_2)^{\beta_1} + O(\rho)\right] \\
&\quad +\frac{iG_{13}}{2}\left[-F_1(-1)\,2^{\alpha_1}\frac{1}{\sin\pi\beta_1}(-z_3)^{\beta_1} + O(\rho)\right] \\
&\quad +\frac{iG_{15}}{2}\left[-F_1(-1)\,2^{\alpha_1}\frac{1}{\sin\pi\beta_1}(-z_4)^{\beta_1} + O(\rho)\right] \\
&\quad -\frac{iG_{10}}{2}\left[-F_2(-1)\,2^{\alpha_1}\frac{1}{\sin\pi\beta_1}(-z_1)^{\beta_1} + O(\rho)\right] \\
&\quad -\frac{iG_{12}}{2}\left[-F_2(-1)\,2^{\alpha_1}\frac{1}{\sin\pi\beta_1}(-z_2)^{\beta_1} + O(\rho)\right] \\
&\quad +\frac{iG_{14}}{2}\left[-F_2(-1)\,2^{\alpha_1}\frac{1}{\sin\pi\beta_1}(-z_3)^{\beta_1} + O(\rho)\right] \\
&\quad +\frac{iG_{16}}{2}\left[-F_2(-1)\,2^{\alpha_1}\frac{1}{\sin\pi\beta_1}(-z_4)^{\beta_1} + O(\rho)\right] \cong -\sigma_0
\end{aligned}
\tag{6.29}
$$

and

$$
\begin{aligned}
&\pi C_{43}\left[-F_3(-1)\,2^{\alpha_2}\cot\pi\beta_2\,(s_2+1)^{\beta_2} + F_3(1)\,2^{\beta_2}\cot\pi\alpha_2\,(1-s_2)^{\alpha_2}\right] \\
&+\ \pi C_{44}\left[-F_4(-1)\,2^{\alpha_2}\cot\pi\beta_2\,(s_2+1)^{\beta_2} + F_4(1)\,2^{\beta_2}\cot\pi\alpha_2\,(1-s_2)^{\alpha_2}\right] \\
&\quad -\frac{iG_{17}}{2}\left[-F_1(-1)\,2^{\alpha_1}\frac{1}{\sin\pi\beta_1}(-z_1)^{\beta_1} + 0(\rho)\right] \\
&\quad -\frac{iG_{19}}{2}\left[-F_1(-1)\,2^{\alpha_1}\frac{1}{\sin\pi\beta_1}(-z_2)^{\beta_1} + 0(\rho)\right] \\
&\quad +\frac{iG_{21}}{2}\left[-F_1(-1)\,2^{\alpha_1}\frac{1}{\sin\pi\beta_1}(-z_3)^{\beta_1} + 0(\rho)\right] \\
&\quad +\frac{iG_{23}}{2}\left[-F_1(-1)\,2^{\alpha_1}\frac{1}{\sin\pi\beta_1}(-z_4)^{\beta_1} + 0(\rho)\right] \\
&\quad -\frac{iG_{18}}{2}\left[-F_2(-1)\,2^{\alpha_1}\frac{1}{\sin\pi\beta_1}(-z_1)^{\beta_1} + 0(\rho)\right] \\
&\quad -\frac{iG_{20}}{2}\left[-F_2(-1)\,2^{\alpha_1}\frac{1}{\sin\pi\beta_1}(-z_2)^{\beta_1} + 0(\rho)\right] \\
&\quad +\frac{iG_{22}}{2}\left[-F_2(-1)\,2^{\alpha_1}\frac{1}{\sin\pi\beta_1}(-z_3)^{\beta_1} + 0(\rho)\right] \\
&\quad +\frac{iG_{24}}{2}\left[-F_2(-1)\,2^{\alpha_1}\frac{1}{\sin\pi\beta_1}(-z_4)^{\beta_1} + 0(\rho)\right] \cong 0
\end{aligned}
\tag{6.30}
$$

Substituting back for $w_1 \ldots w_4$ in (6,27) and examining behavior at x_d (ie. multiplying (6.27) by $\lim (1-s_1)^{-\alpha 1}$ where $-1<\alpha_1<0$) we have: $\lim\limits_{s_1 \to 1} (1-s_1)^{-\alpha_1}$ $\quad -1 < \alpha_1 < 0$

$F_2(1)\,2^{\beta_1}\cot\pi\alpha_1 = 0$

or

$$\cos\pi\alpha_1 = 0 \;\Rightarrow\; \alpha_1 = -\frac{1}{2}$$

Multiplying now (6.29) or (6.30) by $\lim\limits_{s_2 \to -1} (s_2 + 1)^{-\beta_2}$ $\quad -1 < \beta_2 < 0$ we obtain:

$$-F_3(-1)\, 2^{\alpha_2} \cot\pi\beta_2 = 0$$

or

$$\cot\pi\beta_2 = 0 \;\Rightarrow\; \beta_2 = -\frac{1}{2}$$

Let's examine (6.27-6.30) at $s_1 \to -1$ and $s_2 \to 1$ by multiplying (6.27) and (6.28) by:

$\lim\limits_{s_1 \to -1} (s_1 + 1)^{-\beta}$ and (6.29-6.30) by: $\lim\limits_{s_2 \to 1} (1 - s_2)^{-\beta}$ where $\beta_1 = \alpha_2 = \beta$

We obtain:

$$\begin{aligned}
&-\pi C_{12} F_2(-1) \frac{1}{\sqrt{2}} \cot\pi\beta - \frac{i H_9}{2} F_3(1) \frac{1}{\sqrt{2}} \frac{1}{\sin\pi\beta} [\cos\theta + i \sin\theta(a + ib)]^{\beta} \left(-\frac{x_d}{x_a}\right)^{\beta} - \\
&- \frac{i H_{11}}{2} F_3(1) \frac{1}{\sqrt{2}} \frac{1}{\sin\pi\beta} [\cos\theta + i \sin\theta(c + id)]^{\beta} \left(-\frac{x_d}{x_a}\right)^{\beta} \\
&+ \frac{i H_{13}}{2} F_3(1) \frac{1}{\sqrt{2}} \frac{1}{\sin\pi\beta} [\cos\theta - i \sin\theta(a - ib)]^{\beta} \left(-\frac{x_d}{x_a}\right)^{\beta} \\
&+ \frac{i H_{15}}{2} F_3(1) \frac{1}{\sqrt{2}} \frac{1}{\sin\pi\beta} [\cos\theta - i \sin\theta(c - id)]^{\beta} \left(-\frac{x_d}{x_a}\right)^{\beta} \\
&- \frac{i H_{10}}{2} F_4(1) \frac{1}{\sqrt{2}} \frac{1}{\sin\pi\beta} [\cos\theta + i \sin\theta(a + ib)]^{\beta} \left(-\frac{x_d}{x_a}\right)^{\beta} \\
&- \frac{i H_{12}}{2} F_4(1) \frac{1}{\sqrt{2}} \frac{1}{\sin\pi\beta} [\cos\theta + i \sin\theta(c + id)]^{\beta} \left(-\frac{x_d}{x_a}\right)^{\beta} \\
&+ \frac{i H_{14}}{2} F_4(1) \frac{1}{\sqrt{2}} \frac{1}{\sin\pi\beta} [\cos\theta - i \sin\theta(a - ib)]^{\beta} \left(-\frac{x_d}{x_a}\right)^{\beta} \\
&+ \frac{i H_{16}}{2} F_4(1) \frac{1}{\sqrt{2}} \frac{1}{\sin\pi\beta} [\cos\theta - i \sin\theta(c - id)]^{\beta} \left(-\frac{x_d}{x_a}\right) = 0
\end{aligned}$$

or

$$
\begin{aligned}
&F_2(-1)(-\pi C_{12}\cos\pi\beta) + F_3(1)\left(-\frac{x_d}{x_a}\right)^{\beta}\frac{i}{2}\Big[-H_9[\cos\theta + i\sin\theta(a+ib)]^{\beta} \\
&-H_{11}[\cos\theta + i\sin\theta(c+id)]^{\beta} + H_{13}[\cos\theta - i\sin\theta(a-ib)]^{\beta} \\
&+H_{15}[\cos\theta - i\sin\theta(c-id)]^{\beta}\Big] \\
&+F_4(1)\left(-\frac{x_d}{x_a}\right)^{\beta}\frac{i}{2}\Big[-H_{10}[\cos\theta + i\sin\theta(a+ib)]^{\beta} \\
&-H_{12}[\cos\theta + i\sin\theta(c+id)]^{\beta} \\
&+H_{14}[\cos\theta - i\sin\theta(a-ib)]^{\beta} + H_{16}[\cos\theta - i\sin\theta(c-id)]^{\beta}\Big] = 0
\end{aligned}
\tag{6.31}
$$

Analogically from (6.28) we obtain:

$$
\begin{aligned}
&F_1(-1)(-\pi C_{21}\cos\pi\beta) + F_3(1)\left(-\frac{x_d}{x_a}\right)^{\beta}\frac{i}{2}\Big[-H_{17}[\cos\theta + i\sin\theta(a+ib)]^{\beta} \\
&-H_{19}[\cos\theta + i\sin\theta(c+id)]^{\beta} + H_{21}[\cos\theta - i\sin\theta(a-ib)]^{\beta} \\
&+H_{23}[\cos\theta - i\sin\theta(c-id)]^{\beta}\Big] \\
&+F_4(1)\left(-\frac{x_d}{x_a}\right)^{\beta}\frac{i}{2}\Big[-H_{18}[\cos\theta + i\sin\theta(a+ib)]^{\beta} \\
&-H_{20}[\cos\theta + i\sin\theta(c+id)]^{\beta} \\
&+H_{22}[\cos\theta - i\sin\theta(a-ib)]^{\beta} + H_{24}[\cos\theta - i\sin\theta(c-id)]^{\beta}\Big] = 0
\end{aligned}
\tag{6.32}
$$

Examination of (6.29) gives us the following:

$$
\begin{aligned}
&\pi C_{33} F_3(1) \frac{1}{\sqrt{2}} \cot\pi\beta + \pi C_{34} F_4(1) \frac{1}{\sqrt{2}} \cot\pi\beta \\
&+ \frac{i G_9}{2} F_1(-1) \frac{1}{\sqrt{2}} \frac{1}{\sin\pi\beta} [\cos\theta - i \sin\theta\, \omega_1]^\beta \left(-\frac{x_a}{x_d}\right)^\beta \\
&+ \frac{i G_{11}}{2} F_1(-1) \frac{1}{\sqrt{2}} \frac{1}{\sin\pi\beta} [\cos\theta - i \sin\theta\, \omega_2]^\beta \left(-\frac{x_a}{x_d}\right)^\beta \\
&- \frac{i G_{13}}{2} F_1(-1) \frac{1}{\sqrt{2}} \frac{1}{\sin\pi\beta} [\cos\theta + i \sin\theta\, \omega_1]^\beta \left(-\frac{x_a}{x_d}\right)^\beta \\
&- \frac{i G_{15}}{2} F_1(-1) \frac{1}{\sqrt{2}} \frac{1}{\sin\pi\beta} [\cos\theta + i \sin\theta\, \omega_2]^\beta \left(-\frac{x_a}{x_d}\right)^\beta \\
&+ \frac{i G_{10}}{2} F_2(-1) \frac{1}{\sqrt{2}} \frac{1}{\sin\pi\beta} [\cos\theta - i \sin\theta\, \omega_1]^\beta \left(-\frac{x_a}{x_d}\right)^\beta \\
&+ \frac{i G_{12}}{2} F_2(-1) \frac{1}{\sqrt{2}} \frac{1}{\sin\pi\beta} [\cos\theta - i \sin\theta\, \omega_2]^\beta \left(-\frac{x_a}{x_d}\right)^\beta \\
&- \frac{i G_{14}}{2} F_2(-1) \frac{1}{\sqrt{2}} \frac{1}{\sin\pi\beta} [\cos\theta + i \sin\theta\, \omega_1]^\beta \left(-\frac{x_a}{x_d}\right)^\beta \\
&- \frac{i G_{16}}{2} F_2(-1) \frac{1}{\sqrt{2}} \frac{1}{\sin\pi\beta} [\cos\theta + i \sin\theta\, \omega_2]^\beta \left(-\frac{x_a}{x_d}\right)^\beta = 0
\end{aligned}
$$

or

$$
\begin{aligned}
&F_3(1)\, \pi C_{33} \cos\pi\beta + F_4(1)\, \pi C_{34} \cos\pi\beta + F_1(-1) \frac{i}{2} \left(-\frac{x_a}{x_d}\right)^\beta \Big[G_9 [\cos\theta - i \sin\theta\, \omega_1]^\beta \\
&+ G_{11} [\cos\theta - i \sin\theta\, \omega_2]^\beta - G_{13} [\cos\theta + i \sin\theta\, \omega_1]^\beta - G_{15} [\cos\theta + i \sin\theta\, \omega_2]^\beta \Big] \\
&+ F_2(-1) \frac{i}{2} \left(-\frac{x_a}{x_d}\right)^\beta \Big[G_{10} [\cos\theta - i \sin\theta\, \omega_1]^\beta + G_{12} [\cos\theta - i \sin\theta\, \omega_2]^\beta \\
&- G_{14} [\cos\theta + i \sin\theta\, \omega_1]^\beta - G_{16} [\cos\theta + i \sin\theta\, \omega_2]^\beta \Big] = 0 \qquad (6.33)
\end{aligned}
$$

and analogically from (6.30) we have the last equation:

$$F_3(1)\,\pi C_{43}\cos\pi\beta + F_4(1)\,\pi C_{44}\cos\pi\beta + F_1(-1)\,\frac{i}{2}\left(-\frac{X_a}{X_d}\right)^{\beta}\Big[G_{17}[\cos\theta - i\sin\theta\,\omega_1]^{\beta}$$

$$+ G_{19}[\cos\theta - i\sin\theta\,\omega_2]^{\beta} - G_{21}[\cos\theta + i\sin\theta\,\omega_1]^{\beta} - G_{23}[\cos\theta + i\sin\theta\,\omega_2]^{\beta}\Big]$$

$$+ F_2(-1)\,\frac{i}{2}\left(-\frac{X_a}{X_d}\right)^{\beta}\Big[G_{18}[\cos\theta - i\sin\theta\,\omega_1]^{\beta} + G_{20}[\cos\theta - i\sin\theta\,\omega_2]^{\beta}$$

$$- G_{22}[\cos\theta + i\sin\theta\,\omega_1]^{\beta} - G_{24}[\cos\theta + i\sin\theta\,\omega_2]^{\beta}\Big] = 0 \qquad (6.34)$$

The set of equations (6.31-6.34) gives a system of four equations with four unknowns $F_1(-1)$, $F_2(-1)$, $F_3(1)$, $F_4(1)$ and the right hand side equal to zero. We can write the above set in following form:

$$\begin{cases} (-\pi C_{12}\cos\pi\beta)\,F_2(-1) + \left(-\frac{X_d}{X_a}\right)^{\beta}\frac{i}{2}A_{13}\,F_3(1) + \left(-\frac{X_d}{X_a}\right)^{\beta}\frac{i}{2}A_{14}\,F_4(1) = 0 \\ (-\pi C_{21}\cos\pi\beta)\,F_1(-1) + \left(-\frac{X_d}{X_a}\right)^{\beta}\frac{i}{2}A_{23}\,F_3(1) + \left(-\frac{X_d}{X_a}\right)^{\beta}\frac{i}{2}A_{24}\,F_4(1) = 0 \\ \left(-\frac{X_a}{X_d}\right)^{\beta}\frac{i}{2}A_{31}\,F_1(-1) + \left(-\frac{X_a}{X_d}\right)^{\beta}\frac{i}{2}A_{32}\,F_2(-1) \\ \qquad + \pi\cos\pi\beta\,C_{33}\,F_3(1) + \pi\cos\pi\beta\,C_{34}\,F_4(1) = 0 \\ \left(-\frac{X_a}{X_d}\right)^{\beta}\frac{i}{2}A_{41}\,F_1(-1) + \left(-\frac{X_a}{X_d}\right)^{\beta}\frac{i}{2}A_{42}\,F_2(-1) \\ \qquad + \pi\cos\pi\beta\,C_{43}\,F_3(1) + \pi\cos\pi\beta\,C_{44}\,F_4(1) = 0 \end{cases} \qquad (6.35)$$

In order to have a unique solution of this system of equations the determinant of the coefficients must be zero.

$$
\begin{aligned}
&- \pi^4 \cos^4 \pi\beta\, C_{12} C_{21} C_{33} C_{44} - \frac{\pi^2}{4} \cos^2 \pi\beta\, C_{12} C_{34} A_{23} A_{41} \\
&- \frac{\pi^2}{4} \cos^2 \pi\beta\, C_{12} C_{43} A_{24} A_{31} + \frac{\pi^2}{4} \cos^2 \pi\beta\, C_{12} C_{33} A_{24} A_{41} \\
&+ \frac{\pi^2}{4} \cos^2 \pi\beta\, C_{12} C_{44} A_{23} A_{31} + \pi^4 \cos^4 \pi\beta\, C_{12} C_{21} C_{34} C_{43} \\
&+ \frac{\pi^2}{4} \cos^2 \pi\beta\, C_{21} C_{44} A_{13} A_{32} + \frac{1}{16} A_{13} A_{24} A_{31} A_{42} \\
&- \frac{1}{16} A_{13} A_{24} A_{32} A_{41} - \frac{\pi^2}{4} \cos^2 \pi\beta\, C_{21} C_{34} A_{13} A_{42} \\
&- \frac{\pi^2}{4} \cos^2 \pi\beta\, C_{21} C_{43} A_{14} A_{32} - \frac{1}{16} A_{14} A_{23} A_{31} A_{42} \\
&+ \frac{1}{16} A_{14} A_{23} A_{32} A_{41} + \frac{\pi^2}{4} \cos^2 \pi\beta\, C_{21} C_{33} A_{14} A_{42} = 0
\end{aligned}
\tag{6.36}
$$

where:

$$
\begin{aligned}
A_{13} = &- H_9[\cos\theta + i \sin\theta(a + ib)]^\beta - H_{11}[\cos\theta + i \sin\theta(c + id)]^\beta + \\
&+ H_{13}[\cos\theta - i \sin\theta(a - ib)]^\beta + H_{15}[\cos\theta - i \sin\theta(c - id)]^\beta
\end{aligned}
$$

$$
\begin{aligned}
A_{14} = &- H_{10}[\cos\theta + i \sin\theta(a + ib)]^\beta - H_{12}[\cos\theta + i \sin\theta(c + id)]^\beta + \\
&+ H_{14}[\cos\theta - i \sin\theta(a - ib)]^\beta + H_{16}[\cos\theta - i \sin\theta(c - id)]^\beta
\end{aligned}
$$

$$
\begin{aligned}
A_{23} = &- H_{17}[\cos\theta + i \sin\theta(a + ib)]^\beta - H_{19}[\cos\theta + i \sin\theta(c + id)]^\beta + \\
&+ H_{21}[\cos\theta - i \sin\theta(a - ib)]^\beta + H_{23}[\cos\theta - i \sin\theta(c - id)]^\beta
\end{aligned}
$$

$$
\begin{aligned}
A_{24} = &- H_{18}[\cos\theta + i \sin\theta(a + ib)]^\beta - H_{20}[\cos\theta + i \sin\theta(c + id)]^\beta + \\
&+ H_{22}[\cos\theta - i \sin\theta(a - ib)]^\beta + H_{24}[\cos\theta - i \sin\theta(c - id)]^\beta
\end{aligned}
$$

$$
\begin{aligned}
A_{31} = &\; G_9[\cos\theta - i \sin\theta\, \omega_1]^\beta + G_{11}[\cos\theta - i \sin\theta\, \omega_2]^\beta - \\
&- G_{13}[\cos\theta + i \sin\theta\, \omega_1]^\beta - G_{15}[\cos\theta + i \sin\theta\, \omega_2]^\beta
\end{aligned}
$$

$$A_{32} = G_{10}[\cos\theta - i\sin\theta\,\omega_1]^\beta + G_{12}[\cos\theta - i\sin\theta\,\omega_2]^\beta -$$

$$- G_{14}[\cos\theta + i\sin\theta\,\omega_1]^\beta - G_{16}[\cos\theta + i\sin\theta\,\omega_2]^\beta$$

$$A_{41} = G_{17}[\cos\theta - i\sin\theta\,\omega_1]^\beta + G_{19}[\cos\theta - i\sin\theta\,\omega_2]^\beta -$$

$$- G_{21}[\cos\theta + i\sin\theta\,\omega_1]^\beta - G_{23}[\cos\theta + i\sin\theta\,\omega_2]^\beta$$

$$A_{42} = G_{18}[\cos\theta - i\sin\theta\,\omega_1]^\beta + G_{20}[\cos\theta - i\sin\theta\,\omega_2]^\beta -$$

$$- G_{22}[\cos\theta + i\sin\theta\,\omega_1]^\beta - G_{24}[\cos\theta + i\sin\theta\,\omega_2]^\beta$$

The only unknown in (6.36) is β which has to be found so (6.36) is satisfied. Once β is found, two equations from (6.35) can be chosen, that together with (6.11-6.12) become the additional conditions necessary to solve system of integral equations (3.31-3.34) by Gauss-Jacobi or Lobatto-Jacobi method.

It should be pointed out that in order to avoid multivaluedness of solution only one branch of complex number must be taken for the calculations.

The method of choosing the branch is explained as follows. Formula (5.9) is true for representing crack a-b and complex number $z-a=r_1e^{i\phi_1}$ and $z-b=r_2e^{i\phi_2}$ where argument is determined uniquely by making a cut of the complex plane between poles a and b so that $0<\phi_1<2\pi$ and $-\pi<\phi_2<\pi$. In this way, any complex number z taken to real power β will have a unique solution as follows:

$$[\cos\theta - i\sin\theta\,\omega_1]^\beta = \rho_0^\beta[e^{i\phi_0}]^\beta = \rho_0^\beta e^{i\beta\phi_0}$$

VII. Stress intensity factors for skew crack case.

The set of singular integral equations with the generalized Cauchy kernels and four additional conditions in the form of the equations (6.11), (6.12), (6.31) and (6.32) can be solved by Gauss-Jacobi collocation method. We can find t_k as roots of Jacobi polynomial of order n as follows:

$$P_n^{(\alpha,\beta)}(t) = 0$$

Collocation points x_j are found as roots of:

$$P_{n-1}^{(\alpha+1,\beta+1)}(x) = 0$$

and weighting coefficients are calculated according to formula:

$$W_k = -\frac{(2n+\alpha+\beta+2)\,\Gamma(n+\alpha+1)\,\Gamma(n+\beta+1)\,2^{\alpha+\beta}}{(n+1)!\,(n+\alpha+\beta+1)\,\Gamma(n+\alpha+\beta+1)\,P_{n+1}^{(\alpha,\beta)}(t_k)\,\frac{d}{dt}P_n^{(\alpha,\beta)}(t_k)};$$

In order to find expressions for the stress intensity factors we start from definitions (5.1-5.8) and follow the same procedure with different order of singularity.

Starting from (5.10) with x_b=0.

$$k_1(x_a) = \lim_{s_2 \to -1} \sqrt{-x_a}\,\sqrt{-1}\,\sqrt{1+s_2}\;\sigma_{y_2y_2}(s_2,0) \tag{7.1}$$

Since at x_a only the two first terms of (3.33) are singular, using (5.9) we have:

$$\pi C_{33} \frac{1}{\pi} \int_{-1}^{1} \frac{f_3(\tau_2)}{\tau_2 - s_2} d\tau_2 = \pi C_{33} \left[-F_3(-1)\,(2)^{\beta} \frac{e^{(-\pi i)(-\frac{1}{2})}}{\sin(-\frac{\pi}{2})} (s_2 + 1)^{-\frac{1}{2}} + F_3(1) \frac{1}{\sqrt{2}} \frac{1}{\sin \pi\beta} (s_2 - 1)^{\beta} \right]$$

and

$$\pi C_{34} \frac{1}{\pi} \int_{-1}^{1} \frac{f_4(\tau_2)}{\tau_2 - s_2} d\tau_2 = \pi C_{34} \left[-F_4(-1)\,(2)^{\beta} \frac{e^{(-\pi i)(-\frac{1}{2})}}{\sin(-\frac{\pi}{2})} (s_2 + 1)^{-\frac{1}{2}} + F_4(1) \frac{1}{\sqrt{2}} \frac{1}{\sin \pi\beta} (s_2 - 1)^{\beta} \right]$$

Substituting the above results for stress in (7.1) and after some algebra we get:

$$k_1(x_a) = \pi\, 2^{\beta} \sqrt{-x_a} \left[C_{33} F_3(-1) + C_{34} F_4(-1) \right] \tag{7.2}$$

$$k_2(x_a) = \pi\, 2^{\beta} \sqrt{-x_a} \left[C_{43} F_3(-1) + C_{44} F_4(-1) \right] \tag{7.3}$$

$$k_1(x_d) = -\pi\, 2^{\beta} \sqrt{x_d}\; C_{12} F_2(1) \tag{7.4}$$

$$k_2(x_d) = -\pi\, 2^{\beta} \sqrt{x_d}\; C_{21} F_1(1) \tag{7.5}$$

where rest of stress intensity factors were found in similar way.

VIII. Normalized stress intensity factors.

In order to present computational results for two crack configuration and for skew crack configuration , the stress intensity factors are normalized.

Let's define length of the cracks as $x_a x_b = L_1$ and $x_c x_d = L_2$. Then normalized stress intensity factors become:

$$k_i^n = \frac{k_i}{\sigma_0 \sqrt{\frac{L_p}{2}}} \; ; \qquad p = 1,2 \tag{8.1}$$

Thus, the mode one stress intensity factor, for the two crack configuration, at x_a is:

$$k_1^n(x_a) = \frac{\pi}{\sigma_0}\left[C_{33}F_3(-1) + C_{34}F_4(-1)\right] \tag{8.2}$$

and for the skew crack case:

$$k_1^n(x_a) = \frac{\pi}{\sigma_0}\left[C_{33}F_3(-1) + C_{34}F_4(-1)\right] 2^{\beta+\frac{1}{2}} \tag{8.3}$$

IX. Strain Energy Release Rate for x_d.

Let's use the usual definition of the strain energy release rate [3]:

$$G = \frac{d}{da}(U - V) \tag{9.1}$$

where G is the total energy and consists of two parts which represent mode-I (G_I) and mode-II (G_{II}):

$$G = G_I + G_{II} \tag{9.2}$$

at $x = x_d$, we may write [4]:

$$\frac{dU - dV}{da} = \frac{1}{2}\int_{x_d}^{x_d+da} \Big[\sigma_{y_1y_1}(x_1,0)[\,v(x_1 - da,0^+) - v(x_1 - da,0^-)] + \tau_{x_1y_1}(x_1,0)[\,u(x_1 - da,0^+) - u(x_1 - da,0^-)]\Big] dx_1 \tag{9.3}$$

or

$$G_I = \frac{1}{2}\int_{x_d}^{x_d+da} \sigma_{y_1y_1}(x_1,0)\,[\,v(x_1 - da,0^+) - v(x_1 - da,0^-)]\,dx_1 \tag{9.4}$$

$$G_{II} = \frac{1}{2}\int_{x_d}^{x_d+da} \tau_{x_1y_1}(x_1,0)\,[\,u(x_1 - da,0^+) - u(x_1 - da,0^-)\,]\,dx_1 \tag{9.5}$$

To evaluate integral (9.3), the asymptotic expressions of stresses and displacements around the crack tip are needed. The expression of normal and shear stress can be easily obtained by using the following definitions:

$$\sigma_{y_1y_1}(x_1,0) = \frac{k_1(x_d)}{\sqrt{2(x_1 - x_d)}} + \text{higher order terms} \tag{9.6}$$

$$\tau_{x_1y_1}(x_1,0) = \frac{k_2(x_d)}{\sqrt{2(x_1 - x_d)}} + \text{higher order terms} \tag{9.7}$$

Asymptotic expression for the displacements can be obtained using:

$$\Delta u = u(x_1,0^+) - u(x_1,0^-) = \lim_{y_1 \to 0} \int [\,\varepsilon^{(+)}_{x_1x_1} - \varepsilon^{(-)}_{x_1x_1}\,]\,dx_1$$

$$\Delta v = v(x_1,0^+) - v(x_1,0^-) = \lim_{y_1 \to 0} \int [\,\varepsilon^{(+)}_{y_1y_1} - \varepsilon^{(-)}_{y_1y_1}\,]\,dy_1$$

where total strains can be found from (1.22-1.23) from total stresses obtained according to (3.4a,b) using (1.14-1.17) and (3.2-3.3) upon substitution of (3.1) into (2.20-2.25). However, it is known that at x_d only terms with f_1 and f_2 contribute to singular behavior. Thus Δu and Δv can also be found directly us. .g (1.20-1.21), [5].

$$\Delta u = \int f_1(x_1)\, dx_1 \tag{9.8}$$

$$\Delta v = \int f_2(x_1)\, dx_1 \tag{9.9}$$

Starting from this point we shall substitute for f_1, f_2 from (1.29 - 1.30) taking A,B from (1.35-1.36) as:

$$A = K_1 + K_2\omega_2$$
$$B = -K_1 - K_2\omega_1$$

where

$$K_1 = \frac{1}{s^2}\frac{1}{2a_{11}(\omega_1^2 - \omega_2^2)}\int_{x_c}^{x_d} f_1(t_1)\, e^{ist_1}\, dt_1$$

$$K_2 = \frac{|s|}{i\,s^3}\frac{\omega_1\omega_2}{2a_{22}(\omega_1^2 - \omega_2^2)}\int_{x_c}^{x_d} f_2(t_1)\, e^{ist_1}\, dt_1$$

Hence, the normal displacement expression is:

$$\Delta v = \lim_{y_1 \to 0} \frac{-1}{2\pi}\int_{-\infty}^{+\infty}\frac{s^2}{|s|}\left[\frac{A\, e^{-\omega_1|s|y_1^*} + (Ac_1 + Bc_2)\, e^{\omega_1|s|y_1^*}}{\omega_1}(a_{12}\omega_1^2 - a_{22})\right.$$
$$\left. + \frac{B\, e^{-\omega_2|s|y_1^*} + (Ac_3 - Bc_1)\, e^{\omega_2|s|y_1^*}}{\omega_2}(a_{12}\omega_2^2 - a_{22})\right] e^{-isx_1}\, ds \tag{9.10}$$

and for shear displacement the analogical expression is:

$$\Delta u = \lim_{y_1 \to 0} \frac{-1}{2\pi} \int_{-\infty}^{+\infty} \frac{s}{i} \Big[[A\, e^{-\omega_1 |s| y_1^+} - (Ac_1 + Bc_2)\, e^{\omega_1 |s| y_1^-}](a_{11}\omega_1^2 - a_{12})$$

$$+ [B\, e^{-\omega_2 |s| y_1^+} - (Ac_3 - Bc_1)\, e^{\omega_2 |s| y_1^-}](a_{11}\omega_2^2 - a_{12}) \Big] e^{-isx_1}\, ds \qquad (9.11)$$

where c_1, c_2, c_3 are taken from (1.13 a,b,c).

With (9.12-9.15) we obtain:

$$\Delta v = \lim_{y_1 \to 0} \frac{-1}{2\pi} \int_{-\infty}^{+\infty} \frac{1}{2|s|(\omega_1^2 - \omega_2^2)} \left\{ \frac{\int_{x_c}^{x_d} f_1(t_1)\, e^{ist_1} dt_1}{a_{11}} \left[\frac{(a_{12}\omega_1^2 - a_{22})(e^{-\omega_1 |s| y_1^+} - e^{\omega_1 |s| y_1^-})}{\omega_1} \right.\right.$$

$$\left. - \frac{(a_{12}\omega_2^2 - a_{22})(e^{-\omega_2 |s| y_1^+} - e^{\omega_2 |s| y_1^-})}{\omega_2} \right] + \frac{|s|}{i\,s} \frac{\int_{x_c}^{x_d} f_2(t_1)\, e^{ist_1} dt_1}{a_{22}} \Big[(a_{12}\omega_1^2 - a_{22})\omega_2^2$$

$$\left.\left. (e^{-\omega_1 |s| y_1^+} + e^{\omega_1 |s| y_1^-}) - (a_{12}\omega_2^2 - a_{22})\omega_1^2 (e^{-\omega_2 |s| y_1^+} + e^{\omega_2 |s| y_1^-}) \Big] \right\} e^{-isx_1}\, ds \qquad (9.12)$$

and

$$\Delta u = \lim_{y_1 \to 0} \frac{-1}{2\pi} \int_{-\infty}^{+\infty} \frac{1}{i} \frac{1}{2s(\omega_1^2 - \omega_2^2)} \left\{ \frac{\int_{x_c}^{x_d} f_1(t_1)\, e^{ist_1} dt_1}{a_{11}} \left[(a_{11}\omega_1^2 - a_{12})(e^{-\omega_1|s|y_1^+} + e^{\omega_1|s|y_1^-}) \right.\right.$$

$$\left. - (a_{11}\omega_2^2 - a_{12})(e^{-\omega_2|s|y_1^+} + e^{\omega_2|s|y_1^-}) \right] + \frac{|s|}{is} \frac{\int_{x_c}^{x_d} f_2(t_1)\, e^{ist_1} dt_1}{a_{22}} \omega_1\omega_2 \left[(a_{11}\omega_1^2 - a_{12})\, \omega_2 \right.$$

$$\left.\left. (e^{-\omega_1|s|y_1^+} - e^{\omega_1|s|y_1^-}) - (a_{11}\omega_2^2 - a_{12})\omega_1 (e^{-\omega_2|s|y_1^+} - e^{\omega_2|s|y_1^-}) \right] \right\} e^{-isx_1}\, ds \qquad (9.13)$$

For skew crack configuration

$$x_c = 0 \qquad t_1 = \frac{1+\tau}{2} x_d \qquad dt_1 = \frac{1}{2} x_d d\tau \qquad -1 < \tau < 1$$

the equations for displacement now become:

$$\Delta v = \lim_{y_1 \to 0} \frac{-x_d}{8\pi} \int_{-\infty}^{+\infty} \frac{e^{\frac{isx_d}{2}}}{|s|(\omega_1^2 - \omega_2^2)} \left[\int_{-1}^{1} f_1(\tau)\, e^{\frac{isx_d}{2}\tau} d\tau \left[(\omega_1^2 - \frac{a_{12}}{a_{11}})\omega_2 (e^{-\omega_2|s|y_1^+} - e^{\omega_2|s|y_1^-}) \right.\right.$$

$$\left. - (\omega_2^2 - \frac{a_{12}}{a_{11}})\omega_1 (e^{-\omega_1|s|y_1^+} - e^{\omega_1|s|y_1^-}) \right] + \frac{|s|}{is} \int_{-1}^{1} f_2(\tau)\, e^{\frac{isx_d}{2}\tau} d\tau \left[(\omega_1^2 - \frac{a_{12}}{a_{11}}) \right.$$

$$\left.\left. (e^{-\omega_2|s|y_1^+} + e^{\omega_2|s|y_1^-}) - (\omega_2^2 - \frac{a_{12}}{a_{11}})(e^{-\omega_1|s|y_1^+} + e^{\omega_1|s|y_1^-}) \right] \right] e^{-isx_1}\, ds \qquad (9.14)$$

$$\Delta u = \lim_{y_1 \to 0} \frac{-x_d}{8\pi} \int_{-\infty}^{+\infty} \frac{e^{\frac{isx_d}{2}}}{is(\omega_1^2 - \omega_2^2)} \left[\int_{-1}^{1} f_1(\tau)\, e^{\frac{isx_d}{2}\tau} d\tau \, [(\omega_1^2 - \frac{a_{12}}{a_{11}})(e^{-\omega_1|s|y_1^{\bullet}} + e^{\omega_1|s|y_1^{-}}) - \right.$$

$$- (\omega_2^2 - \frac{a_{12}}{a_{11}})(e^{-\omega_2|s|y_1^{\bullet}} + e^{\omega_2|s|y_1^{-}})] + \frac{|s|}{i\, s\omega_1\omega_2} \int_{-1}^{1} f_2(\tau)\, e^{\frac{isx_d}{2}\tau} d\tau \, [(\omega_1^2 - \frac{a_{12}}{a_{11}})\omega_2$$

$$\left. (e^{-\omega_1|s|y_1^{\bullet}} - e^{\omega_1|s|y_1^{-}}) - (\omega_2^2 - \frac{a_{12}}{a_{11}})\omega_1(e^{-\omega_2|s|y_1^{\bullet}} - e^{\omega_2|s|y_1^{-}})] \right] e^{-isx_1} ds \qquad (9.15)$$

First we have to evaluate integrals of terms with variable τ. Note that they all have general form:

$$I_1 = \int_{-1}^{1} f_i(\tau)\, e^{ia\tau} d\tau \overset{(5.9a)}{=} \int_{-1}^{1} e^{ia\tau}(1-\tau)^{\alpha}(1+\tau)^{\beta} F_i(\tau)\, d\tau \qquad (9.16)$$

where $\quad a = \frac{sx_d}{2}$; (9.17)

It was assumed that function F_i can be represented by the following series expansion:

$$F_i(\tau) = \sum_{n=1}^{\infty} c_n^{(i)} P_n^{(\alpha,\beta)}(\tau) \qquad (9.18)$$

Now after substituting this for F_i a series of integrals is obtained

$$I_2 = \int_{-1}^{1} P_n^{(\alpha,\beta)}(\tau)\, e^{ia\tau}(1-\tau)^{\alpha}(1+\tau)^{\beta}\, d\tau$$

Applying the Rodrigues' formula and integrating by parts it reduces to:

$$I_2 = \frac{(-1)^n}{(-2)^n\, n!} \int_{-1}^{1} (i\,a)^n\, e^{ia\tau}(1-\tau)^{\alpha+n}(1+\tau)^{\beta+n} d\tau$$

Now upon transformation $\tau = 2u - 1$, $d\tau = 2du$, $0 < u < 1$ and simple algebra the integral reduces to:

$$I_2 = \frac{(i\,a)^n}{2^n n!} 2^{\alpha+\beta+2n+1} e^{-ia} \int_0^1 e^{i2au}(1-u)^{\alpha+n} u^{\beta+n} du$$

and using the result from [6], it gives:

$$I_2 = \frac{(i\,a)^n}{2^n n!} 2^{\alpha+\beta+2n+1} e^{-ia} \frac{\Gamma(n+\beta+1)\,\Gamma(n+\alpha+1)}{\Gamma(2n+\alpha+\beta+2)} \Phi(\beta+n+1;\, 2n+\alpha+\beta+2;\, 2ai) \tag{9.19}$$

where $\Phi(a;c;z) = {}_1F_1(a;c;z)$ is a confluent hypergeometric function and $\Gamma(x)\Gamma(y)/\Gamma(x+y)=B(x,y)$ is a Beta function. The series expansion is true for any τ from interval $(-1,1)$, so

$$F_1(1) = \sum_{n=1}^{\infty} c_n^{(1)} P_n^{(\alpha,\beta)}(1)$$

$$c_n^{(1)} = \frac{F_1(1)}{P_n^{(\alpha,\beta)}(1)} = \frac{F_1(1)}{(\alpha+1)_n} n! = \frac{F_1(1) n!\,\Gamma(\alpha+1)}{\Gamma(\alpha+1+n)}$$

since

$$\alpha = -\frac{1}{2} \qquad c_n^{(1)} = F_1(1) \frac{n!\;\Gamma(\frac{1}{2})}{\Gamma(n+\frac{1}{2})} \qquad \text{where} \quad \Gamma(\tfrac{1}{2}) = 2\sqrt{\pi} \tag{9.20}$$

and analogically

$$F_2(1) = \sum_{n=1}^{\infty} c_n^{(2)} P_n^{(\alpha,\beta)}(1)$$

$$c_n^{(2)} = \frac{F_2(1)}{P_n^{(\alpha,\beta)}(1)} = \frac{F_2(1)}{(\alpha+1)_n} n! = \frac{F_2(1) n!\,\Gamma(\alpha+1)}{\Gamma(\alpha+1+n)}$$

$$c_n^{(2)} = F_2(1) \frac{n!\;\Gamma(\frac{1}{2})}{\Gamma(n+\frac{1}{2})} \tag{9.21}$$

Applying all these results to equations for Δv and Δu yields:

$$\Delta v = \lim_{y_1 \to 0} A \int_{-\infty}^{+\infty} \frac{s^n}{|s|} \Phi(\beta+n+1;\, 2n+\alpha+\beta+2;\, isx_d)$$

$$\Bigg[c_n^{(1)}[(\omega_1^2 - \frac{a_{12}}{a_{11}})\omega_2(e^{-\omega_2|s|y_1^+} - e^{\omega_2|s|y_1^-})$$

$$- (\omega_2^2 - \frac{a_{12}}{a_{11}})\omega_1(e^{-\omega_1|s|y_1^+} - e^{\omega_1|s|y_1^-})]$$

$$+ \frac{|s|}{is} c_n^{(2)}[(\omega_1^2 - \frac{a_{12}}{a_{11}})(e^{-\omega_2|s|y_1^+} + e^{\omega_2|s|y_1^-})$$

$$- (\omega_2^2 - \frac{a_{12}}{a_{11}})(e^{-\omega_1|s|y_1^+} + e^{\omega_1|s|y_1^-})]\Bigg] e^{-isx_1}\, ds$$

$$\Delta u = \lim_{y_1 \to 0} A \int_{-\infty}^{+\infty} \frac{s^n}{is} \Phi(\beta+n+1;\, 2n+\alpha+\beta+2;\, isx_d)$$

$$\Bigg[c_n^{(1)}[(\omega_1^2 - \frac{a_{12}}{a_{11}})(e^{-\omega_1|s|y_1^+} + e^{\omega_1|s|y_1^-})$$

$$- (\omega_2^2 - \frac{a_{12}}{a_{11}})(e^{-\omega_2|s|y_1^+} + e^{\omega_2|s|y_1^-})]$$

$$+ \frac{|s|}{is\omega_1\omega_2} c_n^{(2)}[(\omega_1^2 - \frac{a_{12}}{a_{11}})\omega_2(e^{-\omega_1|s|y_1^+} - e^{\omega_1|s|y_1^-})$$

$$- (\omega_2^2 - \frac{a_{12}}{a_{11}})\omega_1(e^{-\omega_2|s|y_1^+} - e^{\omega_2|s|y_1^-})]\Bigg] e^{-isx_1}\, ds$$

where

$$A = \frac{-x_d}{4\pi} \frac{(i\,x_d)^n}{(\omega_1^2 - \omega_2^2)} B(n+\beta+1,\, n+\alpha+1) \frac{2^{\alpha+\beta}}{n!}$$

By changing the integration interval to $(0,\infty)$, the above expressions for crack surface displacements become:

$$\Delta v = \lim_{y_1 \to 0} A \int_0^{+\infty} (-1)^{n-1} s^{n-1} \Phi(\beta+n+1;\, 2n+\alpha+\beta+2;\, -isx_d) \Bigg[c_n^{(1)} [(\omega_1^2 - \frac{a_{12}}{a_{11}})\omega_2$$

$$(e^{-\omega_2|s|y_1^+} - e^{\omega_2|s|y_1^-}) - (\omega_2^2 - \frac{a_{12}}{a_{11}})\omega_1 (e^{-\omega_1|s|y_1^+} - e^{\omega_1|s|y_1^-})] - \frac{c_n^{(2)}}{i} [(\omega_1^2 - \frac{a_{12}}{a_{11}})$$

$$(e^{-\omega_2|s|y_1^+} + e^{\omega_2|s|y_1^-}) - (\omega_2^2 - \frac{a_{12}}{a_{11}})(e^{-\omega_1|s|y_1^+} + e^{\omega_1|s|y_1^-})] \Bigg] e^{isx_1}\, ds$$

$$+ s^{n-1} \Phi(\beta+n+1;\, 2n+\alpha+\beta+2;\, isx_d) \Bigg[c_n^{(1)} [(\omega_1^2 - \frac{a_{12}}{a_{11}})\omega_2 (e^{-\omega_2|s|y_1^+} - e^{\omega_2|s|y_1^-}) \tag{9.22}$$

$$- (\omega_2^2 - \frac{a_{12}}{a_{11}})\omega_1 (e^{-\omega_1|s|y_1^+} - e^{\omega_1|s|y_1^-})] + \frac{c_n^{(2)}}{i} [(\omega_1^2 - \frac{a_{12}}{a_{11}})(e^{-\omega_2|s|y_1^+} + e^{\omega_2|s|y_1^-})$$

$$- (\omega_2^2 - \frac{a_{12}}{a_{11}})(e^{-\omega_1|s|y_1^+} + e^{\omega_1|s|y_1^-})] \Bigg] e^{-isx_1}\, ds$$

$$\Delta u = \lim_{y_1 \to 0} \frac{A}{i} \int_0^{+\infty} (-1)^{n-1} s^{n-1} \Phi(\beta+n+1;\, 2n+\alpha+\beta+2;\, -isx_d) \Bigg[c_n^{(1)} [(\omega_1^2 - \frac{a_{12}}{a_{11}})$$

$$(e^{-\omega_1|s|y_1^+} + e^{\omega_1|s|y_1^-}) - (\omega_2^2 - \frac{a_{12}}{a_{11}})(e^{-\omega_2|s|y_1^+} + e^{\omega_2|s|y_1^-})] - \frac{c_n^{(2)}}{i\,\omega_1\omega_2} [(\omega_1^2 - \frac{a_{12}}{a_{11}})$$

$$\omega_2 (e^{-\omega_1|s|y_1^+} - e^{\omega_1|s|y_1^-}) - (\omega_2^2 - \frac{a_{12}}{a_{11}})\omega_1 (e^{-\omega_2|s|y_1^+} - e^{\omega_2|s|y_1^-})] \Bigg] e^{isx_1}\, ds$$

$$+ s^{n-1} \Phi(\beta+n+1;\, 2n+\alpha+\beta+2;\, isx_d) \Bigg[c_n^{(1)} [(\omega_1^2 - \frac{a_{12}}{a_{11}})(e^{-\omega_1|s|y_1^+} + e^{\omega_1|s|y_1^-}) \tag{9.23}$$

$$- (\omega_2^2 - \frac{a_{12}}{a_{11}})(e^{-\omega_2|s|y_1^+} + e^{\omega_2|s|y_1^-})] + \frac{c_n^{(2)}}{i\,\omega_1\omega_2} [(\omega_1^2 - \frac{a_{12}}{a_{11}})\omega_2 (e^{-\omega_1|s|y_1^+} - e^{\omega_1|s|y_1^-})$$

$$- (\omega_2^2 - \frac{a_{12}}{a_{11}})\omega_1 (e^{-\omega_2|s|y_1^+} - e^{\omega_2|s|y_1^-})] \Bigg] e^{-isx_1}\, ds$$

We now apply the asymptotic expansion for confluent hypergeometric functions:

$$\Phi(a; c; x) = \frac{\Gamma(c)}{\Gamma(c-a)}\left[\frac{e^{i\pi\varepsilon}}{x}\right]^{a} + \frac{\Gamma(c)}{\Gamma(a)} e^{x} x^{a-c} \tag{9.24}$$

$\varepsilon = 1$ if $\mathrm{Im}(x) > 0$

$\varepsilon = -1$ if $\mathrm{Im}(x) < 0$

where in our case $a = \beta + n + 1$; $c = 2n + \alpha + \beta + 2$; $x = \pm i s x_d$;

Finally applying this to the equations for displacement we obtain:

$$\Delta v = \lim_{y_1 \to 0} A \int_0^{+\infty} (-1)^{n-1} s^{n-1} \left[\frac{\Gamma(2n+\alpha+\beta+2)}{\Gamma(n+\alpha+1)} \left[\frac{e^{-i\pi}}{-ix_d s} \right]^{\beta+n+1} \right.$$

$$\left. + \frac{\Gamma(2n+\alpha+\beta+2)}{\Gamma(n+\beta+1)} \frac{e^{-isx_d}}{(-ix_d s)^{n+\alpha+1}} \right] \left[c_n^{(1)} [(\omega_1^2 - \frac{a_{12}}{a_{11}})\omega_2 (e^{-\omega_2 |s| y_1^+} - e^{\omega_2 |s| y_1^-}) \right.$$

$$- (\omega_2^2 - \frac{a_{12}}{a_{11}})\omega_1 (e^{-\omega_1 |s| y_1^+} - e^{\omega_1 |s| y_1^-})] - \frac{c_n^{(2)}}{i} [(\omega_1^2 - \frac{a_{12}}{a_{11}})(e^{-\omega_2 |s| y_1^+} + e^{\omega_2 |s| y_1^-})$$

$$\left. - (\omega_2^2 - \frac{a_{12}}{a_{11}})(e^{-\omega_1 |s| y_1^+} + e^{\omega_1 |s| y_1^-})] \right] e^{isx_1} ds$$

$$+ s^{n-1} \left[\frac{\Gamma(2n+\alpha+\beta+2)}{\Gamma(n+\alpha+1)} \left[\frac{e^{i\pi}}{ix_d s} \right]^{\beta+n+1} + \frac{\Gamma(2n+\alpha+\beta+2)}{\Gamma(n+\beta+1)} \frac{e^{isx_d}}{(ix_d s)^{n+\alpha+1}} \right]$$

$$\left[c_n^{(1)} [(\omega_1^2 - \frac{a_{12}}{a_{11}})\omega_2 (e^{-\omega_2 |s| y_1^+} - e^{\omega_2 |s| y_1^-}) - (\omega_2^2 - \frac{a_{12}}{a_{11}})\omega_1 (e^{-\omega_1 |s| y_1^+} - e^{\omega_1 |s| y_1^-})] \right.$$

$$+ \frac{c_n^{(2)}}{i} [(\omega_1^2 - \frac{a_{12}}{a_{11}})(e^{-\omega_2 |s| y_1^+} + e^{\omega_2 |s| y_1^-})$$

$$\left. - (\omega_2^2 - \frac{a_{12}}{a_{11}})(e^{-\omega_1 |s| y_1^+} + e^{\omega_1 |s| y_1^-})] \right] e^{-isx_1} ds \qquad (9.25)$$

$$\Delta u = \lim_{y_1 \to 0} \frac{A}{i} \int_0^{+\infty} (-1)^{n-1} s^{n-1} \left[\frac{\Gamma(2n+\alpha+\beta+2)}{\Gamma(n+\alpha+1)} \left[\frac{e^{-i\pi}}{-ix_d s} \right]^{\beta+n+1} \right.$$

$$\left. + \frac{\Gamma(2n+\alpha+\beta+2)}{\Gamma(n+\beta+1)} \frac{e^{-isx_d}}{(-ix_d s)^{n+\alpha+1}} \right] \left[c_n^{(1)} [(\omega_1^2 - \frac{a_{12}}{a_{11}})(e^{-\omega_1|s|y_1^+} + e^{\omega_1|s|y_1^-})\right.$$

$$- (\omega_2^2 - \frac{a_{12}}{a_{11}})(e^{-\omega_2|s|y_1^+} + e^{\omega_2|s|y_1^-})] - \frac{c_n^{(2)}}{i\,\omega_1\omega_2} [(\omega_1^2 - \frac{a_{12}}{a_{11}})\omega_2(e^{-\omega_1|s|y_1^+} - e^{\omega_1|s|y_1^-})$$

$$\left. - (\omega_2^2 - \frac{a_{12}}{a_{11}})\omega_1(e^{-\omega_2|s|y_1^+} - e^{\omega_2|s|y_1^-})] \right] e^{isx_1}\, ds$$

$$+ s^{n-1} \left[\frac{\Gamma(2n+\alpha+\beta+2)}{\Gamma(n+\alpha+1)} \left[\frac{e^{i\pi}}{ix_d s} \right]^{\beta+n+1} + \frac{\Gamma(2n+\alpha+\beta+2)}{\Gamma(n+\beta+1)} \frac{e^{isx_d}}{(ix_d s)^{n+\alpha+1}} \right]$$

$$\left[c_n^{(1)} [(\omega_1^2 - \frac{a_{12}}{a_{11}})(e^{-\omega_1|s|y_1^+} + e^{\omega_1|s|y_1^-}) - (\omega_2^2 - \frac{a_{12}}{a_{11}})(e^{-\omega_2|s|y_1^+} + e^{\omega_2|s|y_1^-})] \right.$$

$$+ \frac{c_n^{(2)}}{i\,\omega_1\omega_2} [(\omega_1^2 - \frac{a_{12}}{a_{11}})\omega_2(e^{-\omega_1|s|y_1^+} - e^{\omega_1|s|y_1^-})$$

$$\left. - (\omega_2^2 - \frac{a_{12}}{a_{11}})\omega_1(e^{-\omega_2|s|y_1^+} - e^{\omega_2|s|y_1^-})] \right] e^{-isx_1}\, ds \qquad (9.26)$$

Following the integral 3.381 from "Table of integral" by I.S.Gradshteyn and I.M.Ryzhik [7]:

$$\int_0^{\infty} x^{\nu-1} e^{-(p+iq)x} dx = \Gamma(\nu)(p^2+q^2)^{-\frac{\nu}{2}} \exp(-i\nu \operatorname{arc\,tg} \frac{q}{p}) \qquad (9.27)$$

$$p = 0, \quad \nu > -1$$

we obtain:

$$\Delta v = -2^{\beta+\frac{1}{2}} F_1(1)\sqrt{x_d(x_d - x)} \quad + \text{higher order terms} \tag{9.28}$$

and

$$\Delta u = -2^{\beta+\frac{1}{2}} F_2(1)\sqrt{x_d(x_d - x)} \quad + \text{higher order terms} \tag{9.29}$$

where

$$F_1(1) = -\frac{k_2(x_d)}{\pi C_{21}\sqrt{x_d}\,2^{\beta}} \qquad F_2(1) = -\frac{k_1(x_d)}{\pi C_{12}\sqrt{x_d}\,2^{\beta}}$$

for $x_1 < x_d$.

Now , substituting in (9.4-9.5) and integrating we have:

$$G_I = \frac{1}{4}\frac{k_1^2(x_d)}{C_{12}} \quad (9.30) \qquad\qquad G_{II} = \frac{1}{4}\frac{k_2^2(x_d)}{C_{21}} \quad (9.31)$$

or substituting for C_{12} and C_{21} and computing the total strain energy release rate we have:

$$G = \frac{\pi}{2}\left[k_1^2(x_d)\,\omega_1\omega_2(\omega_1 + \omega_2)\,a_{11} + k_2^2(x_d)(\omega_1 + \omega_2)\,a_{11}\right] \tag{9.32}$$

which has the form reported by Cherepanov for the orthotropic case.

For isotropic material and self-similar crack propagation this reduces to the well known form:

$$G = \frac{\pi k_1^2(x_d)}{E} \tag{9.33}$$

APPENDIX REFERENCES

[1] N.I. Muskhelisvili, "Singular Integral Equations", Noordhoff,Groningen, The Netherlands, 1953.

[2] F. Erdogan, "Mixed Boundary-Value Problems in Mechanics", Mechanics Today, edited by S. Nemat-Nasser, Vol. 4, pp. 1-86, Pergamon Press, Oxford, 1978.

[3] G.P. Cherepanow, "Mechanics of Brittle Fracture", McGraw Hill, N.Y., 1979.

[4] F. Delale, "Mode III Fracture of Bonded Nonhomogeneous Materials", Engineering Fracture Mechanics, Vol. 22, pp. 213-226, 1985.

[5] G.D. Gupta, "Strain Energy Release Rate for Mixed Mode Crack Problem", ASME, 76-WA/PVP-7, 1977.

[6] A. Erdelyi, "Higher Transcendental Functions" McGraw Hill, N.Y., 1953.

[7] I.S. Gradshteyn and I.M. Ryzhik, Table of Integral, Series, and Products", Academic Press, N.Y., 1980.

DISTRIBUTION LIST

NON-GOVERNMENT ACTIVITIES (continued)

	NO. OF COPIES
NORTHROP AIRCRAFT CORP., One Northrop Avenue, Hawthorne, CA 90250 (Attn: Dr. M. Ratwani, B. Butler and R. Whitehead). . .	3
PURDUE UNIVERSITY, School of Aeronautics and Astronautics, West Lafayette, IN 47907 (Attn: Dr. C. T. Sun).	1
PROTOTYPE DEVELOPMENT ASSOCIATES, INC., 1560 Brookhollow Drive Santa Ana, CA 92705 (Attn: E. L. Stanton).	1
ROCKWELL INTERNATIONAL, Columbus, OH 43216 (Attn: M. Schweiger).	1
ROCKWELL INTERNATIONAL, Los Angeles, CA 90009 (Attn: Dr. Lackman).	1
(Attn: W. O'Brien).	1
ROCKWELL INTERNATIONAL, Tulsa, OK 74151 (Attn: F. Kaufman).	1
ROHR CORP., Riverside, CA 92503 (Attn: Dr. F. Riel).	1
SIKORSKY AIRCRAFT, Stratford, CT 06622 (Attn: S. Garbo).	1
J. P. STEVENS & CO., INC., New York, NY 10036 (Attn: H. I. Shulock).	1
TELEDYNE RYAN AERONAUTICAL CO., San Diego, CA 92138 (Attn: R. Long).	1
TUSKEGEE UNIVERSITY, School of Engineering and Architecture, Tuskegee, AL 36088 (Attn: Vascar G. Harris, Dean).	1
UNIVERSITY OF DAYTON RESEARCH INSTITUTE, 300 College Park Avenue, Dayton, OH 45469 (Attn: Dr. J. Gallagher).	1
UNIVERSITY OF DELAWARE, Mechanics & Aerospace Eng. Dept., Evans Hall, Newark, DE 19711 (Attn: Dr. R. B. Pipes, Dr. J. R. Vinson and Dr. D.Wilkins .	3
UNIVERSITY OF OKLAHOMA, Norman, OK 73019 (Attn: Dr. C. W. Bert, School of AMNE).	1
UNIVERSITY OF WYOMING, Laramie, WY 82071 (Attn: Dr. D. Adams).	1
VILLANOVA UNIVERSITY, Villanova, PA 19085 (Attn: Dr. P. V. McLaughlin).	1
VIRGINIA POLYTECHNIC INSTITUTE, Blacksburg, VA 24061 (Attn: Dr. K. Reifsnider).	1
WASHINGTON UNIVERSITY, School of Engineering and Applied Science, Materials Research Laboratory, Campus Box 1087, St. Louis, MO 63130 (Attn: T. Hahn).	1

DISTRIBUTION LIST

NON-GOVERNMENT ACTIVITIES (continued)

	NO. OF COPIES
GENERAL ELECTRIC CO., Philadelphia, PA 19101	
(Attn: A. Garber, C. Zweben).	2
GREAT LAKES CARBON CORPORATION, New York, NY 10017	
(Attn: W. R. Benn, Manager, Market Development). . .	1
GRUMMAN CORPORATION, South Oyster Bay Rd., Bethpage, NY 11714	
(Attn: R. Hadcock).	1
(Attn: S. Dastin).	1
HERCULES AEROSPACE DIVISION, P.O. Box 210, Cumberland, MD 21502	
(Attn: Mr. D. Hug).	1
HITCO, 1600 West 135th Street, Gardena, CA 90249	
(Attn: N. Myers).	1
ITT RESEARCH INSTITUTE, Chicago, IL 60616	
(Attn: K. Hofar).	1
KAMAN AIRCRAFT CORP., Bloomfield, CT 06002	
(Attn: Technical Library).	1
LEHIGH UNIVERSITY, Bethlehem, PA 18015	
(Attn: Dr. G. C. Sih).	1
LEONARD ASSOCIATES, INC., 6 East Avenue, Mt. Carmel, PA 17851	
(Attn: Mr. L. Marchinski).	1
LOCKHEED-CALIFORNIA CO., Burbank, CA 91520	
(Attn: E. K. Walker).	1
(Attn: A. James).	1
LOCKHEED-MISSILES & SPACE CO., 1111 Lockheed Way, Sunnyvale, CA 94086	
(Attn: J. A. Bailie).	1
LOCKHEED-CALIFORNIA CO., Rye Canyon Research Laboratory, Burbank, CA 91520	
(Attn: D. E. Pettit).	1
LOCKHEED-GEORGIA CO., Marietta, GA 30063	
(Attn: Technical Information Dept., 72-34, Zone 26). . .	1
LTV AEROSPACE & DEFENSE CO., Vought Missile & Advanced Program Division, P.O. Box 225907, Dallas, TX 75265-0003	
(Attn: R. Knight).	1
MASSACHUSETTS INSTITUTE OF TECHNOLOGY, Technology Laboratory for Advanced Composite, 77 Massachuetts Avenue, Cambridge, MA 02139	
(Attn: Dr. P. A. Lagace).	1
MATERIALS SCIENCES CORP., Spring House, PA 19477	
(Attn: Dr. B. W. Rosen).	
McDONNELL-DOUGLAS CORP., St. Louis, MO 63166	
(Attn: K. Stenberg, R. Garrett, R. Riley, J. Doerr). . .	4
McDONNELL-DOUGLAS CORP. Long Beach, CA 90846	
(Attn: J. Palmer).	1
McDONNELL-DOUGLAS HELICOPTER CO., Bldg. 530, 5000 E. McDowell Rd Mesa, AZ 85258	
(Attn: J. K. Sen, M.S. 338).	1
McDONNELL-DOUGLAS HELICOPTER CO., 5000E. McDowell, M/S B337 Mesa, AZ 85205	
(Attn: Steve Guymon).	1

DISTRIBUTION LIST

NON-GOVERNMENT ACTIVITIES

	NO. OF COPIES
ANAMET LABORATORIES, 100 Industrial Hyw., San Carlos, CA 94070	
(Attn: Dr. R. Arnold).	1
ALCOA DEFENSE SYSTEMS CORP., 16761 Via delCampo Court, San Diego, CA 92127	
(Attn: D. Myers).	1
AVCO, Specialty Materials Div., 2 Industrial Avenue, Lowell, MA 01851	
(Attn: Mr. W. F. Grant).	1
BATTELLE COLUMBUS LABORATORIES, Metals and Ceramics Information Center 505 King Avenue, Columbus, OH 43201.	1
BEECH AIRCRAFT CORP., 4130 Linden Avenue, Dayton, OH 45432	
(Attn: M. B. Goetz).	1
BELL AEROSPACE COMPANY, Buffalo, NY 14240	
(Attn: F. M. Anthony, Zone I-85).	1
BELL HELICOPTER CO., Fort Worth, TX 76101	
(Attn: M. K. Stevenson).	1
BENDIX PRODUCTS, Aerospace Division, South Bend, IN 46619	
(Attn: R. V. Cervelli).	1
BOEING CO., P. O. Box 3707, Seattle, WA 98124	
(Attn: J. Quinliven, and Dr. R. June).	2
BOEING HELICOPTER COMPANY, P.O. Box 16858, Philadelphia, PA 19143	
(Attn: R. L. Pinckney).	1
(Attn: D. Hart).	1
(Attn: C. Albrecht).	1
BOEING CO., Wichita, KS 67277-7730.	1
(Attn: J. Avery).	1
(Attn: R. Waner).	1
CABOT CORPORATION, Billerica Research Center, Billerica, MA 01821.	1
DEPARTMENT OF TRANSPORTATION, Kendall Square, Cambridge, MA 02142.	1
(Attn: Dr. Ping Tong, DTS 76, TSC).	1
DREXEL UNIVERSITY, Philadelphia, PA 19104	
(Attn: Dr. P. C. Chou).	1
(Attn: Dr. A. S. D. Wang).	1
E. I. DuPONT COMPANY, Textile Fibers Department, Chestnut Run Location CR701, Wilmington, DE 19898	
(Attn: V. L. Bertarelli).	1
FAIRCHILD REPUBLIC CO., Farmingdale, L.I., NY 11735	
(Attn: Mr. Frank Costa).	1
GEORGIA INSTITUTE OF TECHNOLOGY, Atlanta, GA 30332	
(Attn: (L. Rehfield)).	1
GENERAL DYNAMICS/CONVAIR, San Diego, CA 92138	
(Attn: Dr. R. Dunbar).	1
GENERAL DYNAMICS, Fort Worth Division, PO Box 748, Fort Worth, TX 76101	
(Attn: J. A. Fant).	1
(Attn: Composite Structures Eng. Dept.).	1

DISTRIBUTION LIST

GOVERNMENT ACTIVITIES - (continued)

	NO. OF COPIES
NAVSHIPRANDCEN, Annapolis, MD 21403	
(Attn: H. Edlestein, Code 2870).	1
NRL, Washington, D.C. 20375	
(Attn: Dr. I. Wolock, Code 6122; Dr. C. I. Chang, and Dr. R. Badaliance).	3
NSWC, WHITE OAK LABORATORY, Silver Spring, MD 20910	
(Attn: Dr. J. Goff, Materials Evaluation Branch, Code R-34	1
(Attn: Dr. J. M. Augl).	2
ONR, 800 N. Quincy St., Arlington, VA 22217	
(Attn: A. Kushner Code 1132 SM; Y. Rajapakse, Code 1132SM)	2
(Attn: R. Jones, Code 1216).	1
ONT, 800 N. Quincy Street, Arlington, VA 22217	
(Attn: Capt. K. Cox, (ONT-21D).	1
PLASTEC, Picatinny Arsenal, Dover, NJ 07801	
(Attn: H. Pebly).	1
(Attn: Librarian, Code DRDAR-SCM-O, Bldg. 351-N).	1
ARMY MATERIALS TECHNOLOGY LABORATORY Watertown, MA 02171	
(Attn: D. Oplinger, SLCMT-MS).	1
U. S. ARMY APPLIED TECHNOLOGY LABORATORY, USARTL, (AVRADCOM), Ft. Eustis, VA 23604-5418	
(Attn: J. Waller; T. Mazza).	2
U. S. ARMY AIR MOBILITY R&D LABORATORY, Ft. Eustis, VA 23604	
(Attn: H. Reddick).	1
U. S. ARMY R&T LABORATORY (AVRADCOM), Ames Research Center, Moffet Field, CA 94035	
(Attn: F. Immen, DAVDL-AS-MS 207-5).	1
U. S. NAVAL ACADEMY, Annapolis, MD 21402	
(Attn: Mechanical Engineering Department).	1
DAVID TAYLOR NAVAL SHIP RESEARCH & DEVELOPMENT CENTER, Annapolis, MD 21402	
(Attn: E. T. Camponeschi, Code 2844; R. Crane, Code 2844).	2
DAVID TAYLOR NAVAL SHIP R&D CENTER Bethesda, MD 20084	
(Attn: A. Macander, Code 1720).	1
NAVAIRDEVCEN, Warminster, PA 18974	
(Attn: Code 8131).	3
(Attn: Code 09L2).	2

DISTRIBUTION LIST

GOVERNMENT ACTIVITIES

	NO. OF COPIES
AFWAL, WPAFB, OH 45433-6553	
(Attn: FIBEC, Dr. G. Sendeckyj).	1
(Attn: FIBC/L. Kelly).	1
(Attn: FIBCA/C. Ramsey).	1
(Attn: FIBE/D. Smith).	1
AFWAL, WPAFB, OH 45433-6533	
(Attn: MLBM/Dr. J. Whitney, M. Knight).	2
(Attn: MLB/F. Cherry).	1
(Attn: MBC/Reinhart).	1
(Attn: MLSE/S. Fecheck).	1
DEPARTMENT OF THE AIR FORCE, Bldg. 410, Bolling Air Force Base, Washington, D.C. 20332	
(Attn: Dr. M. Salkind, Dr. Amos).	2
DEFENSE TECHNICAL INFORMATION CENTER (DTIC), Bldg.#5, Cameron Station Alexandria, VA 22314	
(Attn: Administrator).	2
FAA, Washington, D.C. 20591	
(Attn: J. R. Soderquist, AW-103).	1
FAA, Technical Center, Atlantic City, NJ 08405	
(Attn: L. Neri, Code ACT-330; M. Caiafa, Code ACT-033).	2
NASA HEADQUARTERS, Washington, D. C. 20546	
(Attn: Airframes Branch, FS-120).	1
(Attn: OAST/RM, Dr. D. Mulville).	1
NASA, George C. Marshall Space Flight Center, Huntsville, AL 35812	
(Attn: R. Schwinghamer, S&E-ASTN-M).	1
NASA, Langley Research Center, Hampton, VA 23365	
(Attn: Dr. J. R. Davidson, MS 188E; Dr. J. Starnes, MS-190; Dr. M. Mikulus, H. Bohan, and Dr. C. P. Blakenship MS 189M).	5
NASA, Lewis Research Center, Cleveland, OH 44135	
(Attn: Dr. C. Chamis, MS 49-6; M. Hershberg, MS 49-6).	2
NAVAIRSYSCOM, Washington, D.C. 20361	
(Attn: AIR-00D4).	1
(Attn: AIR-530).	1
(Attn: AIR-5302D).	1
(Attn: AIR-5302).	1
(Attn: AIR-5302F).	1
(Attn: AIR-53032D).	1
(Attn: AIR-931B).	1
NAVPGSCHL, Monterey, CA 95940	
(Attn: Prof. R. Ball, Prof. M. H. Bank, Prof. K. Challenger).	3
NAVSEASYSCOM, Washington, D.C. 20360	
(Attn: C. Zannis, SEA-05R25)).	1
NAVSEC, Arlington, VA 20360	
(Attn: NSEC-6101E).	1

END
DATE
FILMED
6-1988
DTIC